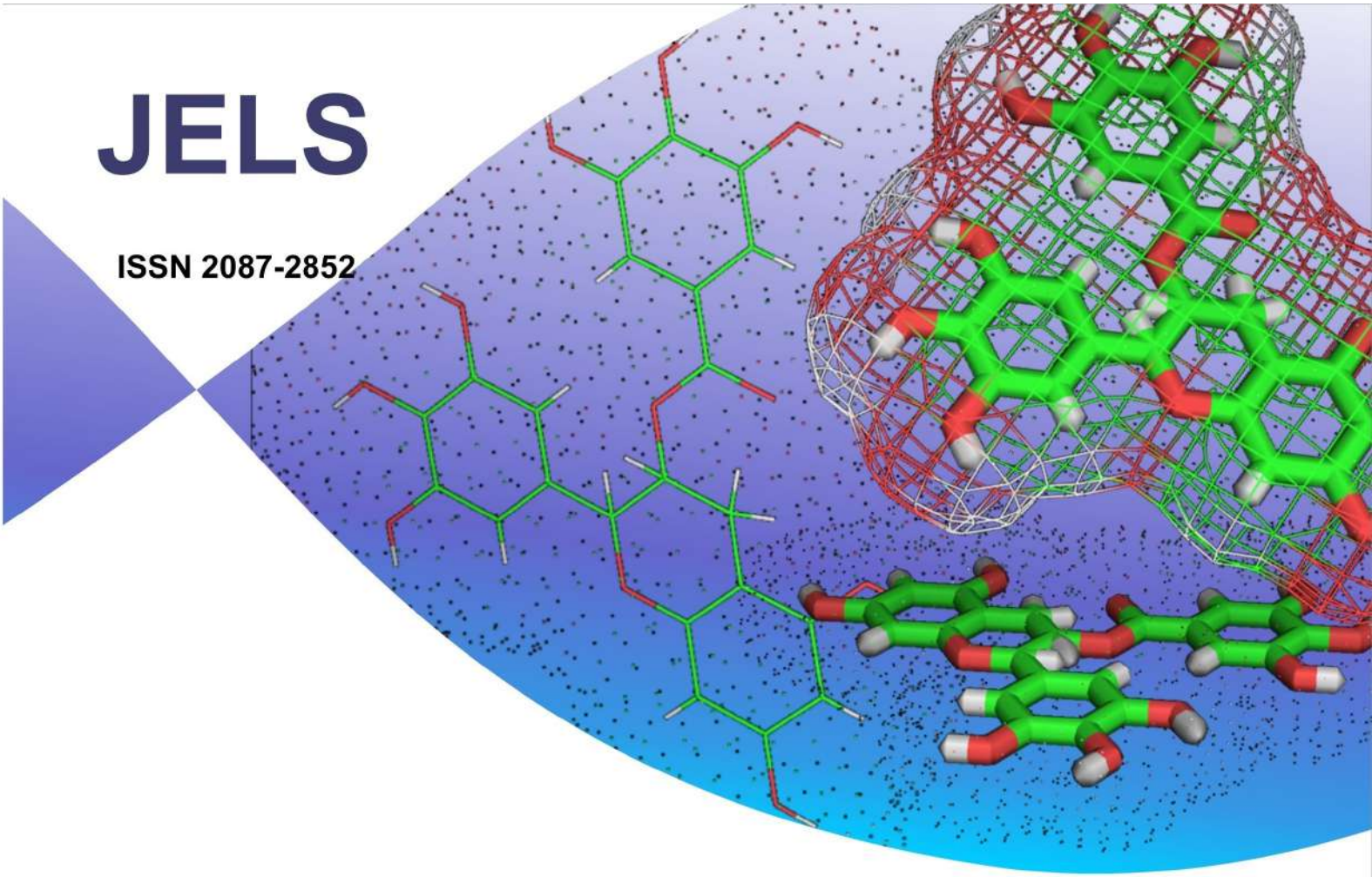

JELS

ISSN 2087-2852

The Journal of EXPERIMENTAL LIFE SCIENCE

J.Exp. Life Sci.	Vol. 13	No. 2	Pages. 67-137	June 2023

Published by :
Graduate Program, Universitas Brawijaya

jels.ub.ac.id

ISSN. 2087-2852
E-ISSN. 2338-1655

The Journal of Experimental Life Science

Discovering Living System Concept through Nano, Molecular and Cellular Biology

Editorial Board

Address
The Journal of Experimental Life Science
Building B, 1st Floor, Postgraduate School, University of Brawijaya
Jl. Mayor Jenderal Haryono 169, Malang, 65145
Telp: (0341) 571260 ; Fax: (0341) 580801
Email: jels@ub.ac.id
Web: http://www.jels.ub.ac.id

ISSN. 2087-2852
E-ISSN. 2338-1655

Table of Content

Re-fermentation of Green Liberica Coffee (*Coffea Liberica*) Beans: Impact on the Caffeine and Antioxidant Content of the Roasted Beans

Wenny Bekti Sunarharum*, Hindun Riza Umami, Annisa Aurora Kartika, Siska Septiana, Tunjung Mahatmanto

Department of Food Science and Biotechnology, Faculty of Agricultural Technology, Universitas Brawijaya, Malang, Indonesia

Abstract

Coffee is renowned for its delightful taste and associated health benefits. A growing preference for lower-caffeine coffee is evident, but traditional decaffeination processes can inadvertently deplete vital bioactive compounds like antioxidants. This research explores the effects of re-fermentation on green liberica coffee beans to alter their caffeine and antioxidant levels. The re-fermentation was achieved using water and coffee cherry extract as media, while a control sample without re-fermentation was used for comparison. The study focused on caffeine content and antioxidant activity, measured as IC_{50}. The results show that re-fermentation, whether with water or coffee cherry extract, led to decreased caffeine content and increased antioxidant activity. The re-fermentation process utilizing coffee cherry extract yielded the lowest caffeine content at 0.12% and exhibited the strongest antioxidant activity with an IC_{50} of 11.00 ± 1.21 ppm.

Keywords: Antioxidant, caffeine, green coffee beans, liberica, re-fermentation.

INTRODUCTION

The popularity of coffee has surged, as it has seamlessly integrated into the lifestyles of many people worldwide. Notably, a growing trend towards reducing caffeine consumption caters to caffeine-sensitive individuals and those mindful of its physiological effects [1]. The caffeine content of coffee varies due to various factors. Low-caffeine coffee can result from blending different species, natural genetic variations that yield lower caffeine levels, specific cultivation conditions, or distinct processes like de-caffeination and brewing [2,3]. In addition to caffeine, coffee contains essential phytochemicals such as polyphenols, including chlorogenic acid, which serve as potent antioxidants [4]. Processes like decaffeination, employed to reduce caffeine, may inadvertently diminish the levels of phenolic acids and the overall antioxidant capacity of coffee [5].

Among the world's popular coffee varieties, liberica coffee (*Coffea liberica*) has been reported to exhibit exceptionally high antioxidant activity compared to arabica and robusta [6]. Typically, liberica coffee beans contain approximately 1.25–1.69% caffeine and are valued for their significant antioxidant profile [6,7]. However, due to its uncharacteristic sensory profile [8], liberica coffee is often used in blends with other coffee, frequently alongside robusta or arabica coffee [6]. Fermentation is a promising approach to enhancing coffee's sensory profile [9].

Fermentation is a process that is typically applied to coffee cherries to remove the mucilage that surrounds the coffee beans through microbial action. This process yields fermented green coffee beans, often referred to as green beans. Beyond its role in shaping the sensory characteristics of coffee, fermentation also impacts the bioactive components of coffee, including caffeine [7] and antioxidants [6]. While the application of fermentation to coffee cherries has been extensively explored, limited research has delved into its application to green coffee beans. Here, we re-fermented green liberica beans using water and coffee cherry extracts and evaluated their effect on the caffeine and antioxidant contents of roasted liberica coffee.

MATERIALS AND METHODS

Materials

The coffee beans used in this study were 10 kg green liberica coffee beans fermented by natural process and 15 kg red liberica coffee cherries from Kalipuro Banyuwangi. The red coffee cherries were de-pulped using a local coffee pulper, and the pulp was collected for preparing the fermentation media.

Preparation of Fermentation Media

The fermentation media were 1000 mL of water (P1) and 1000 mL of coffee cherry extract (P2). The coffee cherry extract was made by pulverizing coffee cherry pulp with water at a ratio of 1:4. The juice was filtered to yield the extract.

Re-Fermentation of Green Coffee Beans

Green liberica coffee beans were soaked in the fermentation media at a ratio of 1:1 in glass jars. The glass jars were tightly closed for 96 hours to allow anaerobic fermentation. The jars were opened for around 5 seconds every 24 hours to release pressure from gas buildup. The resulting re-fermented green coffee beans were washed and sun-dried to below 12.5% moisture. The dry

ISSN. 2087-2852
E-ISSN. 2338-1655

re-fermented coffee beans were roasted at *medium level* (200–220°C) before further analysis (in triplicate). Green liberica coffee beans without re-fermentation were prepared as controls (PK).

Analysis of Caffeine Content

The caffeine content of the roasted beans was analyzed using HPLC (Shimadzu, Prominence LC 20A) with a C18 column, UV-vis and a wavelength of 278 nm. The mobile phase used was methanol: aquabidest (95:5) with a flow rate of 1 mL/min.

Approximately 1.0 g ground coffee was mixed with 10 mL aquabidest and stirred using a magnetic stirrer at 150 rpm for 150 minutes before centrifugation at 6000 rpm for 15 minutes. Approximately 0.1 mL supernatant was diluted with aquabidest in a 25 mL volumetric flask and filtered using a PTFE microfilter (0.45 µm). For the analysis, 20 µL samples were injected into the HPLC.

Caffeine standard stock solution (100 ppm) was prepared before dilution (0, 5, 10, 15, and 20 ppm). Each diluted standard was filtered before injection and run on the HPLC as above to create a caffeine standard curve.

Analysis of Antioxidant Activity

The antioxidant activity of the roasted beans was analyzed using 2,2-diphenyl-1-picrylhydrazyl (DPPH) [11]. A solution of 0.1 mM DPPH in methanol was freshly prepared for the assay. 1 mL sample was added to 1 mL DPPH solution, mixed, and incubated for 30 minutes in the dark at room temperature. The absorbance of the samples was measured using a UV-vis spectrophotometer at 517 nm.

Statistical Data Analysis

The data were tabulated using Microsoft Excel 2013. Analysis of variance (ANOVA) and post-hoc at 95% confidence was performed using XLSTAT version 2015 (Addinsoft, New York, USA).

RESULTS AND DISCUSSIONS

Caffeine Content

The caffeine content in coffee beans is an essential factor influencing coffee's flavor and physiological effects on consumers. Our research findings, summarized in Table 1**,** reveal that the caffeine content in roasted liberica coffee beans ranges between 0.12 and 1.10%. Notably, re-fermentation treatments using either water (P1) or coffee cherry extract (P2) significantly reduced caffeine content. This decrease may be attributed to the leaching and degradation of caffeine during fermentation.

Table 1. Caffeine Content of Roasted Liberica Coffee Beans

Re-fermentation	Caffeine Content (%)
PK (control)	1.10 ± 0.11 a
P1 (using water)	0.60 ± 0.05 b
P2 (using coffee cherry extract)	0.12 ± 0.03 c

Note: Significant differences are indicated with letters (α=0.05)

It is important to note that coffee's caffeine content is subject to many variables, with coffee processing being particularly influential. For example, fermentation and roasting reduced the caffeine levels of liberica coffee to a range of 1.08–1.65%, with variations dependent on the duration of fermentation and roasting levels [7]. Brewing temperatures can also affect the caffeine content of coffee. This is because the solubility of caffeine in water increases with higher temperatures, contributing to lower caffeine content in coffee prepared through cold brewing methods, as opposed to those using hot water [3].

An intriguing observation from our research is the germination of some green coffee beans during the re-fermentation process. This phenomenon may have contributed to the compositional changes in the coffee beans. Indeed, a gradual decline in caffeine content [9] reported ranging from 49.17-62.25% in germinated arabica green coffee beans soaked in water for 12 and 24 hours [10]. The use of coffee cherry extract in the re-fermentation process may also reduce caffeine and other compounds due to biochemical decomposition. Naturally, occurring microorganisms within coffee cherries facilitate the enzymatic decomposition of coffee beans [12]. These intricate interactions and transformations in caffeine content underscore the multifaceted nature of coffee processing and its role in shaping the final chemical composition of coffee.

Antioxidant Activity

Table 2 presents the antioxidant activity results (IC_{50}) in roasted liberica coffee beans. The measured IC_{50} values in these samples ranged from 27.27 ± 17.92 ppm to 40.30 ± 12.85 ppm, indicating a significant range of strong antioxidant activity. This variation in IC_{50} values offers valuable insights into the effect of re-fermentation on the antioxidant potential of coffee beans.

Table 2. Antioxidant Activity (IC_{50}) of Roasted Liberica Coffee Beans

Re-fermentation	IC_{50} (ppm)
PK (control)	40.30 ± 12.85 a
P1 (using water)	31.71 ± 16.14 b
P2 (using coffee cherry extract)	27.27 ± 17.92 c

Note: Significant differences are indicated with letters (α=0.05)

ISSN. 2087-2852
E-ISSN. 2338-1655

Notably, our findings demonstrate that the re-fermentation process, whether through soaking the green beans in water (P1) or coffee cherry extract (P2), led to a substantial decrease in the IC_{50} values. This reduction signifies increased antioxidant activity, indicating that less concentration is required for effective radical scavenging. The enhanced antioxidant potential observed here can be attributed to the intricate biochemical changes driven by the fermentation process. It is assumed that naturally occurring microorganisms, which play a pivotal role during fermentation, contribute to the increased antioxidant activity of roasted beans. In addition, the germination of the green beans during re-fermentation may contribute to the biochemical changes that lead to this increase. For example, coffee polyphenols, predominantly chlorogenic acids (CGAs), may transform coffee processing [4].

In the context of germination, the soaking of green coffee beans has been shown to increase CGAs before a subsequent decrease with prolonged germination time [10]. It is important to note that while polyphenols contribute significantly to antioxidant activity, other compounds may also play pivotal roles. Thus, further exploration is needed to better understand the mechanisms governing the enhancement of antioxidant activity observed in roasted liberica coffee beans after re-fermentation.

CONCLUSION

The significant impact of re-fermentation of green liberica coffee beans on the roasted beans' caffeine content and antioxidant activity. Re-fermentation was found to reduce the caffeine content of liberica coffee while enhancing its antioxidant activity. Further research is needed to explore the complex interactions and effects of re-fermentation, including germination, on the chemical composition and sensory attributes of liberica coffee. This work sets the stage for the development of coffee products that not only cater to caffeine-sensitive individuals but also capitalize on the healthful attributes of coffee, thereby broadening its appeal to a broader audience. In the pursuit of balancing flavor and function, re-fermentation emerges as a promising avenue for the future of liberica coffee.

REFERENCES

[1] Mintel. 2023. The coffee and coffee shop industries: what consumers want in coffee. Available at: https://www.mintel.com.

[2] Kumar, V., G.A. Ravishankar. 2009. Current trends in producing low levels of caffeine in coffee berry and processed coffee powder. *Food Rev. Int.* 25 (3). 175-197.

[3] Olechno, E., A. Puścion-Jakubik, M.E. Zujko, K. Socha. 2021. Influence of various factors on caffeine content in coffee brews. *Foods.* 10. 1208. DOI: 10.3390/foods10061208.

[4] Sunarharum, W.B., T. Mahatmanto, D.Y. Ali, *et al.* 2022. Coffee polyphenols: Biochemical, processing, and health insights. 99-109. In: Ramakrishna, A., P. Giridhar, M. Jeszka-Skowron (Eds). Coffee science: biotechnological advances, economics, and health benefits, 1st Ed. CRC Press.

[5] Vicente, S.J.V., Y.S. Queiroz, S.L. Gotlieb, E.A. Torres. 2014. Stability of phenolic compounds and antioxidant capacity of regular and decaffeinated coffees. *Braz. Arch. Biol. Technol.* 57. 110–118.

[6] Saw, A.K.C., W.S. Yam, K.C. Wong, C.S. Lai. 2015. A comparative study of the volatile constituents of southeast Asian coffea arabica, coffea liberica and coffea robusta green beans and their antioxidant activities. *J. Essent. Oil-Bear. Plants.* 18(1). 64-73.

[7] Wibowo, N.A., W. Mangunwardoyo, T.J. Santoso, Yasman. 2021. Changes in caffeine of fermented Liberica coffee beans cv. Liberoid Meranti on roasting levels. E3S Web of Conferences 306, 01026.

[8] Davis, A.P., Kiwuka, C., A. Faruk. 2022. The re-emergence of Liberica coffee as a major crop plant. *Nat. Plants* 8, 1322–1328.

[9] de Melo Pereira, G.V., V.T. Soccol, S.K. Brar, E. Neto, C.R. Soccol. 2017. Microbial ecology and starter culture technology in coffee processing. *Crit. Rev. Food Sci. Nutr.* 57(13). 2775-2788.

[10] Wang, Y., X. Wang, G. Hu, *et al*. 2023. Anaerobic germination of green coffee beans: A novel strategy to improve the quality of commercial Arabica coffee. *Curr. Res. Food Sci.* 6. 100461.

[11] Molyneux, P. 2004 The use of stable free radical diphenylpicryhydrazyl (DPPH) for estimating antioxidant activity. *J. Sci. Technol.* 26(2). 211-219.

[12] Mahatmanto, T., W.B. Sunarharum, F.A. Putri, *et al.* 2023. The microbiology of arabica and robusta coffee cherries: a comparative study of indigenous bacteria with presumptive impact on coffee quality. *FEMS Microbiol. Lett.* 370. fnad024.

ISSN. 2087-2852
E-ISSN. 2338-1655

Relationship of Circulating Endothelial Cells, Endothelial Progenitor Cells, and Endothelial Dysfunction after High-Intensity Exercise: Role of Nitric Oxide

Rias Gesang Kinanti[1*], Djanggan Sargowo[2], Edi Widjajanto[3], Muhaimin Rifa'i[4]

[1]Department of Sport Science, Universitas Negeri Malang, Malang, Indonesia
[2]Department of Cardiology, Universitas Brawijaya, Malang, Indonesia
[3]Department of Pathology Clinic, Universitas Brawijaya, Malang, Indonesia
[4]Department of Biology, Universitas Brawijaya, Malang, Indonesia

Abstract

Endothelial dysfunction after high-intensity exercise occurs through various mechanisms characterized by decreased nitric oxide (NO) bioavailability. This study aims to determine the relationship between circulating endothelial cells (CEC), endothelial progenitor cells (EPC), and endothelial dysfunction after high-intensity exercise through an experiment using male Wistar strain rats. This study uses the randomized control group posttest-only design. A total of 32 male Wistar rats aged 20-22 weeks with a body weight of 140±20 g were taken randomly and divided into two groups. Group 1 (n=16), the control group, was given low-intensity exercise. Meanwhile, group 2 (n=16), named the treatment group, was given high-intensity exercise. The groups were run on a special treadmill where light-intensity exercise is done at a speed of 5-8 meters.minute^{-1} for 30 minutes and high intensity at 25-30 meters.minute^{-1} for 30 minutes. The treatment was performed at 5 to 10 pm, 3 times weekly for 12 weeks. Blood and aortic tissue samples were taken after the mice were rested for 12 hours after the last exercise. ELISA and Flow cytometry measured NO, CEC, and EPC levels. This research showed that CEC and EPC expression and high-intensity exercise have a positive relationship, yet not significant to the occurrence of endothelial dysfunction (NO), with a value of Sig. (0.111); $p > 0.05$, and the relationship value is r = 0.414 (R^2= 17.15%). In conclusion, endothelial dysfunction after high-intensity exercise is not associated with CEC and EPC expression, which indicates endothelial damage.

Keywords: exercise, circulating endothelial cells, endothelial dysfunction, endothelial progenitor cells, nitric oxide

Introduction

Endothelial cell integrity is one of the indicators and prerequisites for vascular health [1]. The endothelium responds to humoral, neural, and especially hemodynamic stimuli. It regulates several bodily functions, such as platelet function, inflammatory responses, vascular smooth muscle cell growth, and migration, as well as modulating vascular tone by synthesizing and releasing vasoactive substances [2]. When the endothelium is in a dysfunctional state—or termed endothelial dysfunction, characterized by reduced NO bioavailability—it is recognized as one of the preconditions of reversible and early atherosclerosis development. The pathogenesis of endothelial dysfunction is multifactorial. However, the cause of endothelial damage is mainly due to chronic exposure to risk factors that disturb the integrity of endothelial cells [3]. Endothelial dysfunction causes progressive pathophysiological changes as a response that occurs sequentially, namely activation, dysfunction, and endothelial injury [4]. Endothelial dysfunction plays a significant role in initiating and progressing cardiovascular diseases such as atherosclerosis [5]. Endothelial injury can be caused by several stimuli, such as biochemical, immunologic, or hemodynamic [6]. Friction between the blood flow and the endothelial lining of the arterial lumen can cause a force which is called shear stress. The endothelial layer is sensitive to this, where excessively elevated endothelial shear stress (ESS) is associated with plaque susceptibility [5]. Disturbed flow can cause injury endothelium, and affect the integrity of the endothelium, by triggering injury or repair [7].

Exercise is known to affect endothelial dysfunction [8] positively. Regular exercise has a cardio protective effect and improves the body's health quality, especially in improving endothelial function [1]. Despite these benefits, data shows that coronary artery calcification and atherosclerotic plaques are more prevalent in athletes than non-athletes, and athletes have higher coronary artery calcification (CAC) values [9]. Sudden cardiac death (SCD) also happens to many athletes, which is mainly caused by coronary heart disease and myocardial infarction (6.10%), and more than

* Correspondence Address:
Rias Gesang Kinanti
Email : rias.gesang.fik@um.ac.id
Address : University of Brawijaya, Veteran, Malang, Indonesia, 65145.

70% are due to lumen occlusion [10]. Thus, high-intensity physical activity increases the risk of death from cardiovascular disease. Exercise with the intensity of 70-90% MHR (maximal heart rate) or physical activity 6-9 MET, such as running, cycling, aerobics, and tennis competitions [11].

In the status quo, Circulating Endothelial Cells (CEC) level measurement is believed to be able to show endothelial injury and damage [12]. CEC are mature cells detached from the intima layer in response to endothelial injury; It is a distinct cell population from endothelial progenitor cells (EPCs). Endothelial cells line the vascular intima, attached to the basement membrane. In a healthy condition, these cells remain in place; however, in pathological conditions where endothelial damage occurs, it can cause endothelial cells to be released into the bloodstream. While vascular damage happens, CEC will be released into the bloodstream, so CEC and EPC are diagnostic biomarkers of endothelial dysfunction. The CD146 and CD31 markers are the most commonly used markers to detect CEC specificity [13]. As unipotent cells, Endothelial progenitor cells (EPCs) are clonogenic and proliferative and can differentiate into mature endothelial cells to replace vascular endothelium that undergoes necrosis or apoptosis. In addition, EPCs play an essential role in the reendothelialization of damaged blood vessels [14] and contribute to clinically significant vascular repair [15]. EPCs are single-nucleated cells with the marker molecule CD34, a glycoprotein that mediates stem cell attachment to the bone marrow extracellular matrix, and CD 133, a stem cell marker glycoprotein [16]. Measurement of CEC and EPC is vital for assessing endothelial injury and its repair [17]. Endothelial cell damage disrupts the balance between vasodilation and vasoconstriction, initiating several processes by decreasing NO production or activity [18].

The result of a previous study done by *Sapp et al.* [17] shows that acute exercise done at moderate and high intensity does not change the level of CEC in the body. On the other hand, according to Kourek *et al.* [19], who analyzed heart failure samples, high-intensity interval training (HIIT) increased the number of EPCs. This result is supported by the research done by Ribeiro *et al.* [20], where high-intensity acute aerobic exercise and high-intensity resistance exercise (80% VO2 max) are known to increase the number of EPC immediately after exercise. The EPC level peaked 6 hours after the exercise but decreased after 24 hours. Other studies have shown that moderate-intensity exercise does not reduce NO, while high-intensity exercise reduces NO [21]. At the same time, the research of Souza *et al.* [14] proved that ten weeks of moderate to vigorous physical activity (MVPA) significantly increased the number of EPCs in healthy children and may be associated with increased NO levels. Lastly, according to *Djindjić et al.* [22], the relationship between CEC, EPC, and the occurrence of endothelial dysfunction after high-intensity exercise is still unclear.

This study aims to determine the relationship between CEC, EPC, and the occurrence of endothelial dysfunction. Early detection of endothelial dysfunction after high-intensity exercise has clinical significance, especially as an effort to prevent the development of endothelial dysfunction in the human body.

MATERIALS AND METHODS

Animals and training protocol

All research procedures were approved by the Ethics Committee of Faculty Medicine, Universitas Brawijaya, Malang, Indonesia. This experiment used a randomized sample of twenty-weeks-old male Wistar rats divided into two groups. The first group, or the control group, was given low-intensity exercise with a running speed of 5-8 $m.min^{-1}$. The second group, or the treatment, was given high-intensity exercise (HIE) with a speed of 27-30 $m.min^{-1}$. All the rats used in this experiment are in good condition, proven by body conditioning score > 3 and weight of about 140–160 g. The rats were kept under the same condition in the Experimental Animal Center of the Faculty of Sport Science, Malang University. Every cage used has a partition so that it can hold two rats. The cages are conditioned with approximately 24℃ room temperature, humidity maintained at 79%–86%, a regular light cycle (12:12 h of light and dark), and Br 1 standard feed with a dose of 40 $g.day^{-1}$. The feeding is measured in order to achieve rats with normal body weight. The composition contains 20% crude protein, 5% crude fat, a maximum of 3-5% crude fiber, 1% calcium, 5% ash, 6% phosphor, and 3000 $kcal.kg^{-1}$ energy; tap water is freely accessible, and all experimental environments reached specific pathogen-free.

ISSN. 2087-2852
E-ISSN. 2338-1655

The rats were trained on a treadmill, consisting of 6 tracks, with a track length of 45 cm, a track speed of 25-30 m.min^{-1}, a shock voltage of 50 volts, a frequency of 3 Hz, for 12 weeks intervention, 3 times a week and 45-60 min each time. The treadmill inclination of each training group was 0. After the experiment, the rats were euthanized, whole blood was withdrawn from its heart. This study protocol has an ethical clearance from the Health Research Ethics Committee of medicine faculty Brawijaya University, Malang (No.153/EC/KEPK-S3/06/2022, approved on 15 June 2022).

Flowcytometry analysis

Protein expression was isolated from blood and measured using Flowcytometry analysis. The measurement of the number of circulating endothelial cells (CEC); Cell surface marker (CD45-CD146). Antibody cell surface marker (a) Anti-Human CD45 FITC (Biolegend), (b) Anti-Human CD146 PE (Biolegend). The measurement of the number of endothelial progenitor cells (EPC); Sel surface marker (CD34-CD133). Antibody cell surface marker (a) Anti-Human CD34 FITC (Biolegend), (b) Anti-Human CD133 PE (Biolegend).

Analysis of biochemical parameters

NO was tested using the Enzymatic Assay Nitric Oxide (Nitrate/Nitrite) kit or *Enzyme-Linked Immunosorbent Assay* (ELISA) kit, Bioassay Technology Laboratory, China. The test method is based on the measurement of the total sample of nitrite using the Griess Reagent. Prepared reagents: microplate, sample dilution buffer, standard nitrate, reductase nitrate. Buffer reductase nitrate, NADH, reagent A (sulfonamide in 3N HCl) and reagent B (N-(1-Naphthyl) ethylenediamine dihydrochloride in H_2O).

Statistical Analysis

All data is processed using statistical evaluations, namely the normality and homogeneity test, followed by correlation analysis. The statistical significance value was set at $p < 0.05$. All data is processed using the SPSS software.

RESULTS

Change of EPC in the Peripheral Blood Mononuclear Cells (PBMC)

We used Flowcytometry to detect the expression of EPC with marker CD 34 and CD 133 in the PBMC of rats (Fig. 1). The results showed that high-intensity exercise did not significantly reduce EPC expression. It was indicated by the value of sig.2tailed (0.251) > 0.05. However, from the mean value, it appears that there is a decrease of 6.625% in the number of EPCs (Fig. 2).

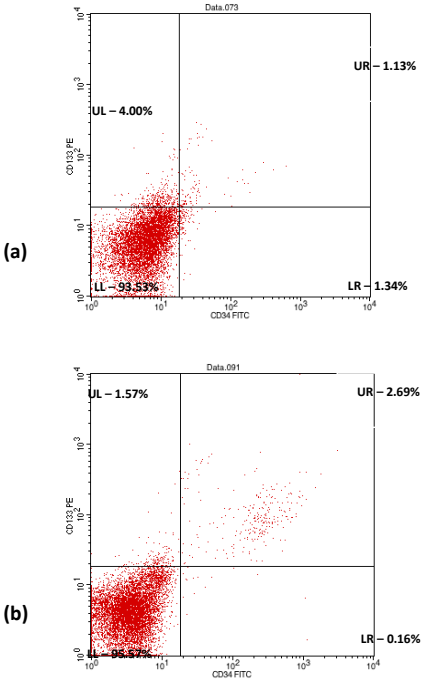

Figure 1. Flowcytometry analysis result of EPC measurement after high intensity (a) and low intensity exercise (b)

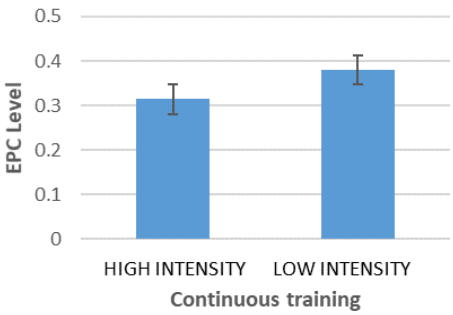

Figure 2. Effects of low intensity and high-intensity continuous training on EPC expression in rats. Rats Wistar were trained on the treadmill with low and high intensities for 12 weeks.

Change of CEC in the Peripheral Blood Mononuclear Cells (PBMC)

We used Flowcytometry to detect the expression of CEC with marker CD 146 and CD 45 in the PBMC of rats. The data analysis shows that high-intensity exercise for 12 weeks increases the number of CEC, but the increase is insignificant. This relationship is shown by the value of sig.2tailed (0.325) > 0.05. However, from the mean value, there appears to be an increase in CEC number, as much as 5.874% (Fig. 3).

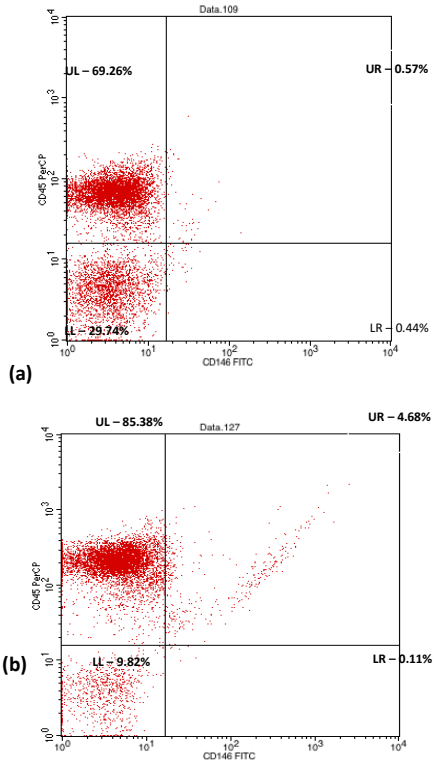

Figure 3. CEC level after high intensity exercise (a) and low intensity exercise (b) using flowcytometry

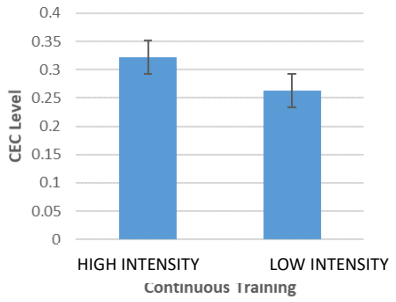

Figure 4. Effects of high-intensity continuous training on CEC expression in rats. Wistar rats were trained on the treadmill with low-intensity and high-intensity exercise for 12 weeks. After training, the expression of CEC and CEC in PBMC were analyzed using Flowcytometry. CEC expression increased.

Change of NO in the Peripheral Blood Mononuclear Cells (PBMC)

Nitric Oxide (NO) is produced by endothelial cells, as the main mediator and marker for endothelial function, including NO metabolites (nitrate/nitrite). Based on the mean value, there is a difference in NO levels in each group. In the high-intensity exercise group, the NO levels were lower (61.7570 mol.L^{-1}) than in the low-intensity exercise group (71.3295 mol.L^{-1}). While high-intensity exercise affects decreasing NO levels, the decrease is insignificant. It is indicated by the value of Sig.2 tailed (0.160) > 0.05 (Fig. 5).

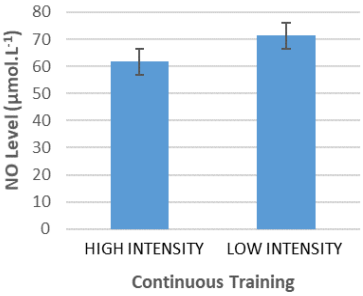

Figure 5. Effects of high-intensity continuous training on NO in rats. Wistar rats were trained on the treadmill with low-intensity and high-intensity exercise for 12 weeks. The level of NO decreased in high-intensity exercise with $p > 0.05$.

Relationship between CEC, EPC and the Occurrence of Endothelial Dysfunction (NO) after Strenuous Exercise

Based on the correlation test, this study uncovers the relationship of CEC and EPC expression on the occurrence of endothelial dysfunction (NO) after high-intensity exercise, with the value of Sig (2-tailed) (0.000), p <0.05. CEC and EPC expression is not significantly related to the occurrence of endothelial dysfunction (NO) after high-intensity exercise, with a value of Sig. (0.111) ; $p > 0.05$, and the relationship value is r = 0.414 (R^2= 17.15%). The regression test results between the number of CEC and EPC after high-intensity exercise with the occurrence of endothelial dysfunction (NO) obtained an R^2 value of 17.15%. The remaining 82.85% was caused by factors other than high-intensity exercise (Fig. 6).

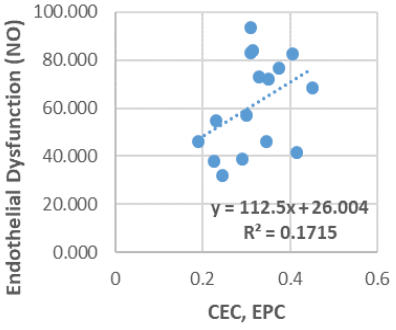

Figure 6. Regression test after high intensity exercise

DISCUSSION

The results show that high-intensity exercise does not significantly reduce EPC expression and does not increase CEC expression significantly. While the expression of CEC and EPC had a significant effect on the occurrence of endothelial dysfunction (NO), the expression of CEC and EPC was not significantly related to the occurrence of endothelial dysfunction (NO) after high-intensity exercise.

Exercise is one example of the many physical stressors that can cause changes in the human body's regulation system. It activates the inflammation signal, increasing the number of leukocytes and induces the proinflammatory cytokines, namely IL-1 and TNF alpha. Exercise affects the hypothalamus-pituitary-adrenal axis, which regulates cortisol secretion as a stress hormone [23]. Prolonged endurance exercise promotes oxidative stress in humans [24]. Damage to the endothelial cell membrane and the integrity of the endothelial monolayer in response to high-intensity exercise stress is thought to affect decreased vascular function.

By measuring peripheral blood CEC—a biomarker of endothelial damage or injury released from the monolayer—, this study can view impaired endothelial cell integrity, an essential marker of endothelial dysfunction. Exercise intensity plays an important role in changes in vascular excitability that affect endothelial function [17]. After the experiment, it was found that CEC levels increased slightly after 12 weeks of high-intensity exercise, indicating that there was no shedding of the endothelial monolayer during exercise. The number of CECs reflects the extent of endothelial injury, where high cell counts have been observed in diseases with extensive vascular damage. Elevated CEC counts are also associated with vascular damage to the blood. Increasing the number of CECs to predict or as a risk factor for future vascular disease events [25].

Endothelial cells can be activated by various stimuli, such as pro-inflammatory cytokines, growth factors, infectious agents, lipoproteins, or oxidative stress. Irreversible loss of endothelial lining integrity leads to endothelial cell release via apoptotic and necrotic mechanisms [26]. CEC level in the body reflects endothelial damage; exposure to risk factors can lead to endothelial cell release and increased levels of CEC in the blood. In in vitro studies, CEC significantly inhibited the proliferation, migration, and expression of eNOS in EPCs, possibly impairing vascular repair's functional capacity. An increase in EPC will offset a decrease in CEC; the decrease in EPC by CEC does not occur universally. Otherwise, the presence of vascular injury will never heal [8].

The mechanism of CEC detachment involves multiple factors, such as mechanical injury, changes in endothelial or sub endothelial cellular adhesion molecules, breakdown of bonds with matrix anchoring proteins, and cell apoptosis with decreased function of cytoskeletal proteins. The number of CECs is associated with conditions of endothelial dysfunction, as evidenced by the findings that there is an inverse relationship between CEC and NO [13]. This study's results differ from those of a study conducted by Sapp *et al.* [17], where the amount of CEC did not change after 30 minutes of high-intensity interval acute exercise. It may be due to differences in the sample used and the duration of the intervention, where 12 weeks of training might have already built adaptation.

In the EPC population, high-intensity exercise decreased CD34 or CD133 compared to the control group, but the decrease was insignificant. The EPC population plays the maintenance of endothelial integrity, where EPCs are exercise-responsive cells. Exercise has a significant role in the repair and maintenance of blood vessels through the mobilization of EPC cells; the clinical condition and exercise modality influence the degree of EPC mobilization, and the magnitude of EPC increases [15]. Decreased peripheral blood EPCs have been associated with endothelial dysfunction and high cardiovascular risk [27].

After 12 weeks of high-intensity exercise, NO levels decreased. Decreased NO synthesis and bioavailability are indicators of the development of endothelial dysfunction. NO, as a major factor of endothelial-dependent vasodilation, considered the most important marker of endothelial function, has a short half-life. Hence, plasma levels of the oxidative degradation products of NO, namely nitrite (NO2-), nitrate (NO3-), and nitrosothiol, were used as indexes. Substitute for NO [5]. NO is a labile inert gas, has a short half-life of less than 1 minute, and will react quickly with free radicals derived from oxygen, especially superoxide anion (O2-). NO acts locally and reacts immediately with water and oxygen to form nitrite and nitrate. NO is produced and degraded very dynamically in endothelial cells

ISSN. 2087-2852
E-ISSN. 2338-1655

[4]. Plasma levels of NO derivatives (nitrosyl/nitroso species) decrease in conditions of endothelial dysfunction [7].

This study has proven that there is no relationship between the expression of CEC, EPC cells, and the occurrence of endothelial dysfunction (NO). This result might be caused by using different measuring instruments while calculating the CEC, EPC, and NO levels. Furthermore, the result may be caused by the length of the experiment, which was done 90 days, where there is a possibility that the rats have grown adaptive to the high-intensity exercise. EPC stem cells originate from the bone marrow, regulated by the vascular endothelial growth factor receptor (VEGFR), enzymes, ligands, surface receptors, and blood flow. During high-intensity exercise, reperfusion ischemia occurs, which is the most potent stimulus and increases EPC expression [28]. Exercise can modify the expression of endothelial cells through a mechanical transduction system through increased shear stress on the endothelial surface, which distorts the monolayer cells. A stable rhythmic flow during exercise increases membrane instability to initiate the process of mitogen-activated protein kinase (MAPK) activation in cells [29]. EPC mobilization from bone marrow to circulation is influenced by eNOS activity and NO bioavailability. In this study, ROS production increased, the possibility of peroxynitrite also increased, and eNOS uncoupling occurred, thereby inhibiting the mobilization of EPC expression, ROS production increased, the possibility of increasing apoptotic/necrotic cells so that the number of CECs increases [26].

EPC mobilization after high-intensity exercise due to shear stress and ischemia/ hypoxia conditions. Shear stress appears to increase endothelial nitric oxide (NO) synthase activity and NO production, contributing to the increased number and activity of EPCs. Ischemia/hypoxia may be related to the upregulation of stromal cell-derived factor 1 and vascular endothelial growth factor (VEGF), increasing the proliferative and migratory capacity of circulating EPCs [30]. Oscillatory shear stress leads to pro-inflammatory endothelial activation with increased monocyte adhesion and endothelial cell apoptosis. Injured endothelial cells release inflammatory mediators, causing a decrease in endothelial function [31], as evidenced by decreased NO levels.

CONCLUSION

In summary, this study proves a relationship between CEC, EPC, and the occurrence of endothelial dysfunction by measuring NO. Similar research must be done with better methods and the same measuring instrument.

Acknowledgments

The authors thank the Institute for Research and Community Service (LP2M), the State Malang University of Malang, as this research was supported. The authors thank the participating technicians of Biomedic Laboratories, State Brawijaya University of Malang, Indonesia, and participating technicians of Sport Science Laboratory and the Biology Laboratory, State University of Malang.

REFERENCES

[1] Chacon, D., B. Fiani. 2020. A review of mechanisms on the beneficial effect of exercise on atherosclerosis. *Cureus.* 12(11). e11641.

[2] Cahill, P.A., E.M. Redmond. 2016. Vascular endothelium - gatekeeper of vessel health. *Atherosclerosis.* 248. 97–109. DOI: 10.1016/j.atherosclerosis.2016.03.007.

[3] Cai, H., D.G. Harrison. 2000. Endothelial dysfunction in cardiovascular diseases: the role of oxidant stress. *Circ. Res.* 87(10). 840–844.

[4] Mudau, M., A. Genis, A. Lochner, H. Strijdom. 2012. Endothelial dysfunction: the early predictor of atherosclerosis. *Cardiovasc. J. Afr.* 23(4). 222–231.

[5] Park, K.H., W.J. Park. 2015. Endothelial dysfunction: Clinical implications in cardiovascular disease and therapeutic approaches. *J. Korean Med. Sci.* 30(9). 1213–1225. DOI: 10.3346/jkms.2015.30.9.1213.

[6] Piepoli, M.F., A.W. Hoes, S. Agewall, C. Albus, C. Brotons, A.L. Catapano, *et al.* 2016. 2016 European guidelines on cardiovascular disease prevention in clinical practice. *Eur. Heart J.* 37(29). 2315–2381.

[7] Gimbrone, M.A., G. García-Cardeña. 2016. Endothelial cell dysfunction and the pathobiology of atherosclerosis. *Circ. Res.* 118(4). 620–636.

[8] Boff, W., A.M. da Silva, J.B. Farinha, J. Rodrigues-Krause, A. Reischak-Oliveira, B. Tschiedel, *et al.* 2019. Superior effects of

high-intensity interval vs. moderate-intensity continuous training on endothelial function and cardiorespiratory fitness in patients with Type 1 Diabetes: A randomized controlled trial. *Front. Physiol.* 10. 450. DOI: 10.3389/fphys.2019.00450.

[9] O'Keefe, J.H., H.R. Patil, C.J. Lavie, A. Magalski, R.A. Vogel, P.A. McCullough. 2012. Potential adverse cardiovascular effects from excessive endurance exercise. *Mayo Clin. Proc.* 87(6): 587–595.

[10] Harmon, K.G., I.M. Asif, J.J. Maleszewski, D.S. Owens, J.M. Prutkin, J.C. Salerno, *et al.* 2015. incidence, cause, and comparative frequency of sudden cardiac death in National Collegiate Athletic Association athletes: A decade in review. *Circulation.* 132(1). 10–19.

[11] Norton, K., L. Norton, D. Sadgrove. 2009. Position statement on physical activity and exercise intensity terminology. *J. Sci. Med. Sport.* 13. 496–502.

[12] Erdbruegger, U., M. Haubitz, A. Woywodt. 2006. Circulating endothelial cells: A novel marker of endothelial damage. *Clinica Chimica Acta.* 373(1–2). 17–26.

[13] Farinacci, M., T. Krahn, W. Dinh, H.D. Volk, H.D. Düngen, *et al.* 2019. Circulating endothelial cells as biomarker for cardiovascular diseases. *Res. Prac. Thromb. Haemost.* 3(1). 49.

[14] Victorino, L., F. De Meneck, V. Oliveira, E. Higa, E. Akamine, M. Franco. 2019. Beneficial impact of moderate to vigorous physical activity program on circulating number and functional capacity of endothelial progenitor cells in children: the crucial role of nitric oxide and VEGF-A. *Pediatr. Exerc. Sci.* 31(3). 322–329.

[15] Ferentinos, P., P. Ferentinos, C. Tsakirides, M. Swainson, A. Davison, M. Martyn-St James, T. Ispoglou, e*t al.* 2022. The impact of different forms of exercise on circulating endothelial progenitor cells in cardiovascular and metabolic disease. *Eur. J. Appl. Physiol.* 122(4). 815–860.

[16] Incalza, M.A., R. D'Oria, A. Natalicchio, S. Perrini, L. Laviola, F. Giorgino. 2018. Oxidative stress and reactive oxygen species in endothelial dysfunction associated with cardiovascular and metabolic diseases. *Vascul. Pharmacol.* 100. 1–19.

[17] Sapp, R.M., W.S. Evans, L.E. Eagan, C.A. Chesney, E.M. Zietowski, S.J. Prior, *et al.* 2019. The effects of moderate and high-intensity exercise on circulating markers of endothelial integrity and activation in young, healthy men. *J. Appl. Physiol.* 127(5). 1245–1256.

[18] Khosravi, M., A. Poursaleh G. Ghasempour, S. Farhad, M. Najafi. 2019. The effects of oxidative stress on the development of atherosclerosis. *Biol. Chem.* 400(6). 711–732.

[19] Kourek, C., M. Alshamari, G. Mitsiou, K. Psarra, D. Delis, V. Linardatou, *et al.* 2021. The acute and long-term effects of a cardiac rehabilitation program on endothelial progenitor cells in chronic heart failure patients: comparing two different exercise training protocols. *Int. J. Cardiol. Heart Vasc.* 32. 100702.

[20] Ribeiro, F., I.P. Ribeiro, A.C. Gonçalves, A.J. Alves, E. Melo, R. Fernandes, *et al.* 2017. Effects of resistance exercise on endothelial progenitor cell mobilization in women. *Scientific Reports.* 7(1). 1–9.

[21] Fang, Y., W. Ying, C. Yu, X. Daliao, S. Lijun. 2019. Impact of moderate- and high-intensity exercise on the endothelial ultrastructure and function in mesenteric arteries from hypertensive rats. *Life Sci.* 222. 36–45.

[22] Djindjić, B.J., Z.L. Radovanović, T. Kostić, N.M. Djindjić, M.V. Lazović. 2017. The Changes of Oxidative Stress and Endothelial function biomarkers after 6 weeks of aerobic physical training in patients with stable ischemic coronary disease. *Vojnosanit Pregl.* 74(11). 1060–1065.

[23] Huldani, I. Pattelongi, M.N. Massi, I. Idris, A. Bukhari, A.D.W. Widodo, *et al.* 2020. Cortisol, IL-6, TNF Alfa, Leukocytes and DAMP on Exercise. *Sys. Rev. Pharm.* 11(6). 474–485.

[24] Powers, S.K., R. Deminice, M. Ozdemir, T. Yoshihara, M.P. Bomkamp, H. Hyatta, *et al.* 2020. Exercise-induced oxidative stress: friend or foe? *J. Sport Health Sci.* 9(5). 415–425.

[25] Erdbruegger, U., A. Dhaygude, M. Haubitz, A. Woywodt. 2010. Circulating Endothelial Cells: Markers and Mediators of Vascular Damage. *Curr. Stem Cell Res. Ther.* 5(4). 294–302.

[26] Pober, J.S., W. Min, J.R. Bradley. 2009. Mechanisms of endothelial dysfunction, injury, and death. *Annu. Rev. Pathol. Mech. Dis.* 4. 71–95.

ISSN. 2087-2852
E-ISSN. 2338-1655

[27] Koutroumpi, M., S. Dimopoulos, K. Psarra, T. Kyprianou, S. Nanas 2012. circulating endothelial and progenitor cells: Evidence from acute and long-term exercise effects. *World J. Cardiol.* 4(12). 312.
[28] Green, D.J., K.J. Smith. 2018. Effects of exercise on vascular function, structure, and health in humans. *Cold Spring Harb. Perspec. Med.* 8(4). a029819.
[29] van Agtmaal, E.L., R. Bierings, B.S. Dragt, T.A. Leyen, M. Fernandez-Borja, A.J.G. Horrevoets, J. Voorberg. 2012. The shear stress-induced transcription factor KLF2 affects dynamics and angiopoietin-2 content of weibel-palade bodies. *PLOS ONE* 7(6). e38399. DOI: 10.1371/journal.pone.0038399.
[30] Kourek, C., E. Karatzanos, K. Psarra, K. Ntalianis, G. Mitsiou, D. Dells, et al. 2021. Endothelial progenitor cells mobilization after maximal exercise in patients with chronic heart failure. *Hell. J. Cardiol.* 62(1). 70–72.
[31] Theofilis, P., M. Sagris, E. Oikonomou, A.S. Antonopoulos, G. Siasos, C. Tsioufis, D. Tousoulis. 2021. Inflammatory mechanisms contributing to endothelial dysfunction. *Biomedicines.* 9(7). 781.

ISSN. 2087-2852
E-ISSN. 2338-1655

Piper betle L. Leaves Extract Potentially Reduce the Nitric Oxide Production on LPS-Induced RAW 264.7 Cell Lines

Dinia Rizqi Dwijayanti[1*], Sapti Puspitarini[2], Nashi Widodo[1]

[1]Department of Biology, Faculty of Mathematic and Natural Sciences, University of Brawijaya, Malang, Indonesia
[2]Study Program of Sains Education, Faculty of Mathematics and Natural Sciences, State University of Surabaya, Surabaya, Indonesia

Abstract

Chronic inflammation can lead to several diseases that represent the leading causes of mortality worldwide. Conventional treatment of inflammation can carry some risks. Therefore, research on herbal medicine that are suspected of having anti-inflammatory effects, such as *Piper betle* L., is important. This study aims to investigate the effect of *P. betle* L. extract on nitric oxide as a pro-inflammatory mediator. The dried leaves of *P. betle* L. were extracted by ethanol. RAW 264.7 cells were treated with LPS and *P. betle* L. extract (PBE). Nitric oxide was measured by the Griess method. Antioxidant activity was determined using 2,2–Diphenyl-1-picrylhydrazyl (DPPH) method. Total flavonoids and phenolic content were also identified by aluminium chloride and Folin–Ciocalteu colorimetric assay, respectively. This study demonstrated that the PBE has excellent NO suppression activity with the IC_{50} 56.22±16.41 $\mu g.mL^{-1}$, without cytotoxicity. PBE also has DPPH inhibitory concentration IC_{50} values of 279.67±11.36 ppm. Interestingly, PBE has a flavonoid content of 50.17±3.14 mg QE.g^{-1} and phenolic content of 128.92±1.2 mg GAE.g^{-1}. These compounds are thought to be responsible for its anti-inflammatory as well as antioxidant. This study proved that *P. betle* L. leaves extract could be used as a candidate for anti-inflammatory drugs. Nevertheless, further research about the biological activity mechanism and their bioactive compounds' purification is still required.

Keywords: Inflammation, lipopolysaccharide, Macrophage, Nitric Oxide, *Piper betle.*

INTRODUCTION

Inflammation is a natural process that occurs when the body's immune system responds to an irritant, such as an injury or infection. It is a key aspect of the body's immune defenses and plays a role in healing [1]. Although inflammation is a natural process that plays a role in healing, chronic inflammation can lead to several diseases that collectively represent the leading causes of disability and mortality worldwide. Inflammation may lead to chronic inflammation, which can contribute to the development of certain diseases, including autoimmune diseases like rheumatoid arthritis, cardiovascular diseases like high blood pressure and heart disease, gastrointestinal disorders like inflammatory bowel disease, lung diseases like asthma, mental illnesses like depression, metabolic syndrome, type 2 diabetes, cancer, arthritis, and bowel diseases like Crohn's disease and ulcerative colitis [2].

Nitric oxide (NO) is a signaling molecule that plays a key role in the pathogenesis of inflammation [3]. NO is synthesized and released into the endothelial cells with the help of NOSs that convert arginine into citrulline producing. NO gives an anti-inflammatory effect under normal physiological conditions, but it is a pro-inflammatory mediator that induces inflammation due to overproduction in abnormal situations [3]. Nitric oxide may amplify inflammation by altering the balance and increasing the proliferation of Th_2 lymphocytes [4]. The heme oxygenase-1/carbon monoxide pathway may mediate the protective role of localized nitric oxide production during inflammation [5]. Even in special conditions such as renal ischemia-reperfusion, it has been shown that high iNOS and low eNOS levels are involved in increased inflammation [6]. Therapeutic strategies for inhibiting inducible nitric oxide synthase have the potential for a novel class of anti-inflammatory [3].

Inflammation can be treated in several ways depending on the cause and severity. Some of these treatments include medication, lifestyle changes, and surgery. However, conventional treatment of inflammation can carry some risks, depending on the type of treatment and the individual's health status. Corticosteroids used to treat inflammation can cause side effects such as weight gain, high blood pressure, and increased risk of infection [7].

*Correspondence Address:
Dinia Rizqi Dwijayanti
E-mail : rd.dinia@ub.ac.id
Address : Dept. Biology, University of Brawijaya, Veteran Malang, 65145.

ISSN. 2087-2852
E-ISSN. 2338-1655

Biologics used to treat inflammatory conditions can also increase the risk of infection and may cause allergic reactions. In addition to the risks associated with specific treatments, chronic inflammation is associated with several diseases, such as cardiovascular disease, cancer, Alzheimer's disease, obesity, diabetes, and infectious diseases [7]. Several studies have shown a positive association between increased intake of dietary antioxidants and reduced risk for chronic inflammatory diseases. Antioxidants help to counteract oxidative stress, neutralizing excess free radicals to protect cells, prevent illness, and reduce inflammation [8].

Piper betle L. has been used for centuries in traditional medicine in South-East Asian countries to treat various health conditions due to its antioxidant properties [9]. The extract of *P. betle* L. leaves has been known to have anti-inflammatory, immunomodulatory, and antioxidant effects [9-12]. The plant contains numerous phytochemicals, including alkaloids, tannins, glycosides, reducing sugars, and saponins, depending on its botanical origin and the solvent used for extraction [13]. Some phenylpropanoids isolated from *P. betle* L. have in vitro anti-inflammatory activities [14]. However, the anti-inflammatory mechanism of this plant, especially regarding the suppression of NO, has yet to be widely studied. Thus, this study aims to investigate the effect of *P. betle* L. extract on the nitric oxide produced by LPS-induced RAW 264.7 cell lines.

METHODS

Plant material and extraction

The dried leaves of *P. betle* L. were purchased from Balai Materia Medica, Batu, Malang, Indonesia. The dried leaves were extracted with 96% ethanol at a ratio of 1:10 (w/v) for 24 hours according to the maceration procedure and repeated five times. The *P. betle* L. ethanol extracts (PBE) were filtered and evaporated by a rotary evaporator (Bunchi R-114) at 60°C. It was diluted in DMSO for the following assay.

RAW Cell Culture 264.7 and treatment

The mouse macrophage cell line RAW 264.7 was purchased from American Type Culture Collection (ATCC; United States). The cells were seeded in 24-well plates with a density of $2x10^5$ cells.well^{-1} and incubated for 24 hours in a 5% CO_2 incubator at 37°C. The culture medium used was DMEM (D6429, Sigma Aldrich, Merck, German) enriched by 10 % fetal bovine serum (F2442, Sigma Aldrich, Merck, German) and 1 % penicillin (100 U.mL^{-1})/streptomycin (100 µg.mL^{-1}) (A5955, Sigma Aldrich, Merck, German). The cells were treated with or without 4 µg.mL^{-1} lipopolysaccharide (LPS; Sigma Aldrich, Merck, German) and the PBE (25, 50, 100 µg.mL^{-1}) for 24 h.

Determination of nitric oxide production

The RAW 264.7 cells were treated with or without LPS and PBE at 37°C for 24 h. The nitrite levels in the culture medium were measured by Griess modified reagent from Sigma Aldrich (G4410). As much as 75 µL of the medium or sodium nitrite ($NaNO_2$) as standard was reacted with 75 µL of Griess reagent in a 96-well plate for 5 min at room temperature, and the microplate reader measured the absorbance at 571 nm. The experiment was repeated thrice with different passage number cells to determine NO inhibition's half-maximal inhibitory concentrations (IC_{50}).

Cell viability assessment

After the NO assay, the RAW 164.7 cell culture medium was replaced with a new medium containing WST-1 reagent (Roche; 11644807001). It was then incubated for 20 in a 5% CO_2 incubator at 37°C. After 20 min, 100 µL of media was transferred to a 96-well plate and then the absorbance at 450 nm was measured by a microplate reader.

Free radical scavenging activity assay

Antioxidant activity was determined using 2,2–Diphenyl-1-picrylhydrazyl (DPPH) method. In 96-well plates, 100 L of PBE was mixed with 100 L of 0.4 mM DPPH. After 30 min, absorbance was measured by microplate reader at 490 nm. Equation (1) was used to alter the proportion of inhibition of scavenging action. Using Equation (2), the IC_{50} value was determined from linear regression of the antioxidant chart.

$$\%\ \text{scavenging of DPPH:}\frac{(\text{Abs control} - \text{Abs extract})}{\text{Abs control}}\ x\ 100\% \quad (1)$$

$$Y = ax + b, where\ Y = 50\%; X = IC50\ dose \quad (2)$$

Total flavonoids content

The total flavonoid content (TFC) of *P. betle* L. was calculated using aluminium chloride ($AlCl_3$) methods, with Quercetin as the standard. The 10 µL of $AlCl_3$ (10% w/v) and 50 µL of PBE or Quercetin were mixed, followed by 150 µL of 96% ethanol. Then, 10 µL of 1M CH_3COONa was added and incubated for 40

ISSN. 2087-2852
E-ISSN. 2338-1655

min at room temperature in the dark. A microplate reader was used to detect absorbance at 405 nm. The TFC was obtained by calculating the absorbance value extract with the standard curve equation ($y= 0.0023x + 0.0583$, $R^2 = 0.9992$) of 0–100 µg.mL^{-1} Quercetin. The TFC was expressed in milligrams of quercetin equivalents (QE) per gram dry extract weight (QE.g^{-1}).

Total phenolic assay

The total phenolic content (TPC) was identified using the Folin–Ciocalteu colorimetric assay with Gallic acid functioning as the standard. The 100 µL of PBE or Gallic acid was mixed with 1.0 mL of the Folin-Ciocalteu reagent. After 5 min, 1.0 mL of Na_2CO_3 (7.5% w/v) was added, then incubated for 90 min at room temperature in the dark. The total phenolic content was determined by a spectrophotometer at 725 nm. The TPC was obtained by calculating the absorbance value extract with the standard curve equation ($y = 0.0042x + 0.0246$, $R^2 = 0.9974$) of gallic acid (0–50 µg.mL^{-1}). The TPC was expressed in milligrams of gallic acid equivalents per gram dry extract weight (GAE.g^{-1}).

Statistical Analysis

The data presented in the figures and tables are representative of at least three independent experiments from different passages of the cell lines that yielded similar results. The values are presented as the means ± standard deviation (SD). The differences were analyzed using Student's t-test. The statistical significance was set at $p < 0.05$ and $p < 0.01$.

RESULTS AND DISCUSSION

***Piper betle* L. Leaves Extract Suppressed the NO Production in RAW 264.7 Cell Line**

We examined the effect of PBE on NO production in LPS-induced RAW 264.7 cells. This study demonstrated that PBE dose-dependently suppressed the levels of NO production in LPS-induced RAW 264.7 cells (Fig. 1). Furthermore, the half-maximal inhibitory concentrations (IC_{50}) were determined to know the potency of PBE in inhibiting NO production. PBE demonstrated excellent NO suppression activity, with IC_{50} values 56.22±16.41 µg.mL^{-1}. The previous study conducted on rats with arthritis supported these findings that showed the PBE was able to reduce inflammation in the rats by down-regulate the transcription of iNOS, which leads to the decreased generation of reactive nitrogen species [11]. Another study also found that the anti-inflammatory and anti-arthritic activity of *P. betle* L. is attributable to its ability to down-regulate the generation of reactive nitrogen species [9]. It means that *P. betle* L. can be used as a candidate for anti-inflammatory drugs with the specific target of inhibiting NO production during inflammation conditions.

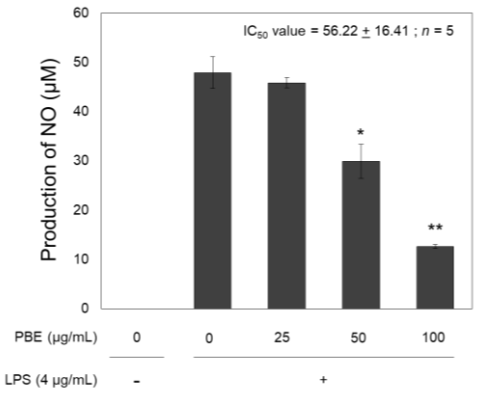

Figure 1. *Piper betle* L. ethanol extract (PBE) suppresses nitric oxide (NO) production in LPS-induced RAW 264.7. The RAW 264.7 cells were treated with LPS and PBE for 24 h. The NO levels in the medium were measured in triplicate and are shown as a means ± standard deviation (SD). * $P < 0.05$ and ** $P < 0.01$ versus LPS alone.

Cell viability after PBE exposure

The cell viability assessment was used to ensure that the reduction of NO by PBE was not caused by cell death. As shown in Figure 2, the number of viable cells after LPS and PBE exposure was more than 80% which means that the selected dose range of PBE in this study has no toxicity to RAW 264.7 cells. Previous studies used the brine shrimp lethality assay to evaluate the cytotoxic activity of the methanol, ethanol, and crude aqueous extracts of PBE. The study found that the methanol and ethanol extracts have cytotoxic effects on the brine shrimp at respectively doses 23.65 µg.mL^{-1} and 85.50 µg.mL^{-1} [15]. It means that PBE was highly toxic (LC_{50} 0-100 µg.mL^{-1}) in shrimp.

Nevertheless, the study conducted on rats has shown that PBE does not cause any explicit indication of toxicity, hepatotoxicity, nephrotoxicity, or any adverse side effects after administration of a highly potent dosage of 1500 mg.kg^{-1} BW. It also does not exert any physical sign of toxicity, stress, or aversive behaviors on rats [16]. Another study found that PBE did not cause toxicity in Wistar rats [17]. Overall, the available studies, including this study, suggest that PBE is safe and does not

cause any significant toxicity at the recommended doses. Thus, PBE is suspected to be effective and safe as an anti-inflammatory drug candidate.

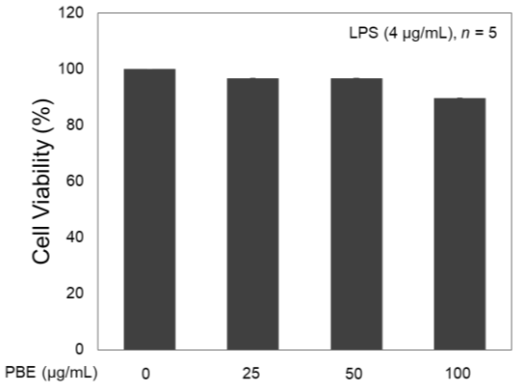

Figure 2. The viability of cells after LPS and PBE exposure was assessed by WST-1 assay. The RAW 264.7 cells were treated with LPS and/or PBE for 24 h. The concentration of 0 µg.mL^{-1} (LPS alone group) was set to have 100% viable cells. The number of viable cells in the other groups was compared to the LPS alone group.

DPPH radical scavenging activity of PBE

Furthermore, we examined the DPPH radical scavenging activity of PBE to find out the radical-scavenging activity of PBE. DPPH-H has a lower absorbance than DPPH because of the lower amount of hydrogen. Thus, the color of the DPPH reagent changed from purple to yellow. Figure 3 shows the DPPH radical scavenging activity of the PBE—the percentage inhibition of free radicals by PBE due to hydrogen donation from the antioxidant. PBE has DPPH inhibitory concentration IC_{50} values of 279.67 ± 11.36 ppm (Table 1). This DPPH radical scavenging activity supported previous research about the antioxidant activity of PBE. Several studies proved that the leaves of *P. betle* L. have been shown to have a higher amount of antioxidant activity, and the ethanol and methanolic extracts of the leaves have been shown to have significant antioxidant activity [17,18].

Table 1. Total flavonoid and Total phenolic of PBE

Assay	Value
DPPH (ppm)	279.67 ± 11.36
TFC (mgQE.g^{-1})	50.17 ± 3.14
TPC (mgGAE.g^{-1})	128.92 ± 1.20

Notes: The data were expressed as mean ± standard deviation (*n* = 3). DPPH: 2,2–Diphenyl-1-picrylhydrazyl, TFC: Total Flavonoid Content, TPC: Total Phenolic Content.

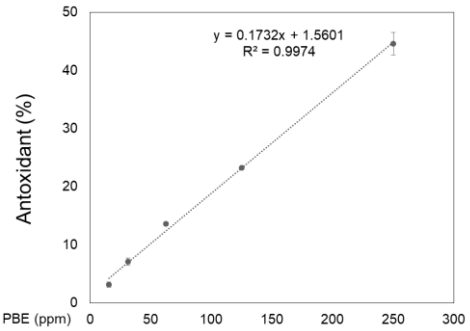

Figure 3. DPPH radical scavenging activity of PBE. The IC_{50} value was determined from linear regression of the antioxidant chart.

Total Flavonoid and Phenolic Content of PBE

Table 1 shows that PBE has a flavonoid content of 50.17 ± 3.14 mg QE.g^{-1} and phenolic content of 128.92±1.2 mg GAE.g^{-1}. The result of this study about TFC and TPC of PBE was supported by another study about *P. betle* L. *Piper betle* L. is a medicinal plant that contains a large number of bioactive compounds, such as tannins, flavonoids (Quercetin), eugenol, hydroxychavicol, chavibetol, chavicol, allylpyrocatechol, and cadinene [12,17,19,20]. The leaves of *P. betle* L. contain hydroxychavicol, eugenol, and gallic acid, which are highly bioactive compounds [12,21]. Twelve phenolic compounds were identified in *P. betle* L. leaves, including six flavonoid derivatives. Hydroxychavicol was the major compound in both aqueous and ethanol extracts, but the aqueous extract presented a greater diversity of compounds. The study also found that both extracts showed intense activity against both acetyl- and butyrylcholinesterase, which can be due, at least partially, to the phenolic composition [22].

Phenol, polyphenol, and tannin are compounds found in plants that have been found to suppress nitric oxide [12,17]. Phenolic compounds from herbal medicine have long been believed to have the potential to inhibit nitric oxide production [23]. Another study also found that polyphenols exert beneficial effects against vascular diseases by restoring the impairment of nitric oxide production [24]. To summarize, this study suggests that the phenol, polyphenol, and tannin content of PBE may be responsible for its anti-inflammatory and antioxidant effects through NO suppression activity.

CONCLUSION

This study demonstrated that the leaves of *P. betle* L. have excellent NO suppression

activity without showing any cytotoxicity to the LPS-induced RAW 264.7 cell line. This NO suppression activity may be associated with its antioxidant activity since this plant also showed DPPH radical scavenging activity. The active compounds from *P. betle* L., especially phenolic compounds and flavonoids, are thought to be responsible for their antioxidant and anti-inflammatory activity. Although *P. Betle* L. leaves extract can be used as a candidate for anti-inflammatory drugs, further research about the detailed mechanism of biological activity and purification of bioactive compounds is still required.

REFERENCES

[1] InformedHealth.org. 2018. What is an inflammation? Cologne, Germany: Institute for Quality and Efficiency in Health Care (IQWiG). Available at: https://www.ncbi.nlm.nih.gov/books/NBK279298/.

[2] Furman, D., J. Campisi, E. Verdin, P. Carrera-Bastos, S. Targ, C. Franceschi, *et al.* 2019. Chronic inflammation in the etiology of disease across the life span. *Nat. Med*. 25. 1822–1832. DOI: 10.1038/s41591-019-0675-0.

[3] Sharma, J.N., A. Al-Omran, S.S. Parvathy. 2007. Role of nitric oxide in inflammatory diseases. *Inflammopharmacology.* 15. 252–259. DOI: 10.1007/s10787-007-0013-x.

[4] Zamora, R., Y. Vodovotz, T.R. Billiar. 2000. Inducible nitric oxide synthase and inflammatory diseases. *Mol. Med.* 6. 347–373. DOI: 10.1007/BF03401781.

[5] Iwata, M., T. Inoue, Y. Asai, K. Hori, M. Fujiwara, S. Matsuo, *et al*. 2020. The protective role of localized nitric oxide production during inflammation may be mediated by the heme oxygenase-1/carbon monoxide pathway. *Biochem. Biophys. Rep*. 23. 100790. DOI: 10.1016/j.bbrep.2020.100790.

[6] Papi, S., F. Ahmadizar, A. Hasanvand. 2019. The role of nitric oxide in inflammation and oxidative stress. *Immunopathol. Persa*. 5(1).e08. DOI: 10.15171/ipp.2019.08.

[7] Damião, A.O.M.C., M.F.C. de Azevedo, A.S. Carlos, M.Y. Wada, T.V.M. Silva, F.C. Feitosa. 2019. Conventional therapy for moderate to severe inflammatory bowel disease: A systematic literature review. *World J. Gastroenterol*. 25(9). 1142-1157. DOI: 10.3748/wjg.v25.i9.1142.

[8] Roy, A., S. Das, I. Chatterjee, S. Roy, R. Chakraborty. 2022. Anti-inflammatory effects of different dietary antioxidants. In: Ekiert, H.M., K.G. Ramawat, J. Arora (Eds). Plant Antioxidants and Health. Reference Series in Phytochemistry. Springer, Cham. DOI: 10.1007/978-3-030-78160-6_20.

[9] Seo, J., U. Lee, S. Seo, A.A. Wibowo, O.B. Pongtuluran, K. Lee, S.B. Han, S. Cho. 2022. Anti-inflammatory and antioxidant activities of methanol extract of *Piper betle* Linn. (*Piper betle* L.) leaves and stems by inhibiting NF-κB/MAPK/Nrf2 signaling pathways in RAW 264.7 macrophages. *Biomed. Pharmacother*. 155. 113734. DOI: 10.1016/j.biopha.2022.113734.

[10] Alam, B., F. Akter, N. Parvin, P.R. Sharmin, S. Akter, J. Chowdhury, *et al*. 2013. Antioxidant, analgesic and anti-inflammatory activities of the methanolic extract of *Piper betle* leaves. *Avicenna J. Phytomed*. 3(2). 112-125.

[11] Ganguly, S., S. Mula, S. Chattopadhyay, M. Chatterjee, 2007. An ethanol extract of *Piper betle* Linn. mediates its anti-inflammatory activity via down-regulation of nitric oxide. *J. Pharm. Pharmacol*. 59(5). 711-8. DOI: 10.1211/jpp.59.5.0012.

[12] Aara, A., V. Chappidi, M.N. Ramadas. 2020. Antioxidant activity of eugenol in *Piper betle* leaf extract. *J. Fam. Med. Prim. Care*. 9(1). 327-331. DOI: 10.4103/jfmpc.jfmpc_809_19.

[13] Nayaka, N.M.D.M.W., M.M.V. Sasadara, D.A. Sanjaya, P.E.S.K. Yuda, N.L.K.A.A. Dewi, E. Cahyaningsih, Hartati, R. 2021. *Piper betle* (L): recent review of antibacterial and antifungal properties, safety profiles, and commercial applications. *Molecules*. 26(8). 2321. DOI: 10.3390/molecules26082321.

[14] Williams, L.A.D., E.A. Vasquez, P.P. Milan, C. Zebitz, W. Kraus. 2002. In Vitro anti-inflammatory and antimicrobial activities of phenylpropanoids from *Piper betle* L. (Piperaceae). In: Rauter, A.P., F.B. Palma, J. Justino, M.E. Araújo, S.P. dos Santos (Eds). Natural Products in the New Millennium: Prospects and Industrial Application. *Proc. Phytochem. Soc. Eur*. 47. DOI: 10.1007/978-94-015-9876-7_22.

[15] Del Socorro, M.M.L., C.P. Bendoy, C.M.L. Dacayana. 2014. Cytotoxic effects of betel vine, *Piper betle* Linn. leaf extracts using *Artemia salina* leach (Brine shrimp lethality assay). *J. Multidiscip. Stud*. 3(1). 100-111. DOI: 10.7828/jmds.v3i1.629.

[16] Azahar, N.I., N.M. Mokhtar, M.A. Arifin, 2020. *Piper betle*: a review on its bioactive compounds, pharmacological properties, and extraction process. *IOP Conf. Ser.: Mater. Sci. Engin.* 991. 012044. DOI: 10.1088/1757-899X/991/1/012044.

[17] Saravanan, R., P.N. Rajendra, K.V. Pugalendi. 2003. Effect of *Piper betle* leaf extract on alcoholic toxicity in the rat brain. *J. Med. Food*. 6(3). 261-265. DOI: 10.1089/10966200360716689.

[18] Dasgupta, N., B. De. 2004. Antioxidant activity of *Piper betle* L. leaf extract in vitro. *Food Chem.* 88(2). 219-224.

[19] Ghosh, K., T.K. Bhattacharya. 2005. Chemical constituents of *Piper betle* Linn. (Piperaceae) roots. *Molecules.* 10(7). 798-802. DOI: 10.3390/10070798.

[20] Shah, S.K., G. Garg, Jhade, Deenanath, N. Patel. 2016. *Piper betle*: Phytochemical, pharmacological and nutritional value in health management. *Int. J. Pharm. Sci. Rev. Res*. 38. 181-189.

[21] Nguyen, L.T.T., T.T. Nguyen, H.N. Nguyen, Q.T.P. Bui. 2020. Simultaneous determination of active compounds in *Piper betle* Linn. leaf extract and effect of extracting solvents on bioactivity. *Eng. Rep*. 2(10). e12246. DOI: 10.1002/eng2. 12246.

[22] Ferreres, F., A.P. Oliveira, A. Gil-Izquierdo, P. Valentão, P.B. Andrade. 2014. *Piper betle* leaves: profiling phenolic compounds by HPLC/DAD-ESI/MS(n) and anti-cholinesterase activity. *Phytochem. Anal.* 25(5). 453-460. DOI: 10.1002/pca. 2515.

[23] Conforti, F., F. Menichini. 2011. Phenolic compounds from plants as nitric oxide production inhibitors. *Curr. Med. Chem*. 18(8). 1137-1145. DOI: 10.2174/09298671 1795029690.

[24] Forte, M., V. Conti, A. Damato, M. Ambrosio, A.A. Puca, S. Sciarretta, *et al.* 2016. Targeting nitric oxide with natural derived compounds as a therapeutic strategy in vascular diseases. *Oxid. Med. Cell. Longev*. 2016. 7364138. DOI: 10.1155/2016/7364138.

ISSN. 2087-2852
E-ISSN. 2338-1655

The Effect of *Alpinia Purpurata* K. Schum Rhizome Extract Supplementation in Tris-Egg Yolk Extender on the Quality of Cryopreserved Bali Bull Sperm

Firlina Laila Putri[1], Sri Rahayu[2*], Agung Pramana Warih Marhendra[3]

[1]Master Program of Biology, Faculty of Mathematics and Natural Sciences, University of Brawijaya, Malang, Indonesia

[2,3]Department of Biology, Faculty of Mathematics and Natural Sciences, University of Brawijaya, Malang, Indonesia

Abstract

This study aimed to analyze the effect of *Alpinia purpurata* K. Schum rhizome extract (APRE) supplementation into tris-egg yolk extender on the sperm quality of Bali bull after freezing. This study used experimental method with a completely randomized design (CRD), consisting of five treatments, denoted as P_0 (semen diluted using 100% Tris-Egg Yolk (TEY)), P_1 (semen diluted using 98% TEY and 2% APRE), P_2 (semen diluted using 96% TEY extender + 4% APRE), P_3 (semen diluted using 94% TEY + 6% APRE), and P_4 (semen diluted using 92% TEY + 8% APRE). Semen quality was assessed both before and after freezing, using several indicators such as motility, viability, and abnormality of sperm. The antioxidant activity of RGE was determined using the DPPH (1,1-diphenils-2-picrylhydrazils) technique. The data were analyzed using ANOVA with further analysis using post hoc tests in the SPSS 25 program. The results showed that APRE has strong antioxidant activity, with an IC_{50} value 38.004 $\mu g.mL^{-1}$. Meanwhile, this research has shown that the addition of 6% RGE in the tris-Tris-egg yolk extender was able to maintain sperm quality before and after freezing.

Keywords: *Alpinia purpurata* K. Schum, sperm quality, tris-egg yolk.

INTRODUCTION*

The increasing demand for animal protein in Indonesia can be handled by increasing the number of livestock populations, including the Bali bull, because it is a good type of beef cattle, with a carcass percentage of around 51.22% [1]. It needs to be preserved as an Indonesian germplasm, as claimed by the Decree of the Minister of Agriculture No. 325/Kpts/OT.140/1/2010.

Artificial insemination (AI) is widely known as an effective method in reproductive biotechnology that could improve genetic quality and livestock populations. Cryopreservation of sperm is an essential technique in Artificial Insemination (AI). Cryopreservation is advantageous because sperm can be stored longer in liquid nitrogen [2]. However, the freezing and thawing process could damage the sperm cells, which leads to reduced quality [3].

During the cryopreservation process, it can cause a decrease in semen quality, including a decrease in the percentage of motility, viability and an increase in the percentage of spermatozoa abnormalities. During the semen dilution process, extreme changes in osmolarity occur due to the diluent used and cold shock to spermatozoa during the freezing process due to a drastic temperature drop below the freezing point of water [4]**.** When frozen semen is to be used, it is thawed again, where there is a drastic change in temperature from below 0 to 37°C. Extreme changes in temperature and osmolarity cause an increase in the metabolic activity of spermatozoa [5].

During the semen storage process, a diluent is needed, which contains energy for spermatozoa and protects spermatozoa so they survive during storage. One type of diluent that can be used by tris-egg yolk because the lipoprotein and lecithin content in egg yolk spermatozoa from cold shock, tris aminomethane functions as a buffer, raffinose and lactose as energy sources, and penicillin and streptomycin as antibiotics [6]. Tris-egg yolk extender can better maintain spermatozoa motility in sapera goats than skim milk [7].

The addition of plant-based ingredients containing antioxidants to semen diluent can maintain semen quality by reducing damage caused by free radicals. Red galangal rhizome (*Alpinia purpurata* K. Schum) is one of the vegetable ingredients that can be utilized because it contains high levels of antioxidants in the form of phenolic and flavonoid compounds [8]. The antioxidant activity of red

*Correspondence address:
Sri Rahayu
Email : srahayu@ub.ac.id
Address : Dept. Biology, University of Brawijaya, Veteran Malang, Malang 65145

galangal comes from quercetin, kaemferol, and galangin [9]. The red galangal extract's antioxidant activity is tested using the DPPH spectrophotometer method. It showed an IC_{50} value of 62.89 $\mu g.mL^{-1}$, indicating that red galangal extract has relatively strong antioxidant activity [10].

The content of flavonoids as antioxidants has been shown to reduce the effects of free radicals. The flavonoid content of peeling dragon fruits added to tris- egg yolk extender functions as an antioxidant to counteract free radicals. So, it can maintain the quality of ettawah crossbred ram frozen semen [11]. The antioxidant activity of flavonoid compounds contained in the n-hexane fraction of red galangal ethanol extract (FHEERL) can be affected the quality of spermatozoa by preventing excess activity of reactive oxygen species (ROS) produced through oxidative stress [12]. Based on previous research, it is necessary to carry out related research with the aimed to analyze the effect of *Alpinia purpurata* K. Schum rhizome extract (APRE) supplementation into tris-egg yolk extender on the sperm quality of Bali bull after freezing.

MATERIAL AND METHOD

Alpinia Purpurata Rhizome Ethanol Extract (APRE) Preparation

The simplicia powder of *Alpinia Purpurata* K. Schum Rhizome was obtained from UPT Herbal Laboratory of Materia Medica, Batu, East Java. The extraction process was performed at the Biochemical Laboratory of the Department of Chemistry, Brawijaya University. Simplicia powder was extracted with 70% ethanol at 25°C for three days. The solution was filtered using filter paper (Whatman no. 3), and the macerate formed was separated. Macerate was evaporated using a rotary evaporator at 60°C. The APRE was stored at 5°C until used [13].

DPPH Analysis of *Alpinia purpurata* Rhizome Extract

The DPPH (2,2-diphenil-1-picrylhydrazil) analysis was used to assess the antioxidant activity of APRE. The APRE was diluted using ethanol 70% at 10, 20, 30, 40 and 50 ppm. Afterward, 0.5, 1, 1.5, 2, and 2.5 mL of each solution were combined with 4.5, 4, 3.5, 3, and 2.5 mL of DPPH. The solution was incubated in a dark room for 30 minutes. Therefore, the sample was examined using a spectrophotometer with a wavelength of 517 nm [14].

The effect DPPH scavenging was calculated by the formula [15]:

$$\%\text{inhibition} = \frac{\text{blank absorbance} - \text{material absorbance}}{\text{blank absorbance}} \text{ x } 100$$

The IC_{50} value of the sample APRE is calculated from the linear regression curve between % absorption inhibition (y) to the concentration of the extract or the solution test (x), using the following formula:

$$\text{IC50} = \frac{50 - \text{a}}{\text{b}}$$

Description:
a = a constant
b = the coefficient of X

Tris -Egg Yolk Preparation

Tris-Egg Yolk extender was made by mixing 20% egg yolk in 2.5% raffinose solution, 0.9% citric acid, 1.6% tris aminomethane, 1.4% lactose, and 80% aquabides. Then followed by giving penicillin and streptomycin antibiotics [16].

Bali Bull Semen Collection

Bali bull semen was collected at National Artificial Insemination, Singosari, Malang. It is collected once a week using an artificial vagina (AV). Ejaculate was evaluated both macroscopically (volume, color, pH, and consistency of semen) and microscopically (concentration, motility, viability, and abnormalities of spermatozoa).

Adding of Semen Extender

Ejaculation that passed the macroscopic and microscopic test was continued by diluting using a tris-egg yolk (TEY) extender added with APRE, based on research [17], with different extracts used and the addition of extract percentages. There were five treatments such as P_0 (100% TEY + 0% APRE), P_1 (98% TEY + 2% APRE), P_2 (96% TEY + 4% APRE), P_3 (94% TEY + 6% APRE), and P_4 (92% TEY + 8% APRE).

Liquid Semen Quality Test (Before Freezing)

Treatment semen was cooled in a cool top with temperatures ranging from 4-5°C for 2-3 hours. Then, a liquid semen test or BF (Before Freezing) was carried out by dripping semen on a glass object and observing. It used a microscope with a magnification of 400x. After that, the percentage of motility, viability, and abnormalities of spermatozoa were measured [16].

ISSN. 2087-2852
E-ISSN. 2338-1655

Semen Freezing

The 0.25 mL of semen was filled into the straw with a concentration of 25 million spermatozoa. The straw was closed by attaching the straw using heating tweezers. Semen is frozen in two stages. The first was pre-freezing, which involved reducing the temperature from 4-5°C to -140°C by inserting straws filled with semen into the cool digits for 7 minutes. The second was the freezing process. It was to put the straw into a container containing liquid N_2 at a temperature of -196°C [16].

Sperm Quality Analysis

Sperm quality was assessed both before and after freezing. Sperm motility was observed using a microscope at 400x magnification. The sperm viability and abnormalities were examined under 400x magnifications using an eosin eosin-negrosin staining procedure.

Experimental Design and Data Analysis

This study employed an experimental method with a Completely Randomized Design (CRD). There were five treatments with five replications each. The research data obtained were statistically processed by one-way analysis of variance (ANOVA). If the ANOVA test shows a significant difference, it will be continued with a Tukey post hoc test using SPSS 25 software.

RESULT AND DISCUSSION

DPPH of *Alpinia purpurata* Rhizome Extract

Based on the results of the antioxidant activity test of *A. purpurata* rhizome extract using the DPPH method, it was found that the percentage inhibition value of *A. purpurata* rhizome extract samples increased as the concentration of the extract increased (Fig. 1).

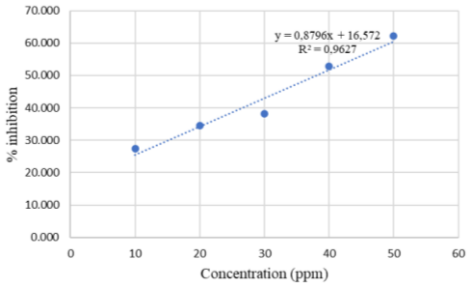

Figure 1. Antioxidant activity curve of *A. purpurata* rhizome extract

Based on the results of research [18], it was concluded that the percentage of antioxidant inhibition contained in red galangal (*Alpinia purpurata*) rhizome extract increased according to the increase in the extract concentration. Following the regression curve equation obtained, the IC50 value of *A. purpurata* rhizome extract was 38.004 $\mu g.mL^{-1}$. This value indicates that the antioxidant activity of *A. purpurata* rhizome was very strong (IC_{50}<50 $\mu g.mL^{-1}$). In accordance with the opinion of [19] that antioxidants that produce IC_{50} values < 50 $\mu g.mL^{-1}$, the antioxidant activity of the samples was classified as very strong.

Fresh Semen Quality of Bali Bull

The assessment of fresh semen quality was conducted through two approaches, those were macroscopic and microscopic evaluations. Macroscopic assessment involved the examination of the volume, pH, color, and consistency of semen. Meanwhile, microscopic evaluation involved calculating the percentage of spermatozoa motility, viability, and abnormalities. The average yield data from testing the quality of fresh semen for Bali bull is shown in Table 1.

Table 1. Average macroscopic and microscopic observations of fresh semen of Bali bull

Parameter	Mean ± SD
Volume (mL)	5.48 ± 1.81
pH	6.52 ± 0.11
Color	Milk white (ps)
Consistency	Concentrated (p)
Concentration (million.mL^{-1})	1671 ± 8.60
Individual Motility (%)	74,28 ± 1,4
Viability (%)	85.80 ± 0.50
Abnormality (%)	6.90 ± 1.71

Table 1 showed that the average volume of fresh semen for Bali bull was 5.48 ± 1.81 mL. The differences in the volume of semen each ejaculate were affected by age. Bali bull used as samples were more than 12 years old. So, semen production was low because the average volume of semen produced by adult bulls was 6.73 mL [20]. Bull semen production begins to increase at two years. It continues to increase until eight years, due to the growth of the testes, so that the seminiferous tubules become longer and the diameter of the lumen increases, followed by the development of the accessory gland and the resulting accessory fluid increases, thereby affecting the volume of semen [21]. However, in old bulls, testicular function declines. Thus, the volume of semen produced decreases [22].

The mean value of the degree of acidity (pH) of Bali bull ejaculate is 6.52 ± 0.11. These results aligned with a previous study [23] that bovine semen has a pH ranging from 6.2 to 7.8. According to Sunami and Wahjuningsih [24], pH

ISSN. 2087-2852
E-ISSN. 2338-1655

is related to the concentration of spermatozoa. High concentrations of spermatozoa have an impact on the pH of semen, which tends to become acidic due to the increasing number of spermatozoa, the accumulation of lactic acid resulting from cell metabolism, specifically the breakdown of fructose which is used as energy by spermatozoa.

On average, the semen of Bali bull was milky white (ps). These results are one hand, with the opinion of Feradis [25] that the average bull semen was milky white or cream due to the influence of the presence of riboflavin secreted by the vesicular glands. The color of semen was related to the concentration of semen; semen was milky white or cream, indicating that the semen concentration was high [26]. It can be seen from the observation that the semen of the Bali bull was milky white (ps) and had an average concentration of 1671x10^6 spermatozoa.mL^{-1}, classified as high-concentration semen.

In addition, the concentration was also related to the consistency of the semen. Semen with a >1500 x 10^6 spermatozoa.mL^{-1} concentration shows a thick consistency. It was the same opinion of Suyadi *et al.* [27] that consistency was related to color and semen concentration. Semen with a thick consistency and cream or milky white (ps) color has a higher concentration than semen with a thinner consistency and a more apparent color.

The mean percentage of motility in the fresh semen samples of the Bali bull examined was 74.28 ± 1.4%. It means that semen is suitable for further processing. According to regulations [28], the minimum motility for fresh semen of a bull is 70%. Normal spermatozoa motility ranges from 70-90% with fast movement [29]. Spermatozoa move because of the role of the spermatozoa tail, due to the tail of the spermatozoa containing many mitochondria that act as energy producers in the form of ATP so that spermatozoa move forward [30]. Sperm motility of ejaculate had been affected by the temperature at the time of storage and during examination. Low temperatures will inhibit spermatozoa motility, while higher and optimal temperatures of 37°C will increase spermatozoa motility. Urine and feces contaminated semen when it was collected.

The mean viability percentage of the ejaculate examined for Bali bull was 85.80 ± 0.50%. These results indicated that the viability of Bali bull spermatozoa was relatively high and belonged to the good category. It is feasible to process frozen semen. Based on the statement of Ducha *et al.* [31], the requirements for ejaculation were good and can be processed to the next stage for freezing. It was semen, a percentage of live spermatozoa >70%.

The abnormal percentage of Bali bull semen examined was 6.90 ± 1.71%. This value was relatively low compared to research [32], it was found that the percentage of abnormal ongole bull ejaculate was 12%. In addition, according to the Indonesian National Standard (SNI) requires that the semen of bull that is classified as good has a percentage value of both primary and secondary abnormalities that is < 20% [28]. This was based on the statement [33], that males with an abnormality percentage of > 17% showed low fertility.

Motility Percentage of Before Freezing and Post Thawing

The average percentage of spermatozoa motility after dilution using a tris-egg yolk (TEY) extender with the addition of *A. purpurata* rhizome extract (APRE) with different percentages according to treatment was shown in Table 2. Decreasing motility percentage before freezing was influenced by the cooling process at 45°C, causing a decrease in the phospholipid content, which protects spermatozoa from cold shock [34]. In addition, temperature changes caused an increase in the metabolic activity of spermatozoa, and accumulation of lactic acid, thus causing a decrease in pH and conditions becoming increasingly acidic, which are toxic to spermatozoa, causing the function of cell organelles to decrease, so that the percentage of motility also decreases [35].

Table 2. Average percentage of motility before freezing and post thawing

Treatment	Mean motility ± SD (%)	
	Before freezing	Post thawing
P_0	56.00 ± 4.18^{ab}	41.20 ± 2.28^{b}
P_1	55.00 ± 5.00^{ab}	39.00 ± 1.87^{ab}
P_2	56.00 ± 4.18^{ab}	39.60 ± 3.21^{ab}
P_3	60.00 ± 5.00^{b}	41.60 ± 3.21^{b}
P_4	47.00 ± 6.71^{a}	34.80 ± 4.55^{a}

Notes: Different superscript letters in the same column indicate a significant difference (P <0.05) between treatments. (P_0) Control, (P_1) treatment 98% TEY + 2% APRE, (P_2) treatment 96% TEY + 4% APRE, (P_3) treatment 94% TEY + 6% APRE, (P_4) treatment 92% TEY + 8% APRE.

ISSN. 2087-2852
E-ISSN. 2338-1655

However, semen can be processed to the freezing stage because the minimum requirement for before-freezing motility was 55% [36]. The diluent content of egg yolk played a role in maintaining the motility before freezing. Lipoprotein and lecithin content in egg yolk protect spermatozoa from cold shock [37]. Rafinosa serves as an energy source for spermatozoa [38].

The motility percentage increased from treatment P_0 to P_3 but decreased in treatment P_4. It happened because adding the extract to the diluent with an excessive percentage harmed the spermatozoa. Antioxidants in spermatozoa have been excess, causing spermatozoa can not receive antioxidants from outside, resulting in prooxidants that cause oxidation. Oxidation reactions can produce excess free radicals, which can cause damage to the spermatozoa membrane, so the percentage of motility decreases [37]. These results are in accordance with previous research [39], which showed that the addition of 30% moringa leaf extract, which also contains antioxidants of 70% egg yolk tris, actually showed the lowest percentage of motility compared to the addition of a smaller percentage of extract, because the higher concentration of the extract, the acidity level of the semen increased, thus affecting the quality of semen. Similar to the results of Ghalehkandi *et al.* [40], the addition of 15 cc of shallot extract to the semen of male rats showed a decrease in motility due to low membrane stability due to high extract concentrations.

The Motility percentage before and after thawing showed a significant difference between treatments ($P<0.05$), with the highest percentage value before freezing and after thawing at P_3 of 60.00 ± 5.00% and 41.60 ± 3.21%. The results of the percentage of motility P_0 and P_3 are suitable for insemination. According to the Ministry of Agriculture [36], in the post-thawing motility (PTM) test, bull spermatozoa's minimum percentage of motility is 40%.

It can occur due to the influence of the lactose content in the egg yolk, which plays a role in helping to remove water from the cells so that it can help prevent the formation of ice crystals, which can reduce the motility of spermatozoa during the freezing process [41]. The addition of red galangal extract, which contains antioxidants, can reduce levels of free radicals resulting from metabolic processes, so that damage to spermatozoa can be minimized and semen quality can be maintained [37]. Flavonoids can reduce the intensity of free radicals because flavonoids have a structure where the aromatic ring contains hydroxyl groups and other groups that can accept or remove free electrons from free radicals through a single electron transfer mechanism or hydrogen atom donor so that free radicals become stable and not toxic to cells [42]. Free radicals that have reacted with antioxidants will not react with other compounds, so the mitochondrial membrane, as a producer of the energy source of the spermatozoa tail, will be protected from free radicals. Thus mitochondria can produce energy in the form of ATP so spermatozoa can move. If the available energy is sufficient, the motility percentage can be maintained, even increased [43].

Percentage of Viability of Spermatozoa

The viability percentage of spermatozoa can be calculated using eosin-negrosin staining to determine live and dead spermatozoa. The eosin dye will be colored pink to the dead spermatozoa because of the damage to the spermatozoa membrane; thus, the dye enters the cell. Meanwhile, the negrosin dye has a function to give color background become blackish blue. Indeed, spermatozoa are easier to observe. Therefore the live spermatozoa will not be stained [31] (Fig. 2).

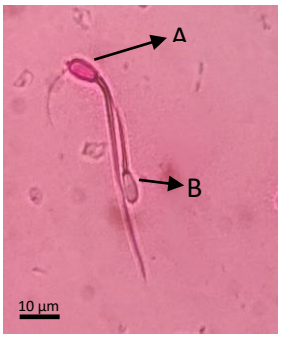

Figure 2. Live and Dead Spermatozoa Stained with Eosin and Negrosin, A. Dead sperm and B. Live sperm

The mean percentage of viability of spermatozoa after dilution using tris-egg yolk (TEY) extender with the addition of *A. purpurata* rhizome extract (APRE) with different percentages according to treatment is shown in Table 3. There was a decrease in the average percentage of viability before freezing. It can occur due to the cooling process that is carried out, causing a decrease

ISSN. 2087-2852
E-ISSN. 2338-1655

in the phospholipid content so that protection from cold shock is reduced. In addition, the content of lactic acid left over from cell metabolism causes conditions to become increasingly acidic due to a decrease in pH, so it can be toxic to cells and result in increased cell death [33].

Meanwhile, decreasing viability percentage of post-thawing can occur due to changes in temperature during freezing or thawing. Drastic temperature changes can increase the production of reactive oxygen species (ROS), which can cause lipid peroxidation in the plasma membrane. It affects the productivity of cells in producing energy; if it does continuously, the cells will weaken until they die [44].

Table 3. Average percentage of viability before freezing and post thawing

Treatment	Mean viability ± SD (%)	
	Before freezing	Post thawing
P_0	77.80 ± 4.44	43.40 ± 2.30^a
P_1	75.60 ± 6.43	44.40 ± 2.70^a
P_2	76.00 ± 2.12	47.80 ± 4.71^a
P_3	76.60 ± 6.23	59.80 ± 5.26^b
P_4	81.80 ± 4.15	46.80 ± 6.87^a

Notes: Different superscript letters in the same column indicate a significant difference (P <0.05) between treatments. (P_0) Control, (P_1) treatment 98% TEY + 2% APRE, (P_2) treatment 96% TEY + 4% APRE, (P_3) treatment 94% TEY + 6% APRE, (P_4) treatment 92% TEY + 8% APRE.

Results mean percentage of viability before freezing showed that the addition of *A. purpurata* rhizome extract in various treatments increased from P_1, P_2, P_3 to P_4. Statistical test results show that viability before freezing is not significantly different between treatments (P>0.05). In comparison, the average percentage of viability post-thawing increased from P_1 to P_3 but decreased at P_4. It happened because the highest percentage of the extract caused a build-up of dissolved materials. Hence, the formation of ice crystals increased, causing sperm viability to decrease. Following Toelihere [37], during the freezing process, ice crystals form and build-up of electrolytes and other materials in the solution or cells. So the lipoprotein sheath of the spermatozoa membrane dissolved, so the membrane's permeability changes, which causes cell death.

Statistical analysis of post-thawing viability showed a significant difference between treatments (P<0.05). Treatment of 6% APRE in 96% TEY (P_3) showed the highest viability percentage compared to other treatments, 59.80 ± 5.26%.

Percentage of Spermatozoa Abnormalities

The average percentage of abnormality data is shown in Table 4. Increasing abnormality can occur because, during the cooling process, intracellular fluids are exchanged with intracellular cryoprotectants, which results in cell expansion and subsequent shrinkage. Thus, the cell organelles are intolerant of changes in osmolarity [45]. It caused an increase in the percentage of abnormalities. It is in line with the research [46] so that the cryopreservation process can cause changes in the morphology of spermatozoa.

Table 4. Average percentage of abnormality before freezing and post thawing

Treatment	Mean Abnormality ± SD (%)	
	Before freezing	Post thawing
P_0	8.60 ± 1.14^{ab}	8.40 ± 2.30^a
P_1	8.60 ± 1.51^{ab}	8.60 ± 1.14^a
P_2	8.20 ± 1.64^{ab}	8.20 ± 2.05^a
P_3	7.20 ± 0.84^a	7.00 ± 2.00^a
P_4	10.80 ± 2.39^b	12.40 ± 1.52^b

Notes: Different superscript letters in the same column indicate a significant difference (P <0.05) between treatments. (P_0) Control, (P_1) treatment 98% TEY + 2% APRE, (P_2) treatment 96% TEY + 4% APRE, (P_3) treatment 94% TEY + 6% APRE, (P_4) treatment 92% TEY + 8% APRE.

Increasing abnormalities percentage from before freezing to post-thawing was due to spermatozoa having experienced cold shock during the cooling and freezing process and heat shock during the thawing process. Changes in temperature cause cell metabolism and ROS production to increase, where an increase in ROS causes damage to the plasma membrane of spermatozoa, which can affect the morphology of spermatozoa; in line with Suyadi *et al.* research [27], the higher the damage to the plasma membrane, abnormalities also increases. However, abnormalities were still considered normal. Morphological abnormalities below 20% are still considered normal [47] because the influence of the flavonoid content in *A. purpurata* rhizome extract prevents damage to spermatozoa and reduces spermatozoa abnormalities caused by free radicals. In accordance with Memon *et al.* research [48], which proved that the addition of antioxidants suppresses spermatozoa abnormalities.

However, among the results of the average abnormal spermatozoa, there was an increase

ISSN. 2087-2852
E-ISSN. 2338-1655

in the P_4 treatment because of the higher dose of the extract given. It has a harmful effect on spermatozoa. Cahyadi *et al.* research [49] explained that excessive flavonoid content can reduce the quality of spermatozoa. In line with the statement of Sabile *et al.* [50], the antioxidant content in too much amount changes its properties to become a pro-oxidant. So it causes oxidation. The occurrence of a reaction between unsaturated fatty acids in the spermatozoa membrane with excess oxygen causes cell oxidative metabolism, which causes damage to the cell membrane [25]. Damage to the cell membrane increases the abnormality of spermatozoa.

Several types of abnormalities were found between before freezing and post-thawing of the Bali bull from treatment P_0 to P_4, such as the tapered head, macrocephalic, microcephalic, double tail, shoe hook tail, coiled tail, bent tail, detached tail, broken tail, and detached head (Fig. 3). Types of abnormalities in the tail, those coiled tail and bent tail (Fig. 4), were found due to the influencing series of dilution and cooling processes, which can cause membrane damage, changes in osmotic pressure, and exposure to chemicals in the diluent, such as glycerol which functions as a cryoprotectant [51]. When cryoprotectants enter and leave the cell, it can cause a change in the composition of the water inside the cell. Thus, the tail of the spermatozoa becomes curled or looks crooked [52].

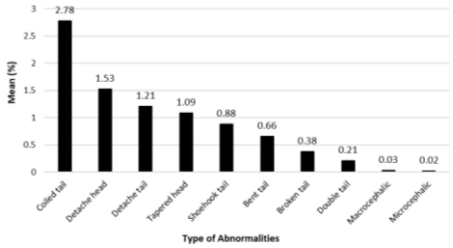

Figure 3. Type of Abnormalities Sperm

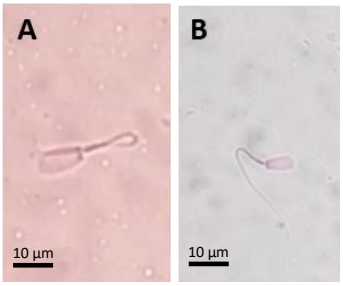

Figure 4. Types of Bali bull Spermatozoa Abnormalities. (A) Coiled tails, (B) Bent tails

CONCLUSION

The results of the research that has been done concluded that the addition of 6% *A. purpurata* rhizome extract in 94% tris-egg yolk extender was effective in maintaining Bali bull spermatozoa quality during the freezing process. Based on the result of this research, further research should be carried out regarding adding A. purpurata rhizome extract with more diverse proportions to find the most optimal proportion.

ACKNOWLEDGEMENTS

The researcher would like to thank the Professor Research grant of the Faculty of Mathematics and Natural Sciences, University of Brawijaya, Indonesia, with contract number 3084.9/UN10.F09/PN/2022. Authors also thank all parties from the Singosari Artificial Insemination Centre (BBIB) and the Department of Mathematics and Natural Sciences, University of Brawijaya, who have allowed the use of the laboratory and provided the facilities for carrying out this research.

REFERENCES

[1] Ismail, M., H. Nuraini, R. Priyanto. 2014. Effect of body fatness to carcass and non carcass productivity of small frame size beef cattle (Bali and Madura). *Vet. J.* 15(3). 417–424.

[2] Sayoko, Y., M. Hartono, P.E. Silotonga. 2011. Faktor-faktor yang mempengaruhi persentase spermatozoa hidup semen beku sapi pada berbagai inseminator di Lampung Tengah [Factors that affect the live spermatozoa of cattle frozen semen on various inseminator in Central Lampung]. Bachelor Thesis. Department of Livestrock Production. Faculty of Agriculture. Universitas Lampung.

[3] Jain, J.K., R.J. Paulson. 2006. Oocyte cryopreservation. *Fertil. Steril*. 86(4 SUPPL.). 1037–1046.

[4] Watson, P.F. 2000. The causes of reduced fertility with cryopreserved semen. *Anim. Reprod. Sci.* 60–61. 481–492.

[5] Moore, A.I., E.L. Squires, J.K. Graham. 2005. Adding Cholesterol to the stallion sperm plasma membrane improves cryosurvival. *Cryobiology*. 51(3). 241–249.

[6] Leboeuf, B., B. Restall, S. Salamon. 2000. Production and storage of goat semen for artificial insemination. *Anim. Reprod. Sci.* 62(1–3). 113–141.

[7] Masyitoh, H., T.W. Suprayogi, R.N. Praja, P. Srianto, S.P. Madyawati, A.L. Saputro.

ISSN. 2087-2852
E-ISSN. 2338-1655

2018. Persentase motilitas dan viabilitas spermatozoa Kambing Sapera dalam pengencer tris kuning telur dan susu skim kuning telur *before freezing*. *J. Med. Vet.* 1(3). 105–112.

[8] Pamungkas, R.N., D. Julaichah, S.D. Prasasti, M. Muslih. 2010. Pemanfaatan lengkuas (*Alpinia purpurata* K. Schum) sebagai bahan pengawet pengganti formalin [Utilization of galangal (*Alpinia purpurata* K. Schum) as a preservative to replace formalin]. Research Report of Student Creativity Program. Universitas Negeri Malang.

[9] Siswandoko, B., S. Zaenab, H. Husamah. 2017. Penambahan ekstrak kulit buah naga ke dalam pengencer tris kuning telur untuk meningkatkan kualitas semen beku kambing peranakan ettawa. *Scr. Biol.* 4(4). 247.

[10] Wathoni, N., T. Rusdiana, R.Y. Hutagaol. 2009. Formasi gel antioksidan ekstrak rimpang lengkuas (*Alpinia galangal* L. Willd) dengan menggunakan basis Aqupec 505 HV. *Farmaka*. 7. 15-27.

[11] Taurina, W., M. Andrie. 2013. Formulation of lengkuas rhizome (*Alpinia galanga* L.) extract's gel as antifungal with hidroxy prophyl methyl cellulosae (HPMC) and carbopol base. *Tradit. Med. J.* 18(3).157-161.

[12] Anas, Y., I. Faozi, Suharjono. 2015. Potensi Fraksi N-heksan ekstrak etanol rimpang lengkuas [*Alpina Galangal* (L) Swartz.] dalam meningkatkan kualitas sperma dan spermatogenesis. Prosiding Seminar Nasional Peluang Herbal sebagai Alternatif Medicine. 7-19.

[13] Riskianto, E.E. Kamal, M. Aris. 2021. Aktivitas antioksidan ekstrak etanol 70% daun kelor (*Moringa oleifera* Lam.). *Jurnal Pro-Life*. 8(2). 168-177.

[14] Valko, M., D. Leibfritz, J. Moncol, M.T. Cronin, M. Mazur, J. Telser. 2007. Free radicals and antioxidants in normal physiological functions and human disease. *Int. J. Biochem. Cell Biol.* 39. 44–84.

[15] Sukardi. 2011. Identifikasidan karakterisasi umbi keladi tikus sebagai zat antioksidan alami. *GAMMA: Jurnal Penelitian Eksakta*. 6(2). 143-151.

[16] Zenichiro, K. Herliantien, Sarastina. 2002. practical instruction technology of frozen semen processing for cattle. Balai Besar Inseminasi Buatan [Singosari Artificial Insemination Centre]. Malang.

[17] Effendi, F.I., S. Wahjuningsih, M.N. Ihsan. Pengaruh pengencer tris aminomethane kuning telur yang disuplementasi sari kulit manggis (*Garcinia mangostana*) terhadap kualitas semen sapi limousin selama penyimpanan suhu dingin 5˚C. *Jurnal Ilmi-Ilmu Peternakan*. 25(3). 69-79.

[18] Mardhiyyah, K., Y.I. Ryandini, Y. Hermawan. 2021. Uji aktivitas antioksidan dan skrining fitokimia perasan lengkuas merah dan lengkuas putih. *Jurnal Jamu Indonesia.* 6(1). 23–31.

[19] Saharuddin, M., C.A. Kondolele. 2020. Uji aktivitas antioksidan ekstrak n-butanol daun rambutan (*Nephelium lappaceum* Linn) dengan metode DPPH (1,1-diphenyl-2-picrylhydrazyl). *Jurnal Kesehatan Yamasi Makassar*. 4(2). 98-103.

[20] Mathevon, M., M.M. Buhr, J.C.M. Dekkers. 1998. Environmental, management, and genetic factors affecting semen production in holstein bulls. *J. Dairy Sci*. 81. 3321.

[21] Konenda, M.T.K., Y.S. Ondho, D. Samsudewa, E. Herwijanti, A. Amaliya, I.A. Setiawan. 2020. Seasonal variation and age-related changes in semen quality of limousin bull in Indonesian Artificial Insemination Center. *Int. J. Vet. Sci.* 9(4). 553–557. DOI : 10.37422/IJVS/20.061.

[22] Kowalczyk, A., E. Gałęska, E. Czerniawska-Piątkowska, A. Szul, L. Hebda. 2021. The impact of regular sperm donation on bulls' seminal plasma hormonal profile and phantom response. *Sci. Rep.* 11(1). 11116. DOI: 10.1038/s41598-021-90630-8.

[23] Ismaya. 2017. Bioteknologi inseminasi buatan pada sapi dan kerbau. Gadjah Mada University Press. Yogyakarta.

[24] Sunami, S., S. Wahjuningsih. 2017. Kualitas semen segar dan *Recovery Rate* (RR) sapi limousin pada musim yang berbeda. *Ternak Tropika*. 18(1). 36-50.

[25] Feradis. 2010. Bioteknologi reproduksi ternak. Alfabeta. Bandung.

[26] Lestari, S., D.M. Saleh, Maidaswar. 2013. Profil kualitas semen segar sapi pejantan limousin dengan umur yang berbeda di Balai Inseminasi Buatan Lembang Jawa Barat. *Jurnal Ilmu Peternakan*. 1(3). 1165-1172.

[27] Suyadi, A., Rachmawati., N. Iswanto. 2012. Pengaruh α-tocopherol yang Berbeda dalam pengencer dasar tris aminimethane-kuning telur terhadap

kualitas semen kambing boer yang disimpan pada suhu 5˚C. *Jurnal Ilmi-Ilmu Peternakan*. 22(3). 1-8.

[28] Badan Standarisasi Nasional [National Standardization Agency of Indonesia]. 2017. SNI 01.4869.1- 2017 on frozen semen of cattle. Ditjen PKH [Directorate General of Livestock]. Jakarta.

[29] Ax, R., M. Dally, B.A. Didion, W. Lenz, C. Love, D. Varner, B. Hafe, M.E. Bellin. 2008. Artificial insemination. In: Hafez, B., E.S.E. Hafez. Reproduction in Farm Animals, 7th Ed. Lippincott Williams and Wikins. Baltimore, Marryland. USA.

[30] Utami, T., T. Considus Tophianong. 2014. Pengaruh suhu thawing pada kualitas spermatozoa sapi pejantan. *Jurnal sains veteriner*. 32(1). 32-39.

[31] Ducha, N., T. Susilawati, A. Aulanni'am, S. Wahyuningsih. 2013. Motilitas dan viabilitas spermatozoa sapi limousin selama penyimpanan pada refrigerator dalam pengencer CEP-2 dengan suplementasi kuning telur. *Jurnal Kedokteran Hewan - Indonesian Journal of Veterinary Sciences.* 7(1). 5-8. DOI: 10.21157/j.ked.hewan.v7i1.555.

[32] Sukmawati, E., R.I. Arifiantini, B. Purwantara. 2015. Freezing capacity of sperm on various type of superior bulls. *Jurnal Ilmu Ternak dan Veteriner.* 19(3). 168–175.

[33] Ball, P.J.H, A.R. Peters. 2004. *Reproduction in Cattle*, 3rd Ed. Blackwell Publishing. Oxford, USA.

[34] Situmorang, P. 2002. The effects of inclusion of exogenous phospholipid in tris diluent containing a different level of egg yolk on the viability of bull spermatozoa. *Jurnal Ilmu Ternak dan Veteriner.* 7(3). 181–187.

[35] Sugiarti, T., E. Triwulaningsih, P. Situmorang, R.G. Sianturi, D.A. Kusumaningrum. 2004. Penggunaan Katalase dalam Produksi Semen Dingin Sapi [Use of Catalase in Cattle Cold Semen Production]. Proceeding of National Technology of Livestock and Veterinery. Bogor, 4-5 Agustus. Livestock Research and Development Center. Bogor. 215-220.

[36] Ditjenak [Directorate General of Livestock]. 2007. Regulation No. 73/PD.410/F/06/2007 on Technical Guidelines for National Beef Cattle Performance Test. Directorate General of Livestock. Ministry of Agriculture.

[37] Toelihere, M.R. 1993. Inseminasi Buatan pada ternak. Penerbit Angkasa. Bandung.

[38] Gunawan, M., E.M. Kainn. 2008. Kualitas sperma sapi beku dalam media tris kuning telur dengan konsentrasi raffinosa yang berbeda. Seminar Nasional Teknologi Peternakan dan Veteriner. 105-110.

[39] Dapawole, R.R., I.P. Sirappa. 2021. Effect concentration of moringa (*Moringa oleifera* Lam) leaf extract in citrate-egg yolk in maintaining motility and viability of spermatozoa of kacang goat. *Jurnal Sain Peternakan Indonesia.* 16(4). 340–346.

[40] Ghalehkandi, J.G., A. Asghari, R. Beheshti, M. Valilu, A. Yeghaneh. 2012. Effect of onion (*Allium cepa*. Linn) aqueous extract on serum concentration of LH, FSH and testosterone compared with zinc sulfate supplementation in the rats. *J. Anim. Vet. Adv.* 11(18). 3346–3349.

[41] Tambing, S.N., M.R. Toelihere, T.L. Yusuf, B. Purwantara, I.K. Sutama, P.Z. Situmorang. 2003. Pengaruh frekuensi ejakulasi terhadap karakteristik semen segar dan kemampuan libido kambing saanen. *Jurnal Sain Veterinary.* XXI(2). 57–65.

[42] Sukmaningsih, A.A.S.A., S. Permana, D.J. D.H. Santjojo, A.Y.P. Wardoyo, S.B. Sumitro. 2018. Investigating natural transition metal coordination anthocyanin complex in java plum (*Syzygium cumini*) fruit as free radical scavenging. *Rasayan Journal Chemistry.* 11(3). 1193–1203.

[43] Ratna Mustikasari, D., N. Qomariyah. 2013. Pengaruh pemberian filtrat daun katuk terhadap konsentrasi dan morfologi normal spermatozoa mencit (M*us musculus*) yang terpapar asap rokok. *LenteraBio*. 2. 155-158.

[44] Hartono, M. 2008. Optimalization of Vitamin E in Egg Yolk Citrate Extender to Preserve Semen Quality of "Boer" Goat. *J. Indon.Trop. Anim Agric*. 33. 11-19.

[45] Medeiros, C.M.O., F. Forell, A.T.D. Oliveira, J.L. Rodrigues. 2002. Current status of sperm cryopreservation: why isn't it better?. *Theriogenology*. 57(1). 327–344.

[46] Sangeeta, S., A. Arangasamy, S. Kulkarni, S. Selvaraju. 2015. Role of amino acids as additives on sperm motility, plasma membrane integrity and lipid peroxidation levels at pre-freeze and post-thawed ram semen. *Anim. Reprod. Sci.* 161. 82–88.

[47] Susilawati, T. 2011. *Spermatology*.

ISSN. 2087-2852
E-ISSN. 2338-1655

Universitas Brawijawa Press. Malang.
[48] Memon, A.A., H. Wahid, Y. Rosnina, Y.M. Goh, M. Ebrahimi, F.M. Nadia. 2012. Effect of Antioxidants on post thaw microscopic, oxidative stress parameter and fertility of boer goat spermatozoa in tris egg yolk glycerol extender. *Anim. Reprod. Sci.* 136 (1–2). 55–60.
[49] Cahyadi, T.R.T., M. Christiyanto, E.T. Setiatin. 2016. Persentase hidup dan abnormalitas sel spermatozoa kambing Peranakan Etawah (PE) dengan pakan yang disuplementasi daun binahong (*Anredera cordifolia* (Ten.) Steenis). *Anim. Agric. J.* 5(3). 23–32.
[50] Sabile, S., A.L. Toleng, M. Yusuf, Zulkharnaim, S. Firmiaty, M. Idrus, Nasriyanto. 2016. Pengaruh penambahan ekstrak buah mengkudu (*Morinda citrifolia* Linn) dalam pengencer terhadap motilitas spermatozoa pada semen cair Sapi Bali. *Aves: Jurnal Ilmu Peternakan.* 10(2). DOI: 10.35457/aves.v10i2.186
[51] Ozkavukcu, S., E. Erdemli, A. Isik, D. Oztuna, S. Karahuseyinoglu. 2008. Effects of Cryopreservation on sperm parameters and ultrastructural morphology of human spermatozoa. *J. Assist. Reprod. Genet.* 25(8). 403-411. DOI: 10.1007/s10815-008-9232-3.
[52] Allamaneni, S.S.R., A. Agrawal, S. Rama, P. Ranganathan, R.K. Sharma. 2005. Comparative study on density gradients and swim-up preparation techniques utilizing neat and cryopreserved spermatozoa. *Asian J. Androl.* 7(1). 86–92. DOI: 10.1111/j.1745-7262.2005.00008.x.

Assessment of Cytotoxicity and Antioxidant Activities of Rice Berry Extracts for Body Cream Products

Tiparat Tikapunya[1], Kanlaya Jumpatong[2], Chaipat Lapinee[3] ,Pahol Samsomchai[4*]

[1] Faculty of Agricultural Technology, Lampang Rajabhat University, Lampang, Thailand
[2,3] Department of Chemistry, School of Science, University of Phayao, Phayao, Thailand
[4] D De Dee Cosmetic Factory, Lamphun, Thailand

Abstract

The utilization of natural extracts as an ingredient in cosmetic products becomes a better choice for customers. Rice berry has been defined as a potential source of anti-free radical properties which is able to be formulated in cosmetic products. Therefore, the objectives of this study are 1) to investigate an antioxidant by ABTS and ABTS assays, total antioxidant compounds by phenolic and total flavonoids assays, and cell viability to fibroblast NIH3T3 (IC80) of ethanol and aqueous extracts of rice berry by MTT test, 2) to evaluate cream stability of each formulates adding different concentrations of rice berry extracts. The results showed that both extraction solvents did not show cytotoxicity to fibroblast NIH3T3 (IC80). However, the ethanol rice berry extracts exhibited a higher total phenolic compound, total flavonoid content, and anthocyanin content than the water rice berry extracts. The physical properties of each cream formulated, including rice berry extracts, showed no unacceptable properties. It can conclude that rice berry extracts have the potential to be a natural ingredient in cosmetic products after studies of the antioxidant properties, antioxidant compounds, cytotoxicity to normal fibroblast, and physical properties after being added to cosmetic cream.

Keywords: Antioxidant, cream stability, flavonoids, normal fibroblasts, rice berry.

INTRODUCTION

The Rice berry extract for the cosmetic ingredient is less in the formation of its biological activity, and the stability of the extract in the cream product has yet to be well known. Rice berry, black-purple-colored rice, is popularly grown in Thailand and easily found in northern Thailand. Rice berry has many benefits and nutritional values for its antioxidants, anti-inflammatory agents, and vital health-promoting compounds, helping lower disease risks [1]. Moreover, other properties of colored rice, such as anti-aging [2] and anti-herpes simplex virus, have been studied [3]. Besides, the rice berry is enriched in health promotion to humankind [4].

Consequently, a screening property is a priority for determining a plant to study further. Rice berry rice provides a long list of incredible health benefits. Herein its mechanism can reduce blood sugar that affects low Glycemic Index (GI) [5]. Thai purple rice assesses with phenolic content, anthocyanin content, and antioxidant activity [3,4,6]. Colored rice can modulate skin for anti-aging with its Oryzanol and phenolic compounds such as Proanthocyanin [7,8], and anthocyanin [9]. The previous study gave information on extracting proanthocyanin-rich red rice extract by ethanol, oryzanol, and other phenolic compounds for skin anti-aging [7].

Moreover, the rice berry content of polyphenol, anthocyanin, and antioxidant activity showed modulation of gastrointestinal digestion [10]. Furthermore, anthocyanin from purple rice has been reported as an efficient compound in cosmetic utility for skin aging [11]. Not long ago, immune-boosting for consumers can be derived from food against COVID-19 [12]. Likewise, anthocyanin has been recommended compound for significant antiviral enhancement to protease enzymes of COVID-19, so COVID-19 cannot increase the cell number or make the virulent to host cell [13].

Rice berry relieves illness in traditional Thai medicine, especially in North Thailand. Investigating biological screening effects, antioxidant activity, related compounds, and the stability of extracted in cream products that is rice berries became an important part of research [1]. Evaluating an effective extract that can modulate NIH3T3 fibroblast cells to develop the extracts to cell viability is a safety test to demonstrate the possibility of Rice berry extract used as an ingredient of cosmetic products.

MATERIALS AND METHODS

Chemicals and Materials

The rice berry was collected from Lamphun, the most northern province of Thailand. The plant was verified using The Plant List (http://www.theplantlist.org) and was identified

* Correspondence Address:
Pahol Sansomchai
Email : Lyw1149@gmail.com
Address : 189/7 Muang-nga, Lamphun, Thailand

ISSN. 2087-2852
E-ISSN. 2338-1655

geographically by a geographer. The whole grains were cleaned and dried in an oven at 40°C, then stored at -20°C until being used. The Whatman qualitative filter paper no.1 was purchased from Northern Chemical and Glassware LTD., Part (Chiang Mai, Thailand). 2,2-Diphenyl-1-picryl hydroxyl (DPPH), 6-hydroxy-2,5,7,8-tetramethyl-chroman-2-carboxylic acid (Trolox), catechin hydrate, and TPTZ (2,4,6-tripyridyl-s-triazine) were purchased from Sigma-Aldrich Chemical Company (St. Louis, MO, USA). Gallic acid was obtained from Fluka (Buchs, Switzerland). Proanthocyanins and anthocyanin were purchased from MySkinRecipies (Bangkok, Thailand). Folin–Ciocalteu phenol reagent was purchased from Merck (Darmstadt, Germany). Sodium hydroxide was obtained from Fisher Chemical (Mumbai, India). KCl, $FeCl_3$, CH_3CO_2K, $K_2S_2O_8$, $AlCl_3.H_{12}O_6$, and CH_3OH were purchased from Ajax Finchem (Auckland, New Zealand). Hexane was obtained from Macron Fine Chemicals (PA, USA). Ethanol 99.9% was purchased from QRëC (New Zealand). All chemicals were of analytical grade. Double-distilled and deionized water was used in the preparation of all solutions.

Sample Preparation of Extracts

Dried samples around one kilogram were grounded to achieve dried powder and then macerated in 4L of 80% (v/v) ethanol mixed water for 24h at room temperature. The extraction process was done twice with the same extraction conditions. The removal of chlorophyll was carried out using the charcoal adsorption process. Then, the extracts without chlorophyll were filtered through Whatman's No. 1 filter paper, and the removal of solvent was done by a vacuum rotary evaporator at room temperature. The lyophilized process was used to concentrate the aqueous portion of the sample extracts to receive the powder of sample products. The crude rice berry extract (RBE) in water (W) and EtOH separate extracts were ready for further experiment.

Assessment of antioxidant activities

The antioxidant activity of rice berry crude extract (RBE) was investigated by conducting the free radical scavenging activity. The DPPH and ABTS inhibition assay has been used to identify the performance of extracts on the antioxidant property, and both methods were slightly modified as described by previous studies [14]. The activity of antioxidant extracts was carried out by monitoring the decrease in absorbance at wavelength 517 nm for DPPH assay and 735 nm ABTS assay, and the percentage of inhibition and IC50 value were also presented.

Total Phenolic and Flavonoid Contents of Crude Extract

The Folin-Ciocalteu and aluminum chloride colorimetric assays have been used to estimate the total phenolic content (TP) and total flavonoid content (TF) in the crude extracts, and the methods have been described in the previous studies [15]. The quantity of TP and TF contents was determined in the unit of milligram gallic acid equivalent per gram extract (mg GE g^{-1} of extracts) for TP and milligram catechin equivalent per gram extract (mg CE g^{-1} of extracts) for TF. Each experiment was done in three replications. The extracts presented with the highest antioxidant activity were identified as antioxidant compounds for use as cosmetic ingredients.

Total Monomeric Anthocyanin Content

The pH differential method [16] was used to determine the total monomeric anthocyanin content (TAC) in the extracts with slight modification. Briefly, the extract of about 0.3 mL was added to 2.7 mL of various buffer solutions such as KCl buffer (0.025 M, pH = 1.0) and sodium acetate buffer (0.4 M, pH = 4.5). All solutions were filtrated by Whatman no.1 before determining the absorbance. The resulting solutions determined the absorbance at wavelength 510 and 700 nm. The form of cyanidin-glucoside (Cyd-3-glu) derived from total anthocyanin was determined and used to calculate the value of TAC using the following equation:

$$TAC\ (mg/g) = (A \times MW \times ditution\ fortor \times 1000)/\varepsilon \times \mathrm{L}$$

Description:

A = ($A_{510\ nm} - A_{700\ nm}$) pH 1.0 - ($A_{510\ nm} - A_{700\ nm}$) pH 4.5
The value of MW for cyd-3-glu = 449.2 g mol^{-1}
The value of Ɛ = 26900 molar extinction coefficients in M^{-1} cm^{-1} for cyd-3-glu
The value of dilution factor = 10

The Assay of Cell Viability

Cell line

The DMEM, 100 U.mL^{-1} penicillin, 100 mg.mL^{-1} streptomycin plus 10% FBS were used to maintain NIH3T3 (ATCC CRL 1658) fibroblast cells. The condition of a humidified incubator with an atmosphere comprised of 95% air and 5% CO_2 at 37°C was used to maintain the culture.

Cell viability assay

The culture was done in DMEM with 10% FBS. The 96-well plate contained the NIH3T3 fibroblast cells (1.0×104 cells.$well^{-1}$). After being cultured for 24h, the concentration of RBEs in EtOH or Water (W) (0-400 mg.mL^{-1}) was varied from 0 to 400 mg.mL^{-1} and incubated for 24h. At the equilibrium point of treatment, the addition of the 15 mL of 3-

ISSN. 2087-2852
E-ISSN. 2338-1655

(4,5-dimethylthiazol-2-yl)-2,5-diphenyltetrazolium bromide (MTT) solution (5 mg.mL^{-1}) was done, and the resulted solution was incubated for 4h. The dissolution of the MTT formazan with dimethyl sulfoxide (DMSO) was carried out. Then the absorbance measurement was placed at wavelength of 570 nm with a reference wavelength of 630 nm.

Evaluation of Formulation

Physical parameters

Each formulated body cream's appearance, color, and homogeneity (Table 1) were determined. The formulated cream procedure was described as follows.

Table 1. Formulated body creams for physical evaluation

Ingredients	RBE1 (g)	RBE2 (g)	RBE3 (g)	RBE4 (g)	RBE5 (g)
RBE	0.00	5.00 (mg)	10.00 (mg)	20.00 (mg)	0.00 (mg)
Cetostearyl alcohol	5.00	5.00	5.00	5.00	5.00
Palmitic acid	2.00	2.00	2.00	2.00	2.00
PEG-200	2.00	2.00	2.00	2.00	2.00
Cetyl alcohol	1.00	1.00	1.00	1.00	1.00
Optiphen	1.00	1.00	1.00	1.00	1.00
Carbopol 940	0.50	0.50	0.50	0.50	0.50
Dimethicone	0.50	0.50	0.50	0.50	0.50
Disodium EDTA	Qs.	Qs.	Qs.	Qs.	Qs.
Triethanolamine	0.50	0.50	0.50	0.50	0.50
Distilled water qs. to 100 g					

Step 1: Aqueous phase

Part 1. Disodium EDTA, optiphen, and RBE were weighed accurately and dissolved in some distilled water. *Part 2.* The remaining distilled water was dispersed with Carbopol 940 while heated to 70°C to swelling using a high-speed shear homogenizer (FJ200-SH, Shanghai Huxi Industrial Company Limited, China).

Step 2: Oil phase

Palmitic acid, acetyl alcohol, dimethicone, and ceto stearyl alcohol were weighed accurately, mixed and heated to 70°C. Then mix oil phase to part 2 of aqueous phase at 70°C with continuous stirring for 30 min till was homogenized and uniformed. Part 1 of aqueous phase was added in the formulated cream when it cools down to 40°C. The formulated cream will be used for further experiments.

For physical parameters were followed Donglikar and Deore [17] method with minor change. The modification was storage samples at room temperature and then at a freeze-thaw condition for 4 cycles.

Thermal stability

The test of cream formulation was carried out in 60-70% RH and 37.0 ± 1.0°C room. The freeze-thaw condition (0°C – 4°C and room temperature) for four cycles was applied for the thermal cycle. The result should not be separated oil or liquidity in the cream to pass the evaluation of the cream test.

pH determination

The variation of pH values was carried out mainly in the range from 5 to 9 for the cream formulation. The variation of cream pH was found around pH 6 to 9. The formulated creams were diluted to 10% dilution with distilled water. The variation of pH ranges of mixtures was monitored using a pH meter.

Viscosity

The Brookfield viscometer (Applied Scientific Instruments Co., Ltd., Dial reading viscometer, Thailand) was used to determine the viscosities of creams. The right spindle was taken at spindle no.4 for the given product, and the operation condition was set up. The cream viscosity was directly measured at a 6 rpm speed by keeping the torque constant.

Statistical analysis

Each experiment was performed in triplication. All values are presented as a mean value (mean ± SD). The statistically significant differences between the means of the samples were calculated by one-way ANOVA. The differences were considered significant at $p<0.05$ (*).

RESULT AND DISCUSSION

Antioxidant properties of crude rice berry extracts

RBE against ABTS and DPPH radicals and their TP, TF, and anthocyanin (A) contents. In this study, rice berries were collected from Lamphun Province. The antioxidant activities of rice berry crude extracts were measured by determining their abilities to scavenge DPPH and ABTS radicals. As shown in Table 2, the antioxidant activities of rice berry extract at 0-200 μg.mL^{-1} were found to inhibit the ABTS-radical and DPPH-radical in a dose-dependent manner when compared with Trolox as a positive control and ascorbic acid, respectively. RBE in the EtOH extract at 200 μg.mL^{-1} displayed the highest inhibitory effect when it inhibited ABTS and DPPH radical, followed by water extract at the same concentration level. This finding agreed well with the evaluation of the TP and TF of each extract (Table 2).

The extracts of RBE were correlated to anti-oxidation against ABTS and DPPH radicals. The IC_{50} of the RBE with EtOH extract against ABTS and DPPH radicals were 54.72 ±1.40 μg.mL^{-1} and 82.04 ±3.16 μg.mL^{-1}, respectively.

ISSN. 2087-2852
E-ISSN. 2338-1655

Table 2. IC_{50} of the RBE against ABTS and DPPH radicals and their TP, TF, and A contents

Extract	IC50 (μg.mL^{-1})		TP (mg GE g^{-1} of ext)	TF (mg CE g^{-1} of ext)	A content (mg.L^{-1})
	ABTS assay	DPPH assay			
Ascorbic acid	54.62±2.42	11.02±0.16	-	-	-
Trolox	10.57±1.55	7.19±1.88	-	-	-
RBE					
EtOH	54.72±1.40	8.20±0.16	158.72±5.50	26.57±4.08	96.42±5.97
W	82.04±3.16*	24.84±0.39	59.53±2.55	25.83±4.63	32.91±4.50

Note: The present value of RBE against ABTS and DPPH radicals and their total phenolic (TP) and total flavonoid (TF) contents are presented as mean ± SD. The differences were considered significant at the level of p<0.05 (*).

The RBE with W extract also showed the IC50 against ABTS and DPPH radicals (8.20 ± 0.16 μg.mL^{-1} and 24.84 ± 0.39 μg.mL^{-1}, respectively). The differences were not considered significant at the p<0.05 (*) level to ascorbic acid and Trolox of ABTS and DPPH assays accept RBE with W extract.

Each extract's total phenolic contents (TP) were analyzed and expressed as milligram gallic acid equivalent per gram extract (mg GE g^{-1} of ext.). It was found that the ethanol and aqueous crude extracts had different TP, which was equal to 158.72 ± 5.50 and 59.53 ± 2.55 of gallic acid, respectively. The total flavonoid content (TF) was determined by aluminum chloride colorimetric assay and expressed as catechin equivalent per gram extract (mg CE g^{-1} of ext.). A high level of TF was also found in the ethanol and aqueous crude extracts. The TF in these extracts was equal to 26.57 ± 4.08 and 25.83 ± 4.63 mg CE g^{-1} of ext. The anthocyanin contents were found in RBE in W and EtOH extracts. The highest anthocyanin content was 96.42 ± 5.97 mg.L^{-1} found in EtOH extraction.

Cell viability assay by MTT test

The present study characterized the cell viability effect of RBE on NIH3T3 fibroblast cells by conducting an MTT assay. Cells were treated with various concentrations of extract for 24h. The viability of cells was moderated with the extracts (Fig. 1). Rice berry extracted with EtOH and water did not affect NIH3T3 fibroblast cells hence the water extract at the concentration of 400 mg.mL^{-1}. The RBE by EtOH and water did not show cytotoxicity to fibroblast NIH3T3 (IC80).

Physical evaluation of formulated cream

In the previous experiment, the RBE by EtOH showed the best antioxidant properties and compounds without cytotoxicity. The RBE by EtOH was used to study physical evaluation. The physical evaluation of color, homogeneity, phase separation, thermal stability, pH, and viscosity of formulated cream was performed after freeze-thaw conditions (Table 3). The freeze-thaw condition provides the cream sample at 0°C for 24 hours and 25°C for 24 hours for four cycles. The difference to the base cream (RBE1) was not shown, and the same ranges of pH and viscosity to RBE1 were observed. The pH of the cream was determined to investigate the possible side effects due to acidic or alkaline pH, which can lead to skin irritation and influence the polymer's hydration rate. In general, the cream should have a pH of 6-9 [17].

All formulations had increased viscosity after storage in freeze-thaw conditions. All samples were oil-in-water creams; hence, their water contents might diminish at fluctuating temperatures. Therefore, the suggested storage condition for these products is a constant temperature.

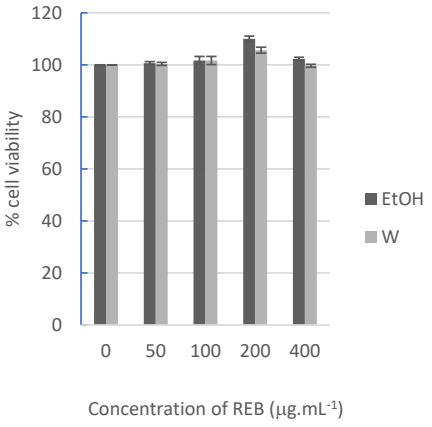

Figure 1. The NIH3T3 fibroblast cell viability to RBEs was tested by MTT assay. The RBEs had no toxicity to fibroblast cells. The RBE can maintain the fibroblast cell with no statistic difference to untreated.

Formulations with suitable viscosity could provide more adhesiveness and spreading efficiency. No phase separation and change in color and odor were observed in all samples after the stability test. However, they seemed to be more viscous. It is observed from the results that the given formulations are relatively stable at

ISSN. 2087-2852
E-ISSN. 2338-1655

accelerated temperature and humidity. The result also gave a slight change in pH value with no statistical difference. The formulated cream with RBEs did not show physical changes compared to the cream base after storage in freeze-thaw conditions. According to these results, the rice berry extracted by ethanol is an excellent natural resource for ingredients in cosmetic products and further applications.

The rice berry has been reported in terms of biological activity with its nutritional value [2,4, 18]. The rice berry from Lamphun, Thailand, was investigated for its advantages. The biological activities, such as antioxidants against free radicals, are linked to bioactive compounds such as terpenes, flavonoids, and polyphenols [19]. These activities are also found in our extract. The rice bran hydrolysate (RBH) extract was composed of total phenolic content (TPC) and showed ferric-reducing antioxidant power (FRAP) [20]. In addition, the bioactive compound in rice berry extracts potential the tyrosinase inhibited in B16 cells [18]. The previous study showed evidence of the antioxidant effect and compounds in colored rice [3,7]. The phenolic compounds and flavonoids had the potential to scavenge free radicals emphasized by Khanema and Manasathien [21]. These studies also emphasized our study that antioxidant compounds are related to antioxidant properties.

The antioxidant compounds found in other plant species are related to antioxidant properties [19,22]. This study showed similar results to a previous study that the monomeric anthocyanin showed ability against free radicals [7] and reduced oxidant properties of ferric [23]. The phenolic compounds modulate antioxidants and involve the sunscreen effect, which increases UV protection [24]. Likewise, using the same protocol as the present study, ethanolic extract of the *Melientha stevia* was found to have SPF maxima 20 [19]. The aromatic or double bond structures are expected as it is a common component in plants with phenolic or flavonoid substances that are the most effective UV radiation absorbers [25]. An earlier study [26] showed that polyphenol extracts from grape seeds are robust to human skin fibroblast against UVA light in vitro [26]. By our studies, the RBE can modulate NIH 3T3 mouse skin fibroblast with no cytotoxicity.

Moreover, some plant extract is a multi-tasking cosmetic ingredient showed its safety and efficacy as an antioxidant, skin lightener, and detoxifying assistant to the skin [27]. The plant extract also showed photoprotective properties with its polyphenols [28]. The RBE from Lamphun, Thailand, also found a polyphenol that can promote health to consumers. Moreover, the polyphenol from the plant extract did not change the physical property of the cream formulation when it was added to the formula [26], which is related to our study that rice berry extract did not show physical changes when compared to the cream base. The aqueous extract of *Polypodium leucotomos* reduces the ultraviolet radiation harmful to the skin without physical change to the cosmetic formula [29]. According to our data, ethanol rice berry extract may be an excellent natural resource for ingredients in body cream products.

Table 3. Physical evaluation of formulated cream

Physical evaluation	RBE1	RBE2	RBE3	RBE4	RBE5
RBE by EtOH	0.000 (mg)	5.000 (mg)	10.000 (mg)	20.000 (mg)	40.000 (mg)
Color	No change	No change	No change	No change	No change
Homogeneity	Yes	Yes	Yes	Yes	Yes
Oil phase separation	No	No	No	No	No
Liquidity separation	No	No	No	No	No
Thermal stability	Stable	Stable	Stable	Stable	Stable
pH	7.0	6.8	6.9	6.9	6.9
Viscosity (cP)	28980	31004	31021	31027	31088

CONCLUSION

The rice berry extract contains various bioactive compounds, such as flavonoids, polyphenols, and anthocyanin, related to its potent anti-oxidative activities. On the other hand, the extract could modulate fibroblast cells because of the antioxidant effect and compounds. The rice berry extract in ethanol also showed the best biological properties. The formulated cream with the RBE did not show physical changes compared to the cream base. Therefore, ethanol rice berry extract is an excellent natural resource for ingredients in cosmetic products.

Acknowledgement

The author thanks the local development project (code: 103001140642) of Lampang Rajabhat University for funding, also the Faculty of Medicine, Chiang Mai University, for laboratory equipment and cell line partially provided by the Bioassay Research Unit, Professor Dr. T. Randall

Lee from Department of Chemistry, University of Houston for his advice as well as Asst. Prof. Yaowat Sirisathitkul and Assoc. Prof. Chitnarong Sirisathitkul for their suggestion on the manuscript. Gratitude will be expressed to Pongsatorn Khamjainuk (staff of Geography, Faculty of Humanities and Social Sciences, Lampang Rajbhat University), who has identified the geographical identification by a geographer.

REFERENCES

[1] Vanavichit, A. 2020. Rice berry rice Thailand's antioxidant-packed nutraceutical and super food. Available at: https://researchoutreach.org/wp-content/uploads/2020/02/Apichart-Vanavichit.pdf.

[2] Poomanee, W., P. Doungsaard, N. Nantharat, P. Leelapornpisid. 2021. Evaluation of biological activities and stability of Thai organic rice berry broken extracts for the anti-aging cosmetology. *Int. J. App. Pharm*. 13(1). 1-4.

[3] Suantai, B., Y. Tragoolpua. 2020. Biological properties of extracts from rice berry and black rice for inhibition of herpes simplex viruses, phytochemical compounds, and antioxidant activities. Proceeding of RSU International Research Conference 2020. Rangsit University. 646-653. Available at: https://rsucon.rsu.ac.th/files/proceedings/inter2020/IN20-232.pdf.

[4] Vanavichit, A. 2021. Rice berry rice for well-being. Open Access Government, Agriculture News. Available at: https://www.openaccessgovernment.org/riceberry-rice-for-well-being/119541/.

[5] Suttireung, P., T. Winuprasith, W. Srichamnong, W. Paemuang, T. Phonyiam, D. Trachootham, 2019. Rice berry rice puddings: rice-based low glycemic dysphagia diets. Asia *Pac. J. Clin. Nutr.* 28(3). 467-475.

[6] Peanparkdee, M., J. Patrawart, S. Iwamoto. 2019. Effect of extraction conditions on phenolic content, anthocyanin content and antioxidant activity of bran extracts from Thai rice cultivars. *J. Cereal Sci*. 86. 86-91.

[7] Yodkeeree, S., P. Thippraphan, W. Punfa, J. Srisomboon, P. Limtrakul, 2018. Skin anti-aging assays of proanthocyanin rich red rice extract, oryzanol and other phenolic compounds. *Nat. Prod. Commun.* 13(8). 967-972.

[8] Saleh, ASM., P. Wang, N. Wang, L. Yang, Z. Xiao. 2019. Brown rice versus white rice: nutritional quality, potential health benefits, development of food products, and preservation technologies. *Compr. Rev. Food Sci. Food Saf.* 18(4). 1070-1096.

[9] Hair, R., J.R. Sakaki, O.K. Chun. 2021. Anthocyanins, microbiome, and health benefits in aging. *Molecules*. 26(537). 1-17.

[10] Anuyahong, T., C. Chusak, S. Adisakwattana, 2020. Incorporation of anthocyanin-rich riceberry rice in yogurts: Effect on physicochemical properties, antioxidant activity and in vitro gastrointestinal digestion. *LWT*. 129. 1-10.

[11] Yamuangmorn, S., C. Prom-u-Thai. 2021. The potential of high-anthocyanin purple rice as a functional ingredient in human health. *Antioxidants (Basel)*. 10(6). 1-21.

[12] Galanakis, C.M., T.M.S. Aldawoud, M. Rizou, N.J. Rowan, S.A. Ibrahim. 2020. Food ingredients and active compounds against the Coronavirus Disease (COVID-19) pandemic: A comprehensive review. *Foods*. 9(11). 1-16.

[13] Mohammadi, P.P., S. Fakhrl, S. Asgary, M.H. Farzaei, J. Echeverria. 2019. The signaling pathways, and therapeutic targets of antiviral agents: Focusing on the antiviral approaches and clinical perspectives of anthocyanins in the management of viral diseases. *Front. Pharmacol*. 10. 1-23.

[14] Abramovic, H., B. Grobin, N.P. Ulrih, B. Cigic. 2018. Relevance and standardization of in vitro antioxidant assays: ABTS, DPPH, and Folin–Ciocalteu. *J. Chem.* 2018. 4608405.

[15] Saansoomchai, P., A. Limmongkon, D. Surangkul, T. Chewonarin, M. Srikummool. 2018. Enhanced VEGF expression in hair follicle dermal papilla cells by Centella asiatica Linn. *Chiang Mai Univ. J. Nat. Sci.* 17(1). 25-37.

[16] Priyanthi, C., R. Sivakanesan. 2021. The total antioxidant capacity and the total phenolic content of rice using water as a solvent. *Int. J. Food Sci.* 2021. 5268584.

[17] Donglikar, M.M., S.L. Deore. 2017. Development and evaluation of herbal sunscreen. *Pharmacog. J.* 9(1). 83-97.

[18] Rodboon, T., S. Okada, P. Suwannalert. 2020. Germinated rice berry rice enhanced protocatechuic acid and vanillic acid to suppress melanogenesis through cellular oxidant-related tyrosinase activity in b16 cells. *Antioxidants (Basel).* 9(3). 1-12.

[19] Sansomchai, P., K. Jumpatong, C. Lapinee, K. Utchariyajit. 2021. *Melientha suavis* Pierre. extract: Antioxidant and sunscreen properties for future cosmetic development. *Chiang Mai Univ. J. Nat. Sci.* 20(1). 1-11.

ISSN. 2087-2852
E-ISSN. 2338-1655

[20] Kaewjumpo, G., S. Thawornchinsombut. 2018. Enhanced storage stability of freeze-dried rice ran hydrolysates by maltodextrin. *Asia-Pac. J. Sci. Technol.* 23(2). 1-11.
[21] Khanema, P., J. Manasathien. 2021. Antioxidant, toxic and cytotoxic activities of Butea superba Roxb. *Asia-Pac. J. Sci. Technol.* 26(4). 1-12.
[22] Peanparkdee, M., J. Patrawart, S. Iwamoto. 2019. Effect of extraction conditions on phenolic content, anthocyanin content and antioxidant activity of bran extracts from Thai rice cultivars. *J. Cereal Sci.* 86. 86-91.
[23] Kittipongpittaya, K., P. Puangploy, P. Kullamethee, P. Fakkheow, P. Kareevate, B. Philkliang. 2021. Antioxidant activities of extract from Makmao seed waste. *Asia-Pac. J. Sci. Technol.* 26(2). 1-7.
[24] Hubner, A., F. Sobreira, A.V. Neto, C.A.S.O. Pinto, M.F. Dario, I.E.C. Diaz, F.R. Lourenco, C. Rosado, A.R. Baby, E.M. Bacchi. 2019. The synergistic behavior of antioxidant phenolic compounds obtained from winemaking waste's valorization, increased the efficacy of a sunscreen system. *Antioxidants (Basel).* 8(11). 1-16.
[25] Aleixandre-Tudo, J.L., W. Toit. 2018. The role of UV-visible spectroscopy for phenolic compounds quantification in winemaking. In: Solís-Oviedo, R.L., Á. de la Cruz Pech-Canul. Frontiers and New Trends in the Science of Fermented Food and Beverages. DOI: 10.5772/intechopen.79550.
[26] Yarovaya, L., N. Waranuch, W. Wisuitiprot. 2021. Effect of grape seed extract on skin fibroblasts exposed to UVA light and its photostability in sunscreen formulation. *J. Cosmet. Dermatol.* 20(4). 1271-1282.
[27] MERCK. 2020. EMBLICA: The ayurvedic key to strengthening your skin. Available at: https://cosmeticsbusiness.com/news/article_page/EMBLICA_The_ayurvedic_key_to_strengthening_your_skin/166091.
[28] Almeida, W.A.S., A.S. Antunes, R.G. Penido, H.S.G. Correa, A.M. Nascimento, A.L. Andrade, *et al.* 2019. Photoprotective activity and increase of SPF in sunscreen formulation using lyophilized red propolis extracts from Alagoas. *Rev. Bras. Farmacogn*. 29(3). 373-380.
[29] Parrado, C., J. Nicolas, A. Juarranz, S. Gonzalez. 2020. The role of the aqueous extract Polypodium leucotomos in photoprotection. *Photochem. Photobiol. Sci.* 19. 831-843.

Morphological Variation of Asian Small Lizards genus *Tytthoscincus* Linkem, Diesmos & Brown (Squamata : Scincidae) in Indonesia

Richo Firmansyah[1*], Awal Riyanto[2], Nia Kurniawan[1]

[1]Department of Biology, Faculty of Mathematics and Natural Sciences, University of Brawijaya, Malang, Indonesia
[2]Museum Zoologicum Bogoriense, Research Center of Biology, National Research and Innovation Agency (BRIN), Bogor, Indonesia

Abstract

Morphological variations in species with a relatively broad distribution, including the genus *Tytthosincus*, were likely a result of island isolation. This research was conducted to map the morphological variations of the genus *Tytthoscincus* in Indonesia. A total of 32 specimens of the Tytthoscincus scientific collection in the Zoologicum Bogoriense Museum (MZB) - National Research and Innovation Agency (BRIN) and identified as *T. temmincki*, *T. textus*, and *T. parvus* have been examined and data collection which includes six morphometric characters and 12 meristic characters. Morphometric data were analyzed in univariate and multivariate. Univariate analysis was carried out by the Kruskal-Wallis test, while multivariate analysis was done with the Principal Component Analysis (PCA) test. The results showed morphology in *T. temmincki* and *T. textus*, namely the number of loreal scales and tympanum diameter. Both *T. temmincki* and *T. textus* consist of two groups, but the morphological variation in *T. temmincki* and *T. textus* in this study has yet to provide certainty as a different species. However, one was *T. textus* Type 2, isolated from other species on Jampea Island, Sulawesi. Further research was needed to clarify the taxonomic status of these variations by increasing the number of adequate samples supported by the molecular analysis approach.

Keywords: meristic, morphometric, species, *Tytthoscincus*, variation.

INTRODUCTION

In 2011, Linkem et al. Classified *Sphenomorphus* species into a new genus, *Tytthoscincus*. Genetic and morphological data show that small mountain species such as *S. butleri* (Boulenger), *S. Ishaki* (Grismer), and others form a monophyletic group centered phylogenetically on the genus *Tytthoscincus* [1]. The morphological characteristics of the genus *Tytthoscincus* are a body size of less than 45 mm (SVL= *Snout Vent Length*), and temporal scales cannot be distinguished from lateral body scales in either size or shape [2]. *Tytthoscincus* weighs around 0.63 – 3.25 grams. The genus *Tytthoscincus* is distributed in the Southeast Asian region such as Malaysia, Indonesia, to the Philippines [3].

Lygosoma temmincki was described by Duméril and Bibron in 1839, with morphological characteristics of this species having jaws parallel to the snout, smooth scales, small longitudinal slit-shaped ear holes, and short limbs. *Lygosoma temmincki* was found on Java Island [4]. Mueller, in 1894 described a species found on the island of Sulawesi at an altitude of 3900 meters above sea level as *Lygosoma texum*. This species has morphological characteristics such as a short and pointed snout, no supranasal, and five supraocular scales. The ventral part of the chin is gray. The head length of *L. texum* is around 50 mm, with a tail of 56 mm [5]. In 1897, *Lygosoma parvum* was described by Boulenger with the morphological characteristics of an elongated body shape with a total body length of 78 mm, a short and blunt snout, scaly lower eyelids, four supraocular scales, eight supraciliary scales, no supranasal, unclear tympanum hole, hind limbs longer than forelimbs, and a brown body with dorsal yellowish brown dots. *Lygosoma parvum* was found in Luhu, Central Sulawesi, at 1000 - 1600 feet [6].

Linkem *et al.* [7] redescribed *T. Parvus* characterized by a small body size of less than 45 mm, small fingers, and a fourth finger longer than or equal to the third finger. This species is found on the island of Sulawesi [7]. Meanwhile, Grismer *et al.* [1] described *T. Temmincki* with morphological characteristics having a range of 4 - 5 supralabial scales, two loreal scales, 68–80 paravertebral scales, 62–72 ventral scales, 9–11 scales on the lamella of the fourth toe, smooth lamella texture, and a dark line on the dorsolateral [1]. The distribution of *T. temmincki* is in Java, Sumatra, and Sulawesi [8]. Grismer *et al.* in 2016 described *T. textus* with a short snout, 42 mm SVL size, reddish brown above with reticulation, and dark limbs [1]. Karin *et al.* in 2016 also hypothesized that *S. textus* belongs to the *Tytthoscincus* group,

*Correspondence address:
Richo Firmansyah
Email : richo.firmansyah25@gmail.com
Address : Dept. Biology, University of Brawijaya, Veteran Malang 65145, Indonesia.

ISSN. 2087-2852
E-ISSN. 2338-1655

characterized by an adult body size of 38 mm and a bright stripe on the postorbital and dorsolateral [2]. This hypothesis was proven by Grismer *et al.* in 2017 by confirming that *S. textus* is included in the phylogeny of the genus *Tytthoscincus* [9]. This study aimed to map the morphological variation of the genus *Tytthoscincus* in Indonesia.

MATERIAL AND METHOD

Data Collection

The research data were taken from scientific collections in the form of wet-preserved specimens at the Museum Zoologicum Bogoriense (MZB), Herpetology Laboratory, Center for Biosystematics and Evolution Research, Indonesian National Research and Innovation Agency (BRIN), Cibinong. Morphometric and meristic character data were collected to compare the genus *Tytthoscincus* in Indonesia (Fig. 1).

Morphometric characters refer to Grismer *et al.* [9], and specimens were measured using Image J software [10]. These morphometric characters include snout-cloaca distance length (SVL = snout-vent length) measured from the rostral end to the cloaca margin, head length (HdL) measured from the anterior edge of the ear hole to the rostral end, tympanum diameter (TD, tympanum depth) measured from the anterior to the posterior edge of the tympanum, length of the distance between the armpit and the thigh fold (AXG, axilla groin length), forelimb length (FL, forelimb limbs), and hind limb length (HL, hind limbs). Meristic characters include the number of supralabials, infralabials, supraoculars, supraoculars attached to frontal scales, loreals (Fig. 2), middle, paravertebral, ventral scale rows, third finger lamellae, fourth finger lamellae, and meristic character with the shape of the tympanum.

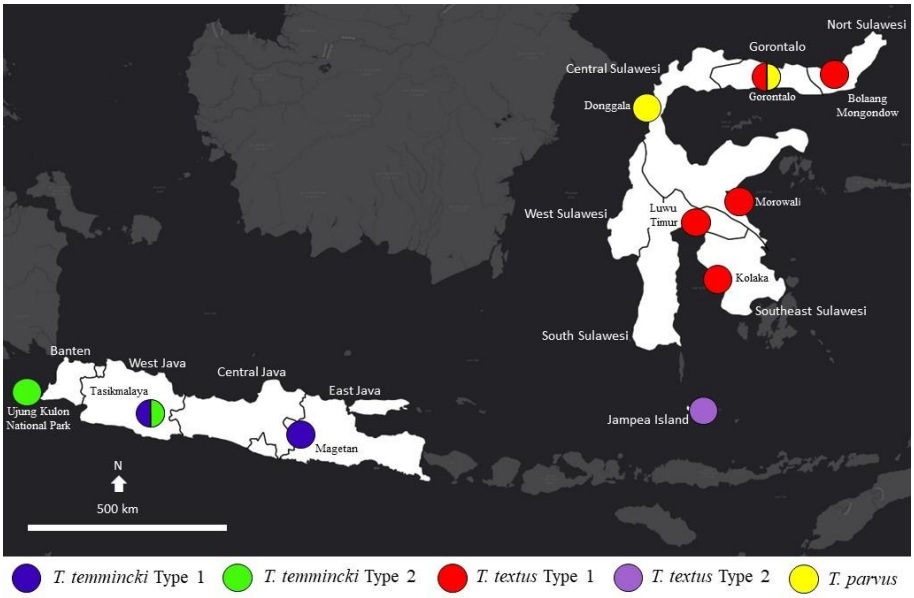

Figure 1. Distribution of variation *Tytthoscincus*.

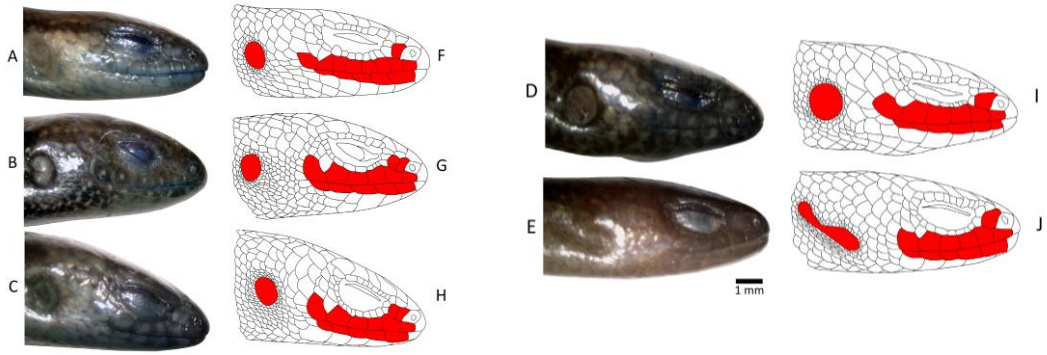

Figure 2. Morphological variation of *Tytthoscincus* based on the loreal scale number and tympanum diameter. A = F, *T. temmincki* type 1; B = G, *T. temmincki* type 2; C = H, *T. textus* type 1; D=I, *T. textus* type 2; E = J, *T. parvus*

ISSN. 2087-2852
E-ISSN. 2338-1655

Data Analysis

A total of 32 adult *Tytthoscincus* specimens (from Java and Sulawesi Island) were used in the analysis, and due to the small sample size, the statistical analysis did not differentiate between males and females. These specimens were initially grouped into four operational taxonomic units (OTU/Operational Taxonomy Units) based on variations of loreal scales number and shape.

Morphometric data were standardized in ratios (HdL/SVL, TD/SVL, AXG/SVL, FL/SVL, HL/SVL, and TD/HdL). Kruskal-Wallis analysis was carried out separately for each morphometric character to determine whether there were differences between OTUs (*T. temmincki* type 1, *T. temmincki* type 2, *T. textus* type 1, *T. textus* type 2 and *T. parvus*). This analysis method followed the Zar method [11]. Each morphometric character is a dependent variable, and OTU is an independent variable or predictor. Multivariate analysis used the principal component analysis (PCA) test to reduce multidimensional correlations into several uncorrelated variables. All analyzes were performed by RStudio statistical software.

RESULT AND DISCUSSION

Tytthoscincus temmincki is grouped into two, namely, type 1 with the characteristic of only having one loreal scale and type 2 for specimens with two loreal scales. The same applies to *T. textus* in type 1 and type 2. Meanwhile, *T. parvus* is only one group because there is no variation in the number of loreal scales (Fig. 2). The results of the Kruskal-Wallis analysis showed that only two ratio characters had significantly different values between OTUs, consist of TD/SVL and TD/HdL (Table 1). Of all OTUs, *T. parvus* had the smallest tympanum size (TD/SVL and TD/HdL). The largest tympanum belonged to *T. textus*, with *T. textus* type 1 and *T. textus* type 2.

Multivariant analysis with PCA on PC1 and PC2 showed that only *T. parvus* separated from *T. temmincki* type 1 and type 2, and *T. textus* type 1 and type 2. PC1 and PC2 cumulatively explained 73.8% of the variation (Table 2, Fig.3). In PC_1, the morphometric ratio AXG/SVL had negative loading, while the other five morphometric ratios TD/SVL, TD/HdL, FL/SVL, HL/SVL, and HdL/SVL had positive loading values. As for PC2, AXG/SVL, TD/HdL, FL/SVL, and TD/SVL had positive loading values, while HL/SVL and HdL/SVL had negative loading values.

Based on this study, *T. parvus* is distinct from *T. temmincki* and *T. textus*. The variation in the number of loreal scales in both *T. temmincki* and *T. textus* should be suspected as a phenomenon of intra-species variation. This variation may be part of the ongoing speciation process. Another possibility is that the number of samples for morphometric analysis in both *T. temmincki* type 1 and type 2 and *T. textus* type 2 needed to be more significant (more samples needed).

The wide distribution area likely influences morphological variation in *T. temmincki* and *T. textus*. The distribution area includes not only one large island but also small islands with complex structures [3]. Geographical barriers play a role in causing variation. The range limit of a species is usually aligned with a significant barrier to dispersal, such as a river, sea, or mountain [12].

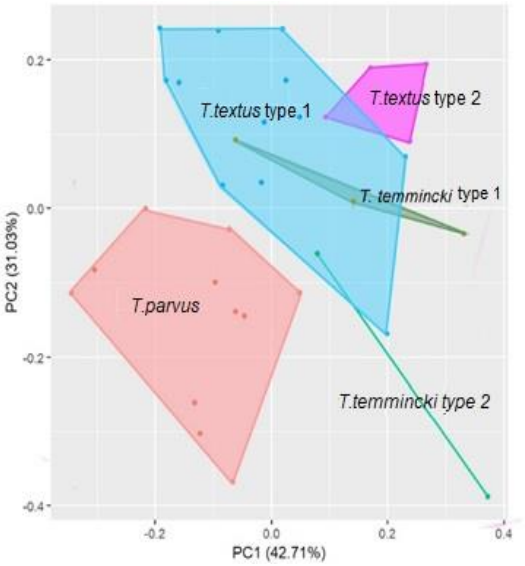

Figure 3. Biplot principal component analysis of *Tytthoscincus* morphological variations on PC1 and PC2

In this study, the distribution of *T. textus* type 2 was isolated from the distribution of other species on Jampea Island (Fig. 1). This allows the variation to be very different from *T. textus* type 1, which originates from Sulawesi Island. The morphological variations found can be used as a future taxonomic review and to provide certainty whether *T. textus* type 2 from Jampea Island is different from *T. textus* type 1 from Sulawesi Island as a distinct species, through molecular analysis and larger/ representative sample size.

ISSN. 2087-2852
E-ISSN. 2338-1655

Table 1. Mean values and Kruskal-Wallis test statistics on variation in morphometric ratios between OTUs and comparison of meristic characters.

Character	OTU					X^2	*P-value*
	T. temmincki type1	*T. temmincki* type2	*T. textus* type1	*T. textus* type2	*T. parvus*		
N	type 1 (n=3)	type 2 (n=2)	type 1(n=12)	type 2 (n=4)	(n=11)		
HdL/SVL	0.203 ± 0.007	0.221 ± 0.017	0.200 ± 0.013	0.206 ± 0.014	0.205 ± 0.015	4.0686	0.3968
SVL	0.033 ± 0.004*	0.033 ± 0.003*	0.034 ± 0.003*	0.040 ± 0.003*	0.024 ± 0.003*	24.825*	5.456e^{-05}*
AXG/SVL	0.545 ± 0.024	0.479 ± 0.103	0.562 ± 0.020	0.536 ± 0.036	0.546 ± 0.025	6.1551	0.1879
FL/SVL	0.185 ± 0.012	0.175 ± 0.005	0.159 ± 0.016	0.173 ± 0.013	0.158 ± 0.016	8.0561	0.08954
HL/SVL	0.283 ± 0.043	0.229 ± 0.013	0.251 ± 0.024	0.272 ± 0.021	0.257 ± 0.022	7.3068	0.1205
TD/HdL	0.164 ± 0.011*	0.148 ± 0.000*	0.170 ± 0.012*	0.196 ± 0.004*	0.116 ± 0.015*	26.624*	2.368e^{-05}*
Supralabials	8(1), 6(2)	6	6	6	7(1), 6(10)		
Infralabials	5	5	5	6(1), 5(3)	5		
Supraoculars	4	4	4	4	4		
Loreals	1	2	2 (10), 1(2)	1	1		
Distribution	West Java, East Java	West Java	Gorontalo, Southeast Sulawesi, Central Sulawesi	South Sulawesi	Sulawesi, Gorontalo, Central Sulawesi		

Notes: * significant; HdL = head length, SVL = snout-vent length, AXG = axilla groin length, FL = forelimb length, HL = hind limb length, and TD = tympanum diameter.

Table 2. Principle component analysis (PCA) and factor loading.

PCA variable	PC1	PC2	PC3	PC4	PC5	PC6
SD	1.601	1.365	0.935	0.709	0.442	0.057
Proportion of variance	0.427	0.310	0.146	0.084	0.033	0.001
Cumulative	0.427	0.738	0.883	0.967	0.999	1.000
Loading						
HdL/SVL	0.304	- 0.452	- 0.462	0.598	0.300	0.208
TD/SVL	0.464	0.427	- 0.347	0.052	0.014	- 0.692
AXG/SVL	-0.316	0.448	0.262	0.780	- 0.149	- 0.011
FL/SVL	0.452	0.035	0.684	0.042	0.569	- 0.004
HL/SVL	0.505	- 0.287	0.295	0.128	- 0.748	0.007
TD/HdL	0.365	0.574	- 0.204	- 0.117	- 0.067	0.691

Notes: HdL = head length, SVL = snout-vent length, AXG = axilla groin length, FL = forelimb length, HL = hind limb length, and TD = tympanum diameter.

The existence of habitat isolation was formed due to evolutionary factors, consisting of population differentiation between isolated islands during the Pleistocene era, which resulted in fluctuating sea levels and the separation of land by shallow seas [13]. Spatial and temporal variation in intraspecific body size or morphology is driven by differences in the heritability of phenotypic traits and the basis of evolution and adaptation to environmental changes [14].

CONCLUSION

Morphological variations in *T. temmincki* and *T. textus* are based on the number of loreal scales and the diameter of the tympanum. As for *T. parvus*, no such variation was found. Both *T. temmincki* and *T. textus* consist of two groups. The morphological variations in this study in *T. temmincki* and *T. textus* do not provide certainty as different species. However, one of them, *T. textus* type 2, is isolated from other species on the Island of Jampea, Sulawesi. Further research is needed to clarify the taxonomic status of these variations by adding an adequate number of samples supported by molecular analysis approaches.

Acknowledgement

This research was supported by the Research Assistant Program from the National Research and Innovation Agency (BRIN) (Number 4/II/HK/2023). We thank Wahyu Trilaksono, who has helped access the samples in this research.

REFERENCES

[1] Grismer, L.L., A.M. Mohd, L.W. Perry, A. JR. Sharhrul, W.L. Charles. 2016. The transfer of two clades of Malaysian Sphenomorphus Fitzinger (Squamata: Scincidae) ointo the genus *Tytthoscincus* Linkem, Diesmos, & Brown and the description of a new Malaysian swamp-

dwelling species. *Zootaxa.* 4092(2). 231–242. DOI: 10.11646/zootaxa.4092.2.6.

[2] Karin, B.R., D. Indraneil, M.B. Aaron. 2016. Two new species of diminutive leaf-litter skinks (Squamata: Scincidae: *Tytthoscincus*) from Gunung Penrissen, Srawak, Malaysia (northern Borneo). *Zootaxa*. DOI: 10.11646/zootaxa.4093.3.7.

[3] Grismer, L.L., L.W. JR. Perry, B.A. Amirrudin, H.B.S. Baizul, S.M. Afiq, A.R. Sayed, H.Q. Evan. 2018. Two new *Tytthoscincus* Linkem, Diesmos & Brown (Squamata: Scincidae) from Peninsular Malaysia and another case of microsyntopy between ecologically specialized, unrelated, leaf-litter species. *Zootaxa.* 4425(1). 087–107. DOI: 10.11646/zootaxa.4425.1.5.

[4] Dumeril, P.A.M.C., G. Bibron. 1839. Erpetologie generale historie naturelle complete des reptiles. Paris, Lidrairie Encyclopedqie De Roret.

[5] Muller, F. 1894. Reptilian und amphibians aus Celebes. Verh.Ges.Basel 10 (3).

[6] Boulenger. 1897. Zoological society of London for the year 1897: 215 Juni 1897. Messrs Longmans Green and Co. London.

[7] Linkem, C.W., C.D. Arvin, M.B. Rafe. 2011. Molecular systematics of the Philippine forest skinks (Squamata: Scincidae: Sphenomorphus): testing morphological hypotheses of interspecific relations. *Zool. J. Linn. Soc.* 163. 1217–1243. DOI: 10.1111/j.1096-3642.2011.00747.x.

[8] The Reptile Database. 2022. Tytthoscincus temmincki (Dumeril & Bibron, 1839). Available at: https://reptile-database.reptarium.cz/species?genus=Tytthoscincus&species=temmincki&search_param=%28%28genus%3D%27Tytthoscincus%27%29%29.

[9] Grismer, L.L., Q. Evan, L.W.Jr. Perry, A. Shahrul, B.N. Ehwan, M.I. Nur Amalina, A. Norhayati. 2017. Systematics, ecomorphology, cryptic speciation and biogeography of the lizard genus Tytthoscincus Linkem Diesmos & Brown (Squamata: Scincidae) from the sky-island archipelago of Peninsular Malaysia. *Zool. J. Linn. Soc.* 20. 1- 37.

[10] Rueden, C., S. Johannes, Mark., E.D. Barry. 2017. Image J2: ImageJ for the next generation of scientific image data. *BMC Bioinformatics*. 18. 529. DOI: 10.1186/ s12859-017-1934-z.

[11] Zar, J.H. 2010. Biostatistical Analysis, 5th Ed. Prentice Hall Inc., USA.

[12] Jaya, I. 2018. Meniliki variasi morfologi Biawak Air dari pulau Buton, Muna, dan Kadatua. *Warta Herpetofauna.* 10(2). 35 – 40.

[13] Barter, M., R.B. Luke, D. Andressa, T.G. Celine, T. Reid, M.S. Glenn, M. Shai, G.C. David. 2022. Predictors of geographic range size in Australian skinks. *Glob. Ecol. Biogeogr.* 31. 113–122. DOI: 10.1111/geb. 13419.

[14] Schmitt, L.H., R.A How, S. Hisheh, J. Goldberg, I. Maryanto. 2000. Geographic pattern in genetic and morphological variationin two skink species along Banda Arcs, South Eastern Indonesia. *J. Herpetol.* 34(2). 240–258. DOI: 10.2307/1565421.

ISSN. 2087-2852
E-ISSN. 2338-1655

Shelf Life and Quality Stability Determination of Drying Shredded Dumbo Catfish (*Clarias Gariepinus*)

Matheus Nugroho[1], Eli Susanti[1], Sugiono Sugiono[2]

[1]Fisheries Product Technology, Faculty of Agriculture, Universitas Yudharta, Pasuruan, Indonesia
[2]Fisheries Agribusiness, Faculty of Agriculture, Universitas Islam Madura, Pamekasan, Indonesia

Abstract

The purpose of this study was to determine the stability of the quality and shelf life of dried shredded African catfish (*Clarias gariepinus*). The method used in this study was quantitative research using an experimental method using a completely randomized design with three different drying treatments. The stability of the drying quality of African catfish shredded (*Clarias Gariepinus*) was the color of African catfish shredded with varying methods of drying, giving panelist scores ranging from 2.36 to 4.4; organoleptic value of African catfish floss ranged from 2.88 to 4.16; panelists' assessment of the texture of African catfish shredded ranged from 2.12 - 4.56; the taste of African catfish floss ranges from 2.08 to 4.44. Shredded African catfish with different drying durations that were most in demand by panelists was sample A3 shredded African catfish steamed and dried for 4 minutes in a spinner machine with a color score of 4.4, aroma 4.16, texture 4.56, and taste 4.44. The results of measurements using distribution turnover explained that the shelf life of shredded catfish could last up to 7 months and was reduced to 6 months to anticipate product damage earlier.

Keywords: quality, shelf life, shredded dumbo catfish.

INTRODUCTION

Fish is a source of animal protein. Besides being consumed directly after cooking, fish can also be processed into other food ingredients that can increase economic added value and extend shelf life while maintaining nutritional content. Various types of fish can be processed into good nutritious food products, such as mackerel, tuna, catfish, and others. Processed food is produced from various fish, such as dumplings, *pempek*, shredded, crackers, *amplang*/*kuku macan* snack, and so on [1].

Catfish is a freshwater fish that is widely consumed by the public. Catfish have good nutritional content for health and contain lower mercury than sea fish. Every 100 g of catfish contains energy (145 calories), protein (15.45 g), fat (9.09 g), sodium (65 mg), cholesterol (82 mg), and saturated fatty acids (2730 mg). Catfish consisting of heads, fish skin, fish meat, and fish bones can be processed into various processed food products. Fish meat can be processed into nuggets, fish sticks, meatballs, amplang, etc. Fish heads and spines can be processed into fish crackers, and catfish skin can be made into skin crackers [2].

Shredded catfish is a processed fishery product made from catfish meat, which includes preparing catfish meat, steaming, grinding fish meat, making shredded seasoning, mixing fish meat and spices and coconut milk, seasoning impregnation, and finally frying the fish meat and then packing it and stored [3]. Shredded is a long-lasting food with high protein and low cholesterol levels. Drying in the production process of shredded catfish is a process that affects the acceptability and shelf life of the shredded catfish. The quality of shredded fish is that it has a soft shape, tastes good, has a distinctive smell, and has a relatively long shelf life [4]. The quality characteristics of shredded fish are influenced by the type of fish used as the main ingredient, the composition of the spices, and the presence of other additives [5]. Determination of the quality of shredded fish refers to the quality requirements for shredded fish as described in SNI 01-3707-1995 [6,7]. Shredded quality parameters and the level of consumer acceptance of organoleptic tests [8], including color, aroma, taste, and texture, were assessed. Based on these descriptions, this research aims to determine the quality, stability, and shelf life of drying shredded catfish (*Clarias gariepinus*).

RESEARCH METHODS

Material

The main ingredient used in shredded is 2 kg of fresh catfish (*Clarias gariepinus*) obtained from catfish farmers in Purwosari Pasuruan. Additional ingredients for making floss are ten pieces of shallots, six pieces of garlic, palm oil, lemongrass, galangal, coriander, pepper, 50 grams of brown sugar, 50 grams of chilies, 50 mL of coconut milk, three pieces of aromatic

* Correspondence Address:
Sugiono
E-mail : sugiono@uim.ac.id
Address : Universitas Islam Madura, JL. Pondok Peantren Miftahul Ulum Bettet, Pamekasan, 69317

ISSN. 2087-2852
E-ISSN. 2338-1655

leaves, three pieces of lime leaves, one piece of lemongrass and salt obtained from a traditional market in Purwosari – Pasuruan.

Method

This research was conducted experimentally using a single factor Complete Randomized Design with three treatments. Treatment A1: shredded African catfish steamed without drying on a spinner machine, A2: shredded African catfish steamed and dried on a spinner machine for 2 minutes, A3: shredded African catfish steamed and dried on a spinner machine for 4 minutes. Parameters observed included color, aroma, texture, taste, and shelf life. Methods of data collection using interview techniques, observation, and organoleptic testing of catfish shredded products using 25 untrained panelists. Determination of shredded shelf life used the conventional method of extended storage studies (ESS) in the form of literature values and distribution turnover.

Stages of Processing Shredded Catfish

Receiving raw materials

Receiving raw materials, namely live catfish received weighing ± 2 kg. The raw material that is received must be organoleptically tested first, then shorted by quality analysis. Handling of catfish raw materials is carried out until the shredded processing is complete. The freshness level of fish will significantly determine the quality of the final product [9]. Materials must remain in good condition until they are used [10].

Washing and weeding process

The catfish was immediately killed and weeded. Weeding is done by removing the head, gills, catfish skin, and stomach contents. The tail of the fish is not cut because it shortens the time. The weeding waste in the form of blood and stomach contents is immediately disposed of so that it does not mix into the clean area [11].

Steaming process

The steaming process is carried out by adding water as much as ¼ of the height of the steamer (± 20 L) to the boiler or boiling device. Steaming is done at ± 95°C for 1 hour. The maturity of the fish meat can be seen from the clearly separated flesh and skin, and the change in the color of the meat to slightly brownish. In undercooked fish, separating the bones, skin, and flesh can be difficult. Whereas if it takes too long, the texture of the meat will be mushy [12].

Shredding process

After the steaming of the fish meat is complete, the catfish meat is shredded. The shredding process involves cutting the fish meat into smaller pieces and separating the meat from the catfish spines. This reduction will affect the long frying time of shredded [13]. Shrinking of fish meat is done until the fish meat is in the form of cotton with a soft and uniform texture [14].

Mixing of spices

The raw materials for spices are mashed with a blender. The spices used include 50 grams of brown sugar, 50 mL of coconut milk, three pieces of aromatic leaves, three pieces of lime leaves, one piece of lemongrass, 25 mL of cooking oil, 1 gram of salt, and 3 grams of white sugar. For the ground spices in the process of making this shredded meat, use ten pieces of shallots, six pieces of garlic, 50 grams of red chilies, one segment of ginger, one segment of galangal, one segment of turmeric, 1 gram of coriander and 1 gram of pepper. The spices are mashed and then put in the shredded catfish meat. Let the spices seep into the catfish meat.

Frying process

The catfish meat that has been mixed with spices is fried until dry and brown. Every three times frying, the oil is changed because the quality of the oil is decreased [15]. During the frying process, there is a reduction in water content which will be replaced by oil. It will also cause changes in color, aroma, texture, and taste, as well as the formation of volatile compounds, which generally come from aromatic compounds.

Process of Draining Oil from Shredded Fish

Shredded fish that has been cooked is put into an oil slicer (spinner) quickly, carefully, and sanitarily, which aims to separate the fish meat from the oil used for frying. After draining in the spinner machine, the shredded catfish is poured into a flat container covered with plastic. While the cooling takes place, the process of selecting the thorns and decomposing the meat that is still lumpy is carried out. The result of slicing is shredded fish with a dry texture because the oil has been separated from the shredded. The main principle of the slicing machine is that the remaining frying oil attached to the shredded can be more thorough and speed up the production process [16]. To produce dry and durable shredded, cooked shredded is pressed to reduce the oil [17,18].

Packaging Process

The packaging process is carried out by weighing the shredded in large and small sizes that have been labeled. After being put into the shredded packaging, it is pressed with a heat sealer to strengthen the packaging. Each pack has a large one, 100 grams, and a small one, 50 grams of shredded. Product packaging is to protect and prevent product damage and extend shelf life.

Storage Process

Shredded fish packed in plastic is pressed with a machine and stored in a storage cupboard. Food storage is placed in cupboards, not on the floor, and storage cabinets are made of anti-rats and insects [10]. Product contamination that is not covered comes from biogenic dust containing mites, fungi, and bacteria [19]. Polyethylene packaging is the best in maintaining quality, both at room temperature and cold storage.

Data collection

Data collection is an essential step for conducting research. With knowing data collection techniques, researchers will get data that meets data standards. The techniques used by the author in this study are as follows.

Questionnaire technique

Questionnaires are data collection techniques that are carried out by providing a series of written questions to respondents or commonly called panelists. There are two types of questionnaire techniques, namely closed and open. In this study, researchers used a closed questionnaire technique to get answers from specific results according to the panelist's experience after tasting or tasting the results of the variables that have been provided. This questionnaire is intended for untrained panelists of 25 respondents with a scale of 1-5 (1 = dislike; 2 = don't like it; 3 = quite like it; 4 = like it; and 5 = really like it).

Extended Storage Studies (ESS) technique

Shelf life assessment techniques in this study used conventional methods (Extended Storage Studies/ESS). The ESS method used in this research is literature value and distribution turnover, which determines the shelf life of food products based on information on similar products available on the market.

Data Analysis

In this research on shredded African catfish with different drying durations, data analysis was carried out using Ms. Excel to look for organoleptic test data using Friedman's test with a significant level of 5% and study of shredded shelf life using conventional methods in the form of literature values and distribution turn over.

Organoleptic analysis and study of the shelf life of shredded African catfish (*Clarias gariepinus*) were conducted with different drying durations. The African catfish shredded product results were then subjected to organoleptic tests using the Friedman test at a significant level of 5%.

RESULTS AND DISCUSSION

Organoleptic Test

Identification and processing of 25 respondent questionnaires include the demographics of the research panelists, i.e. gender, age, education, and institution, in detail presented in Table 1. The percentage of males is 40%, while the percentage of females is 60%. Demographic data on the age of the respondents shows that most respondents are below 26 years old, with a percentage value of 60%, while the lowest percentage is for respondents below 21 years old at 4%.

Demographic education data shows that at least respondents have a junior high school education level. Undergraduate education (bachelor's degree) respondents show the highest percentage. Institutional demographic data shows that respondents from Yudharta University institutions are 32%, while non-Yudharta University respondents are 68%.

Organoleptic test on the three research variables, namely A1 (steamed African catfish + spinner without drying); A2 (dumbo catfish steamed + with spinner drying 2 minutes); A3 (steamed dumbo catfish + spinner drying 4 minutes) includes testing the level of preference for color, aroma, taste, and texture. Based on the results of the African catfish shredded preference test with three different treatments (Table 2), it was shown that the panelists liked the shredded catfish sample (A3), which was steamed and dried for 4 minutes in a spinner machine in terms of color, aroma, texture, and taste [5].

Color

Color performance is an indicator for determining attractiveness, characteristics, and quality attributes [20]. Based on the results of organoleptic tests conducted by 25 panelists, the color of shredded African catfish with different drying methods gave panelist scores ranging from 2.36 to 4.4 (Table 2).

ISSN. 2087-2852
E-ISSN. 2338-1655

Table 1. Demographics of Respondents/ Panelists

Description	number (people)	Percentage (%)
Gender		
Man	10	40
Woma	15	60
Age		
Below 21 years old	1	4
Below 26 years old	15	60
Below 31 years old	4	16
Below 36 years old	3	12
More than 36 years old	2	8
Description	**number (people)**	**Percentage (%)**
Education		
Elementary school	0	0
Junior high school	3	12
Senior High School	10	40
Associate Degree	0	0
Bachelor Degree	12	48
Master Degree	0	0
Institution		
Yudharta University	8	32
Non Yudharta University	17	68

Table 2. Scores of Organoleptic Test Results

Treatment	Parameters Results			
	Color	Scent	Texture	Flavor
A1	2.36	2.88	2.12	2.08
A2	4.20	4.12	4.04	4.00
A3	4.40	4.16	4.56	4.44

In the organoleptic test results for the color of shredded fish, the lowest score was 2.36 (disliked) in treatment A1, while the highest score was 4.4 in treatment A3. The results of the panelists' assessment explained that the African catfish floss in sample A3 had a brown color that looked soft and was almost the same as in sample A2. In contrast, sample A1 had a color that tended to be darker brown (Fig. 1) due to lots of oil deposits because it had not gone through the spinner machine drying process.

Sample A1 **Sample A2** **Sampel A3**

Figure 1. Shredded catfish

The organoleptic value of the color of shredded catfish in this study was lower than that of the color of previous studies with shredded lampam fish (5.24) [21] and shredded tuna [22]. Another value range was 4.70 - 5.23 for shredded tuna [23], a value range of 4.70 - 5.17 for shredded fish [24], and the organoleptic range for the color of shredded fish was 3.76 – 5.08 [25]. The Friedman test results showed a significant difference in the color of African catfish shredded in the different drying duration treatments.

Scent

Based on the results of organoleptic tests on 25 untrained panelists, the aroma value of shredded catfish can be seen in Table 2. The results show that the organoleptic value of the aroma of shredded catfish with different drying methods ranges from 2.88 to 4. 16 (likes). The average value of panelists' preference for the aroma of shredded African catfish is with the lowest score of 2.88 in treatment A1, while the highest score was 4.16 in treatment A3.

Panelists preferred the scent of African catfish floss using the method of steaming and spinner drying for 4 minutes with a value of 4.16, compared to the method of steaming African catfish and spinner drying for 2 minutes and without spinner drying. The panelists further explained that all the African catfish shredded samples had a pleasant scent. It was influenced by the shredded manufacturing process, which used spices of the same type and amount ratio. The type of fish and the composition of the shredded seasoning can

affect the resulting shredded aroma [22]. Previous studies showed that the organoleptic value of aroma ranges from 4.53 to 4.92 in shredded tuna [23], while the value range from 4.78 - 4.92 [24] and 3.95 - 4.79 [25] in shredded fish. The results of the Friedman test show that the F table is smaller than the F count, meaning that there is a significant difference in the scent of shredded catfish with different drying durations.

Texture

The texture of the African catfish shredded can be seen in Table 2. The study results showed that the panelists' assessment of the African catfish shredded texture ranged from 2.12-4.56. Texture is a significant characteristic, both in fresh food and processed products [10]. The freshness and quality of the raw materials will significantly influence fried products' crispness.

Preference will be given to crunchy foods that are hard, easy to bite into, and make a crunchy sound. The organoleptic value of the catfish shredded texture average value of the lowest preference is 2.12 (dislikes) A1, and the highest value is 4.4 from treatment A3. The panelists further explained that the shredded African catfish in sample A3 generally had the most suitable texture for shredded fish, not too oily and brittle. The results of this study were higher than shredded tuna by 2.47 [22], While the results of other studies related to the organoleptic value of shredded fish texture were 4.62-5.08 [23], 4.64-5.30 [24], and 4.12-4.98 [25].

Differences in texture values can occur due to different species and manufacturing methods. Friedman's test results show that significant difference in the texture of African catfish shredded at different drying durations.

Flavor

Based on the results of organoleptic tests on 25 untrained panelists, the taste value of the shredded African catfish can be seen in Table 2. The results showed that the panelists' assessment of the African catfish shredded taste ranged from 2.08 to 4.44. The organoleptic value of the taste of shredded catfish was lower than shredded tuna at 5.3 and shredded tuna at 5.51 [22], shredded lampam fish at 5.04 [21], the organoleptic value of shredded fish flavor at 4.64 - 5.02 [23], 4.97-5.08 [24] and 3.95-5.30 [25].

Sulthoniyah *et al.* [26] explained that taste is a sensation formed from the combination of the composition of the ingredients forming a food product captured by the sense of taste. Therefore taste is the main element in deciding whether a product is accepted. Even though a product's color, scent, and texture are good, consumers will usually reject it if it tastes terrible. Taste is one crucial component that influences consumer acceptance of a product. Taste can affect consumers' acceptance or rejection of a food product [21].

Based on the average panelists' preference for the taste of African catfish shredded, the lowest value was 2.08 (disliked) in sample A1, while the highest value was 4.44 in treatment A3. According to the notes of one of the panelists, shredded African catfish in sample A3, the taste is most in line with shredded catfish in general, has a savory taste, is not greasy, and has a dominant catfish taste. Friedman's test showed a significant difference in the taste of African catfish shredded with different drying durations (α=0.05).

Shelf Life Determination

The shelf life was determined using the Extended Storage Studies (ESS) method with sensory damage parameters (appearance, smell, taste, and texture) according to SNI 7757:2013. Estimating shelf life using the extended storage studies (ESS) method, namely by allowing the product to deteriorate until a particular time and then measuring the parameters of quality changes. The storage temperature used is room temperature (30°C). The results of organoleptic testing by 25 untrained panelists on shredded African catfish stored at 30°C for seven days showed that it did not change physically, and no fungus grew. It is because the shredded catfish product is processed and can last a long time. After all, it is a type of dried food. Determination of the shelf life of African catfish shredded is the determination of the product's shelf-life from the time of production to consumption where the product is in a satisfactory condition based on the characteristics of appearance, taste, scent, and texture.

Several sources related to the shelf life of shredded fish, including the shelf life of shredded skipjack tuna (*Katsuwonus pelamis*) at the Maha Karya micro and medium business unit, Pangandaran Regency, show that the reaction of decreased quality of skipjack tuna products at 30°C (room temperature) last longer 222 days/7.4 months [22]. It was further explained that aluminum foil packaging is

ISSN. 2087-2852
E-ISSN. 2338-1655

recommended for skipjack tuna products and stored at 30°C or room temperature to extend the product's shelf life.

Determining the shelf life in this study also used the distribution turnover method, which determines the shelf life of food products based on information on similar products available on the market. From the analysis of the organoleptic tests carried out, the most preferred treatment by the panelists of the three samples is the A3 treatment, in which the A3 treatment is steamed and dried for 4 minutes in a spinner machine. It is related to the results of interviews or information obtained from business actors similar products, namely in micro and medium enterprises in Sukorejo, namely Processed Catfish, where these small and medium enterprises also use the same method, namely steaming fish and drying it on a spinner machine for 4 minutes.

From the information obtained from small and medium enterprises, the process of steaming and drying with a duration of 4 minutes on shredded catfish that has been running so far, is that the shelf life of the shredded catfish products that are distributed is claimed to last for a period of seven months but reduced by one month to anticipate earlier product damage which is eventually rounded up to six months from the initial production date. This information can eventually become a reference for researchers to determine the shelf life of catfish shredded products when viewed based on the conventional distribution turnover method.

CONCLUSION

The stability of the drying quality of African catfish shredded (*Clarias Gariepinus*) was the color of African catfish shredded with different drying methods giving panelist scores ranging from 2.36 to 4.4; organoleptic value of African catfish floss ranged from 2.88 to 4.16; panelists' assessment of the texture of African catfish shredded ranged from 2.12 - 4.56; the taste of African catfish floss ranges from 2.08 to 4.44. Shredded African catfish with different drying durations that were most in demand by panelists was the sample A3 shredded African catfish that steamed and dried for 4 minutes in a spinner machine with a color score of 4.4, scent 4.16, texture 4.56, and taste 4.44.

The shelf life of shredded African catfish stored at room temperature (±30°C) is seven days, physically unchanged. The shelf life of shredded catfish could last up to seven months and was reduced to six months to anticipate the product damage.

REFERENCES

[1] Salita, L.., P. Suptijah, Nurjannah. 2019. Formulasi dan karakterisasi sambal ikan lele dumbo (*Clarias gariepinus*) Asap. Undergrasuate Thesis. Aquatic Product Technology. IPB University. Bogor.

[2] Afriani K., A.H. Permana, K. Widiana, P.A. Agustin, I.A. Nurhalisa, H.A. Halimah. 2022. Pembuatan aneka produk olahan pangan berbahan dasar ikan lele. *Jurnal Pengabdian Masyarakat AKA.* 2(1). 30-34.

[3] Agustin, I.W., Y.H. Sipahutar. 2022. Feasibility analysis of making shredded dumbo catfish (*Clarias gariepinus*). Proceeding of Nasional Symposium IX Marine and Fisheries. Hasanuddin University. Makassar.

[4] Suryani *et al*. 2007. Abon sebagai makanan olahan yang diberi bumbu. Surabaya – Jakarta.

[5] Jumiati, F.F. 2018. Pemanfaatan jantung pisang dan kluwih pada pembuatan abon ikan tongkol (*Euthynnus affinis*) ditinjau dari analisis proksimat, dan uji asam tiobarbiturat (TBA). *Reka Pangan.* 12(1). 60-66.

[6] Badan Standardisasi Nasional [National Standardization Agency of Indonesia]. 1995. Abon ikan. SNI 01-3707-1995. Badan Standardisasi Nasional Indonesia. Jakarta.

[7] Badan Standardisasi Nasional [National Standardization Agency of Indonesia]. 2006. Cara uji kimia bagian 2: Penentuan kadar air pada produk perikanan. SNI-2354-2-2006. Badan Standardisasi Nasional Indonesia. Jakarta.

[8] Mareta, D.T. 2019. Hedonic test method for measuring instant pindang seasoning powder preferences. *Journal of Science and Applicative Technology.* 3(1). 34-36.

[9] Irianto, H.E., S. Giyatmi. 2015. Teknologi pengolahan hasil perikanan, 2nd Ed. Universitas Terbuka. Tangerang Selatan.

[10] Sucipto, C.D. 2015. Keamanan pangan untuk manusia. Gosyen Publishing. Yogyakarta.

[11] Junianto. 2003. Teknik penanganan ikan. Penebar Swadaya. Jakarta.

[12] Sipahutar, Y.H., R.J. Napitupulu, W.P. Susanto. 2017. Pengaruh penambahan kentang *Solanum tuberosum* terhadap mutu kesukaan konsumen abon lele

kremes. Seminar Nasional Kelautan XII. Universitas Hang Tuah. Surabaya 20 July 2017. 89–98.

[13] Setiawati, I.T., S. Ningsih. 2018. Manajemen usaha pengolahan abon ikan lele (*Clarias gariepinus*) di P2MKP Jaya Mandiri Kecamatan Bulu, Kabupaten Temanggung. *Jurnal Penyuluhan Perikanan dan Kelautan*. 12(2). 95–110.

[14] Angwar, M., E. Rahayu. 2015. Modul pelatihan pembuatan abon ikan lele untuk UKM. LIPI Press.

[15] Riana, A. 2013. Penerapan alat peniris abon lele sistim sentrifugal dengan pengatur waktu dan putaran pada industri kecil rumah tangga. Pekan Ilmiah Mahasiswa Nasional Program Kreativitas Mahasiswa - Teknologi 2013. Indonesian Ministry of Research, Technology and Higher Education. Jakarta.

[16] Siahaan, I.C.M., Y.H. Sipahutar, R. Jannah. 2020. Pengaruh Penggunaan minyak goreng berulang terhadap perubahan nilai gizi mutu keripik belut. Seminar Nasional Tahunan XVII Hasil Penelitian Perikanan dan Kelautan. Universitas Gadjah Mada. 501–507.

[17] Musyaddad, A., A. Ramadhani, M.A. Pratama, Juliyanto, I. Safitri, N. Fitri. 2019. Produksi abon ikan lele sebagai alternatif usaha untuk meningkatkan perekonomian masyarakat Desa Pelutan. *Asian J. Innov. Entrep.* 4. 199–206.

[18] Jayadi, A., B. Anwar, Sukainah, Andi. 2016. Pengaruh suhu penyimpanan dan jenis kemasan terhadap mutu abon ikan terbang. *Jurnal Pendidikan.* 2. 62–69.

[19] Ashar, Y.K. 2020. Dasar kesehatan lingkungan. Universitas Islam Negeri Sumatera Utara. Available at: http://repository.uinsu.ac.id/8798/1/DIKTAT.pdf

[20] Anwar, C., Irhami., M. Kemalawaty. 2018. Pengaruh jenis ikan dan metode pemasakan terhadap mutu abon ikan. *FishtecH – Jurnal Teknologi Hasil Perikanan.* 7(2). 138-147.

[21] Aditya, H.P., Herpandi., S. Lestari. 2016. Karakteristik fisik, kimia dan sensoris abon ikan dari berbagai ikan ekonomis rendah. *FishtecH – Jurnal Teknologi Hasil Perikanan.* 5(1). 61-72.

[22] Huthaimah., Yusriana., Martunis. 2017. Pengaruh jenis ikan dan metode pembuatan abon ikan terhadap karakteristik mutu dan tingkat penerimaan konsumen. *Jurnal Ilmiah Mahasiswa Pertanian Unsyiah.* 2(3). 244-254.

[23] Djamaludin, H., Hardoko., M. Dailami, V. Nurhadianty, D.R. Ananta, D.R. Prayoga. 2022. The peroxide, organoleptic, and proximate content of *Thunnus* sp. shredded fortified with banana blossoms. *Jurnal Sumberdaya Akuatik Indopasifik.* 6(4). 319-330.

[24] Hardoko., E. Suprayitno, T.D. Sulistiyati, B.B. Sasmito, A. Chamidah, M.A.P. Panjaitan, *et al.* 2021. Banana blossom addition to increase food fiber in tuna. (*Thunnus* sp.) floss product as functional food for degenerative disease's patient. *IOP Conf. Series: Earth Environ.l Sci.* 1-8. DOI: 10.1088/1755-1315/1036/1/012095.

[25] Sulistiyati, T.D., J.E. Tambunan, Hardoko., E. Suprayitno, B.B. Sasmito, A. Chamidah, *et al.* 2022. Karakteristik organoleptik abon ikan tuna (*Thunnus* sp.) dengan penambahan jantung pisang. *Journal of Fisheries and Marine Research*. 6(1). 10-19.

[26] Sulthoniyah, S.T.M., T.D. Sulistiyati, E. Suprayitno. 2013. Pengaruh suhu pengukusan terhadap kandungan gizi dan organoleptik abon ikan gabus (*Ophiocephalus striatus*). *THPi Student Journal.* 1(1). 33-45.

ISSN. 2087-2852
E-ISSN. 2338-1655

Analysis of Microbial Abundances in Biofilms and Water in Hypersaline Environments with Different NaCl Levels

Ilham Misbakudin Al Zamzami[1], Yuni Kilawati[2], Zulkisam Pramudia[2], Yogita Ayu Dwi Susanti[2], Andi Kurniawan[2*]

[1]Postgraduate Program, Faculty of Fisheries and Marine Science, University of Brawijaya, Malang, Indonesia
[2]Department of Water Resources and Fisheries Management, Faculty of Fisheries and Marine Science, University of Brawijaya, Malang, Indonesia

Abstract

Biofilm is the dominant habitat for aquatic microbes that can grow in various aquatic conditions, including environments with extreme conditions. One of the extreme conditions found in aquatic ecosystems is a hypersaline environment. As part of aquatic biological resources, microbes can also live in this environment. However, although it is the predominant habitat of microbes, biofilms in hypersaline environments have yet to be widely explored. Understanding biofilms in hypersaline environments, especially salt ponds, will increase knowledge about microbial biofilms. The knowledge can open opportunities for using microbes as aquatic resources, such as aquaculture or environmental biotechnology. This study analyzed microbial abundance in biofilms and water in hypersaline environments. The water is from salt ponds on the South Coast of Malang Regency, Indonesia, with different salinity levels (2%, 25%, and 40%). Microbial abundance was analyzed using the culture method using several culture media (Modified Nutrient Agar, Modified Total Plate Agar, Mannitol Salt Agar, and Casein Medium Agar). The substrate for biofilm growth is HDPE, often used as a bottom coating for salt ponds and shrimp ponds. Moreover, this study also analyzed water quality parameters (pH, dissolved oxygen, turbidity, conductivity, total dissolved solids, temperature) during the biofilms' forming process. The results of this study indicate that the abundance of good microbes that grow in the biofilm or the water around the biofilm is strongly influenced by the type of media used for culturing. The main composition of the most influential media is peptone. The density of microbes in the biofilm is hundreds to thousands of times higher than that in the surrounding water. The results of this study also show that the presence of microbes in both water and biofilm affects the water quality properties in hypersaline environments.

Keywords: aquatic ecosystem, biofilm, hypersaline, microbial ecology.

INTRODUCTION

The utilization of water resources can not be separated from the use of the environment. The aquatic environment has abiotic and biotic components [1]. The abiotic component contains nitrate, phosphate, NaCl, and other minerals. In comparison, one of the biotic components is aquatic microbes. These components have a direct effect on life [2]. One environment that has yet to be optimally explored is the hypersaline environment.

The hypersaline environment is one of the extreme environments with high salt content [3]. A hypersaline environment is an environment with extreme conditions that have limited nutrients for the life of organisms. In this environment, some organisms can live and develop, called extremophiles organisms, a type of halophilic microbe [4]. Many species are considered halophilic microbes because they tolerate high salt levels. Its presence in hypersaline environments is often influenced by self-acclimatization and lack of competition with other phototrophic organisms [5]. Halophilic microbes have a particular characteristic of tolerating hypersaline environments, namely avoiding osmotic shocks by increasing ion concentrations in the cytoplasm [2]. Generally, microorganisms can communicate between cells, forming biofilms in a space/field [1].

Biofilm is a collection of microbes attached to a surface and covered with a carbohydrate adhesive secreted by microbes [6]. The composition of biofilms is microorganism cells, extracellular products, detritus, polysaccharides (adhesive materials), and 97% water (a main constituent) [7]. Polysaccharides (polymers of monosaccharides or simple sugars) produced by microbes and form biofilms include exopolysaccharides (EPS), namely polysaccharides secreted from cells [8]. EPS synthesized by microbial cells differs in composition and chemical and physical properties. Other biofilm constituent materials are proteins, lipids, and lectins [9].

Biofilm is a collection of microbes attached to a surface and covered with a carbohydrate adhesive secreted by microbes [6]. The

* Correspondence Address:
Andi Kurniawan
E-mail : andi_k@ub.ac.id
Address : University of Brawijaya, Veteran Malang, 65145.

ISSN. 2087-2852
E-ISSN. 2338-1655

compositiBiofilm, as a collection of aquatic microbes, has several functions. In aquatic environments, microbes act as decomposers [10]. In fisheries and marine resources, microbes are used as bioremediation agents and management in marine minerals. Generally, previous studies related to biofilms and their forming microbial communities were carried out in typical environments such as seas [11], lakes [12], and rivers [10]. Therefore, research on biofilms under hypersaline conditions is necessary as an initial stage for developing and utilizing halophilic biofilms. The purpose of this study was to analyze the abundance of microbes in specific culture media on biofilms. Moreover, this study also compared the abundance of halophilic microbes that form biofilms with microbes in water.

MATERIAL AND METHOD

Sample Preparation

The water used as a medium for growing biofilms in this study was water taken from salt ponds on the South Coast of Malang Regency, Indonesia. The water used has a salinity level of 2%, 25%, and 40%. This difference in salinity can occur due to the evaporation process in salt ponds to produce salt crystals. There are three stages in the salt production process, from raw materials to salt crystals. The first stage is the evaporation of young water, which occurs at 2% salinity. Furthermore, the evaporation of old water occurs at 25% salinity; in this condition, salt crystals will form. The third stage is called bittern, where the brine remains with 40% salinity [13].

The substrate used for biofilm growth is High-density polyethylene (HDPE) with a thickness of 5 mm. This type of HDPE is widely used to line the bottom of salt ponds and shrimp ponds in Indonesia. HDPE sheets were cut into 15 x 10 cm sizes and put into an aquarium filled with water with different salinity levels. HDPE is bonded to a stainless weight so it can be submerged in a standing position in the water.

The biofilm that grows on HDPE is taken by brushing the biofilm with a soft toothbrush slowly in one direction into 40 mL of distilled water. The suspended biofilm was then homogenized and used as a sample to grow biofilm on different media. All experiments were carried out three times independently. The water around the biofilm was taken as much as 50 mL. This water sample was used for microbial culture on different media. All experiments using water as a sample were also repeated three times independently. Three repetitions were used to minimize data error during testing, and the data obtained will be averaged.

Microbes in the biofilm and the water around the biofilm were cultured using several culture media. The media used were Nutrient Agar modified NaCl (Oxoid), Total Plate Agar modified NaCl (Himedia), Mannitol Salt Agar (Himedia), and Casein Medium Agar [14]. These four selective media are often used to culture halophilic microbes with different nutrient compositions.

Microbial Abundance Analysis

Analysis of microbial abundance in biofilm and water was carried out at the beginning of the study (D_0) and the end (D_{21}). For the case of biofilms, because at the beginning of the study (D_0), there were no growing biofilms, the microbial abundance data obtained was only available at the end of the study (D_{21}). Abundance was calculated using the total plate count method with microbial culture using the spread plate method on each different media. The microbial culture was carried out for seven days, with microbial counts carried out every day. The time of seven days is based on the growth phase of halophilic microbes in general starting the stationary phase at 5-7 days.

Water Quality Measurement

Water quality parameters analyzed in this study were pH, dissolved oxygen, turbidity, conductivity, total dissolved solids, and temperature. pH was measured using a digital pH meter (WQC-22A, DKK TOA Corporation, Japan), dissolved oxygen and temperature were measured using an integrated DO Meter and Digital Thermometer (WQC-22A, DKK TOA Corporation, Japan), and turbidity was measured using a digital turbidity meter (WQC-22A, DKK TOA Corporation, Japan). Total dissolved solids were measured using the turbidity meter (Lutron YK22CTA, USA). All measurements were measured with three repetitions independently.

Data Analysis Method

Data that has been tabulated will be analyzed to get the results of the research. The method used to analyze the data is a quantitative descriptive method. The quantitative descriptive method analyzes data in numbers resulting from observations of the actual situation.

ISSN. 2087-2852
E-ISSN. 2338-1655

RESULT AND DISCUSSION

Halophilic microbial abundance in a hypersaline environment was estimated based on total plate count analysis of four different media. The use of different media aims to analyze the most appropriate media for calculating the abundance of halophilic microbes, especially related to the characteristics of halophilic microbes, which include extremophiles with their uniqueness regarding nutritional needs. The hypersaline environment is an extreme environment with low nutrients [15], so the presence of nutrients in the media can affect bacterial growth, affecting the estimation of the abundance of bacteria present in the biofilm and the surrounding water. Three repetitions were used to minimize data error during testing, and the data obtained will be averaged.

Microbial Abundance in Biofilms

At the beginning of the study (D_0), biofilms had not formed on the surface of HDPE, so the microbial density value in the biofilm could not be shown in this study. The biofilm formation process will occur after the quorum sensing process occurs between the microbes attached to the surface. The results of this study indicate that biofilms in halophilic environments have not yet formed on day 0.

Biofilm takes approximately 14 days to reach the mature biofilm level [16]. In oreder to give time for the biofilms growing on HDPE to reach the mature biofilm stage, the microbial density in the biofilm was analyzed after 21 days (Fig. 1). The results varied based on the calculating microbial abundance in biofilms treated with NaCl levels with different media. The highest abundance was found at 25% NaCl content, with different media having an abundance between 10.0-29.0 x 10^{-1} CFU.mL^{-1}. The abundance of microbes in 2% NaCl treatment with different media is between 8.0 – 24.0 x 10^{-1} CFU.mL^{-1}. In the treatment of 40% NaCl with different media has an abundance between 8.0 – 24.0 x 10^{-1} CFU.mL^{-1}.

The abundance of microbes in the biofilm at 2%, 25%, and 40% NaCl treatment showed different density levels with the same pattern. The halophilic microbial log phase occurred on culture days 1 to 3 in NaCl-modified NA media. The exponential phase occurred on day 4, marked by the emergence of colonies, and increased until day 6. The stationary phase occurred from day 6 to day 7. The death phase in this study was not visible because the Petri dishes were filled with microbial colonies. The same microbial growth phase occurs in NaCl-modified TPA media. In the media treatment, MSA and CMA had the same growth pattern. The lag phase in these two media occurs in microbial culture days 1 and 2.

The exponential phase occurred on day 3, marked by the emergence of colonies, and continued to rise until day 6. The exponential phase on MSA media was faster, presumably due to the effect of mannitol. Mannitol Salt Agar (MSA) was used to determine halophilic (salt-loving) bacteria with the ability to ferment mannitol. These halophilic bacteria can grow on MSA media because of their ability to grow in environments with high salt levels [17]. A positive result of mannitol fermentation is the formation of a yellow halo around the bacterial colonies; this indicates acid production from mannitol breakdown [18]. The ability of halophilic microbes to ferment mannitol makes them anti-edema in cells, so they have an excellent ability to osmoregulate salt ions. In general, non-halophilic microbes do not have this ability, causing the microbes to experience edema in the cytoplasm [17]. On days 5-6, there is no increase in the prohibition, which means it shows a stationary stage. The death phase in this study was not visible because the Petri dishes were filled with microbial colonies. The highest microbial abundance was found in MSA media with 24.0 - 29.0 x 10^{-1} CFU.mL^{-1}.

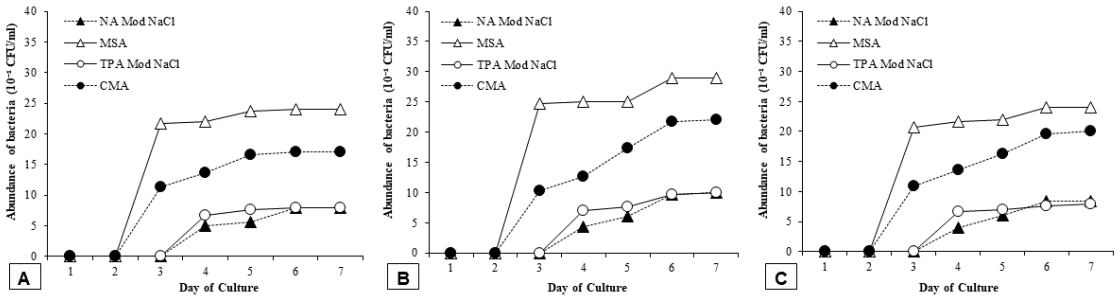

Figure 1. Microbial abundance inside biofilms in hypersaline environment (A=NaCl 2%, B= NaCl 25%, and C= NaCl 4%)

ISSN. 2087-2852
E-ISSN. 2338-1655

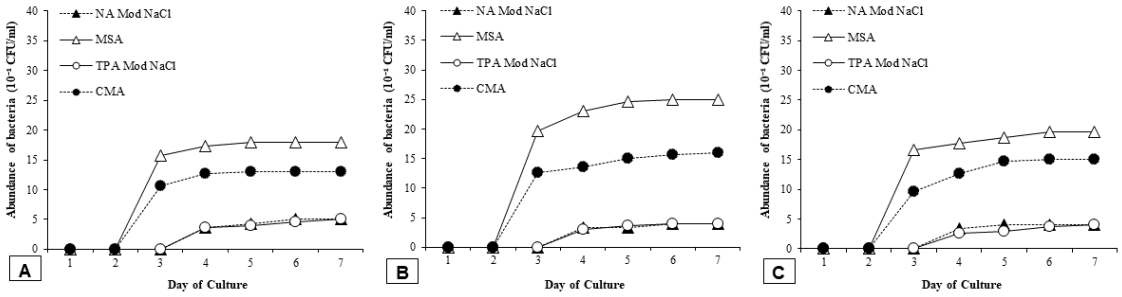

Figure 2. Microbial abundance in the water at start of the study (D0) (A= NaCl 2%; B= NaCl 25%; C= NaCl 40%)

Microbial abundance in water at the start of the study (D_0)

Based on calculating the abundance of microbes in the initial water sample (D_0), the treatment of NaCl levels with different media showed varied results (Fig. 2). The highest abundance was found at 25% NaCl content, with different media having an abundance between 4.0 – 25.0 x 10^{-1} CFU.mL^{-1}. The abundance of microbes in 2% NaCl treatment with different media is between 5.0 – 18.0 x 10^{-1} CFU.mL^{-1}. The 40% NaCl treatment with different media ranges between 4.0 – 19.7 x 10^{-1} CFU.mL^{-1}.

The abundance of microbes in the initial water sample (D_0) at 2%, 25%, and 40% NaCl treatment showed different densities but relatively the same pattern. In NaCl-modified NA media, the halophilic microbial lag phase occurred in culture days 1 to 3. The exponential phase occurred on day four, marked by the emergence of colonies, and increased until day 6. Both media did not contain mannitol as an anti-edema, meaning only a few microbes can live and thrive at high salinity. Halomonas halophilic microbes have a thick cytoplasmic structure, making them one of the halotolerant microbes often found in hypersaline environments [17]. NA media modified by NaCl contained the composition of Lab Lemco Powder (1 g). This material functions as a source of minerals, vitamins [19].

The NaCl-modified TPA media grew with the same abundance range as the NaCl-modified NA media. The composition of the two media is almost the same. The difference is that the TPA media contains dextrose as an additional nutrient. Dextrose or sugar clusters, both monosaccharides and polysaccharides, are additional nutrients for the culture in the media [20]. The presence of dextrose is an additional carbon source in the modified NaCl TPA media [21]. In general, halophilic microbes cultured on NA media will grow in 3-7 days [20]. The stationary phase occurred from day 6 to day 7. The death phase in this study was not visible because the petri dish was filled with microbial colonies.

In the media treatment, MSA and CMA had the same growth pattern. The lag phase in both media occurred on days 1 and 2 of the microbial culture. The exponential phase occurred on day three, marked by the emergence of colonies, and continued to increase until day 6. However, on days 5 and 6, no significant increase in abundance indicates a stationary stage. The death phase in this study was not visible because the Petri dishes were filled with microbial colonies. The highest microbial abundance was found in MSA media with 19.0 - 25.0 x 10^{-1} CFU.mL^{-1}. The overall microbial abundance in the initial water (D_0) was lower than in the biofilm.

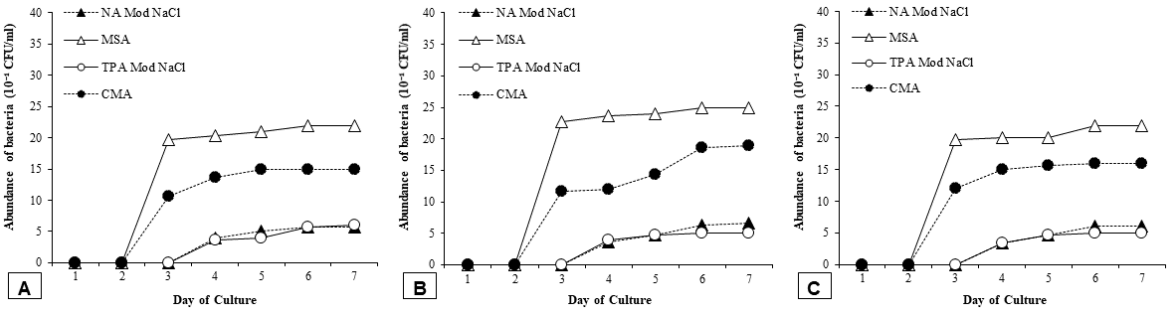

Figure 3. Microbial abundance in the water at finish of the study (D21) (A= NaCl 2%; B= NaCl 25%; C= NaCl 40%)

ISSN. 2087-2852
E-ISSN. 2338-1655

Microbial abundance in water at the end of the study (D_{21})

The results of calculating the microbial abundance in the water samples at the end of the study (D_{21}) indicated that the treatment of NaCl levels with different media showed varied results (Fig. 3). The highest abundance was found at 25% NaCl content, with different media having an abundance between 5.0 – 25.0 x 10^{-1} CFU.mL^{-1}. The abundance of microbes in 2% NaCl treatment for different media is 5.7 – 22.0 x 10^{-1} CFU.mL^{-1}. While for the media with 40% NaCl range between 5.0 – 22.0 x 10^{-1} CFU.mL^{-1}. As at the beginning of the study, the abundance of microbes in the water after 21 days (D_{21}) showed a different abundance with the same growth pattern in 2%, 25%, and 40% NaCl treatments. The halophilic microbial lag phase occurred in culture days 1 to 3 in NaCl-modified NA media. The exponential phase occurred on day four, marked by the emergence of colonies, and increased until day 6. The stationary phase occurred from day 6 to day 7. The same microbial growth phase occurs in NaCl-modified TPA media.

In the media treatment, MSA and CMA had the same growth pattern. The lag phase in both media occurred on days 1 and 2 of the microbial culture. The exponential phase occurred on day three, marked by the emergence of colonies, and continued to increase until day 6. However, on days 5 and 6, no significant increase in abundance indicates a stationary stage. The death phase in this study was not visible because the Petri dishes were filled with microbial colonies. The highest microbial abundance was found in MSA media with 22.0 – 25.0 x 10^{-1} CFU.mL^{-1}.

The abundance of CMA media has a high abundance after MSA media. This abundance is presumably due to the influence of the composition of CMA, which contains Magnesium Chloride and Potassium Chloride. Both of these materials function like mannitol in MSA media as a regulator of osmosis in cells. Adding Magnesium Chloride to the culture medium can increase microbial density because this compound can restore the lost balance between sodium and potassium [22]. Halophilic microbes need this condition to thrive in high salinity and low nutrients. The overall abundance of microbes in the initial water (D_{21}) was lower than that in the biofilm but higher than that in the initial water (D_0).

Effect of media composition on microbial abundance

The four media used in this study were NaCl-modified Nutrient Agar, Mannitol Salt Agar, NaCl-modified Total Plate Agar, and Casein Medium Agar. Each medium has different nutrients. The composition of each media can be seen in Table 1 below.

The composition of the media that gets highlighted in this study is peptone. All media contain peptone with different levels. Analysis was conducted to see the regression of peptone levels in each medium to microbial abundance. The results of the analysis can be seen in Figure 4.

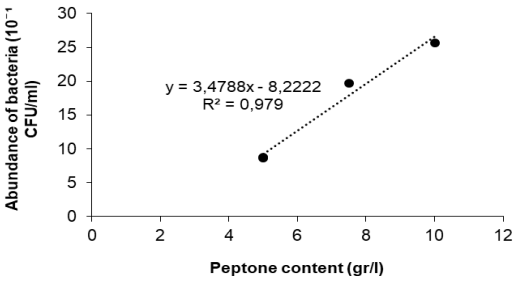

Figure 4. Regression of peptone levels with microbial abundance

Table 1. Halophilic selective media composition

Media Composition	NA Mod NaCl	MSA	TPA Mod NaCl	CMA
Lab-Lemco Powder	1 gr.L^{-1}	1 gr.L^{-1}	-	-
Yeast extract	2 gr.L^{-1}	-	2.5 gr.L^{-1}	5 gr.L^{-1}
Peptone	**5 gr.L^{-1}**	**10 gr.L^{-1}**	**5 gr.L^{-1}**	**7.5 gr.L^{-1}**
Sodium Chloride	5 gr.L^{-1} + 70 gr.L^{-1}	75 gr.L^{-1}	+ 75 gr.L^{-1}	75 gr.L^{-1}
Agar	15 gr.L^{-1}	15 gr.L^{-1}	15 gr.L^{-1}	15 gr.L^{-1}
Dextrose	-	-	1 gr.L^{-1}	-
Mannitol	-	10 gr.L^{-1}	-	-
Phenol red	-	0.025 gr.L^{-1}	-	-
$MgCl_2.6H_2O$	-	-	-	2 gr.L^{-1}
KCl	-	-	-	2 gr.L^{-1}
$CaCl_2$	-	-	-	0.2 gr.L^{-1}
Source	Oxoid	Himedia	Himedia	Microbiological media 4th 2010

ISSN. 2087-2852
E-ISSN. 2338-1655

The analysis results in Figure 4 show that the regression value (R^2) between peptone content and abundance of microbes is 0.979. This result indicates that the level of regression between the two factors is 97.9%. This value is included in the category of solid relationships (>80%).

Peptone is a protein hydrolyzate widely used as a nutritional component in microorganism growth media. Peptone is easily soluble in water and does not experience coagulation when heated [23]. Peptones in microbial growth media serve as a nitrogen source for microorganisms [24].

Water Quality Parameters

pH

Based on the measurement of the pH value of each treatment, the value tends to be stationary from the beginning to the end of the study. The pH value is shown in Figure 5. The 2% NaCl treatment had the highest relative pH value (alkaline), whereas the 25% NaCl treatment had the lowest. This condition is directly proportional to the abundance of microbes in each treatment, where the highest abundance was in the 25% NaCl treatment. The decrease in pH is caused by the accumulation of organic acids and an increase in H^+ protons due to bacterial metabolism due to the decomposition of amino acids [25]. Halophilic bacteria are microorganisms resistant to high salt levels because they accumulate dissolved organic matter in their cytoplasm [26].

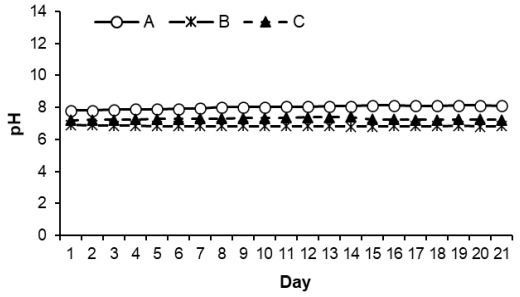

Figure 5. pH during biofim forming process

Dissolved Oxygen

Based on the measurement of each treatment's dissolved oxygen (DO) value, the value tends to be stationary from the beginning to the end of the study. The DO value is shown in Figure 6. The DO value in the observations tends to decrease. The difference in the DO value for each treatment has a different value. The highest DO occurred in treatment A (NaCl 2%), followed by treatment C (NaCl 40%), and the lowest DO value was in treatment B (NaCl 25%). DO concentration affects the ability of microbes in the process of degrading organic matter [27]. DO concentrations decreased from day 1 to day 21 in all treatments. This condition is influenced by the continuous consumption of DO by microbes in degrading organic matter without significant additions from the external environment.

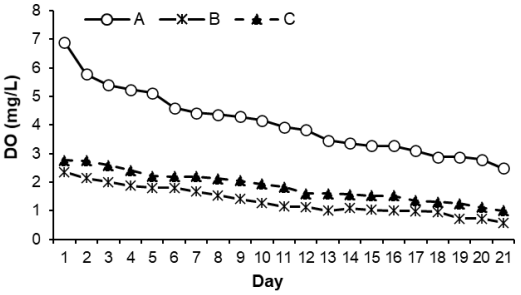

Figure 6. DO during biofilm forming process

Turbidity

The turbidity value during the biofilm formation process was analyzed in this study. Based on the measurement of the turbidity value of each treatment, it shows that each treatment has a turbidity value that tends to be stationary from the beginning to the end of the study (Fig. 7). The level of turbidity in the water sample treatment C (NaCl 40%) has a higher turbidity level than treatment B (NaCl 25%), and treatment A (NaCl 2%) has a low turbidity value. This condition was influenced by the concentration of NaCl in the water sample treatment C, which was higher than treatments B and A, so it affected the turbidity level.

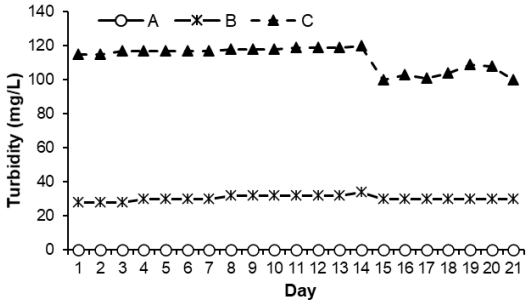

Figure 7. Turbidity during biofilm forming process

Conductivity

The conductivity values of water during the biofilm formation process in a halophilic environment are shown in Figure 8. The conductivity values of each identified treatment tended to be stationary from the beginning to the end of the study. The order of the height of the conductivity level in the sample water is treatment B (25% NaCl) followed by treatment C (40% NaCl). The conductivity value was the lowest in treatment A (NaCl 2%).

ISSN. 2087-2852
E-ISSN. 2338-1655

Conductivity (electrical conductivity) is the ability of water to conduct electricity. The electrical conductivity is more influenced by dissolved minerals in the water, especially ionized NaCl, which is directly proportional to the electrical conductivity. Interestingly, the higher the microbial abundance affected the conductivity value to be higher. This condition can be associated with microbes releasing ions during their metabolic processes [28,29]. Some examples of microbes with this ability are *Staphylococcus* sp. and *E. coli* [30]. The two species come from the phyla Proteobacteria and Firmicutes, where based on metagenomic results, this phylum is the most identified.

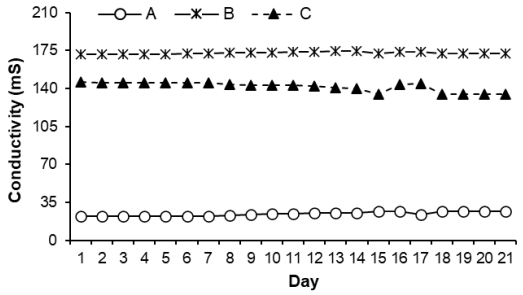

Figure 8. Conductivity of water during biofilm process

Total Dissolved Solid (TDS)

The TDS value in water in this study is shown in Figure 9. The highest TDS value was in treatment B (25% NaCl), followed by treatment C (40% NaCl). A (NaCl 2%) has a very low TDS in treatment. The NaCl content and substances in water affect the TDS level, including microbes. It is assumed that other dissolved materials affect the TDS value. This condition is proportional to the microbial abundance in treatment B, which is higher. TDS is affected by solids dissolved in water in the form of elements, compounds, and colloids [31].

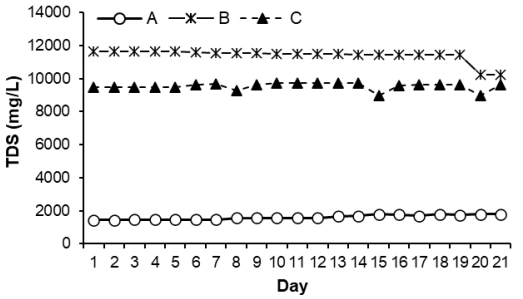

Figure 9. TDS in water during biofilm forming process

Temperature

The water temperature during the biofilm formation process was measured in this study, with the results shown in Figure 10. The temperature in treatments A, B, and C was relatively the same from day 1 to day 21. This condition indicated that the NaCl content in the sample did not affect the sample water temperature considering the research was conducted indoors. Water temperature is greatly influenced by the amount of sunlight on the water's surface [31].

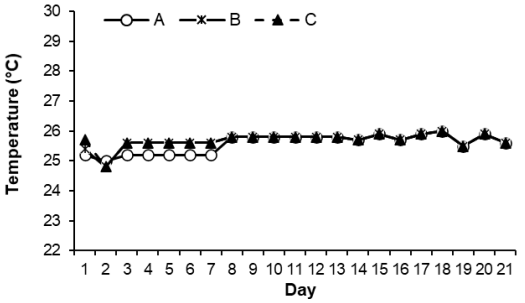

Figure 10. Temperature of water during biofilm forming process

CONCLUSSION

The results of this study indicate that the abundance of microbial abundance in biofilms and water around biofilms that grow in a halophilic environment is analyzed in this study. The results of this study indicate that the good microbes that grow in the biofilm or the water around the biofilm are greatly influenced by the type of media used for culturing. The main composition of the most influential media is peptone. The density of microbes in the biofilm is hundreds to thousands of times higher than that in the surrounding water. The highest abundance of microbes is at 25% NaCl content. The results of this study also show that the presence of microbes in both water and biofilm affects the water quality properties in hypersaline environments.

ACKNOWLEDGMENT

This research received funding from the Hibah Lektor Kepala Program, Faculty of Fisheries and Marine Sciences, Universitas Brawijaya, in 2023 with contract number: 2317/UN10.F06/KS/2023.

REFERENCES

[1] Sauer, K., P. Stoodley, D.M. Goeres, L. Hall-Stoodley, M. Burmølle, P.S. Stewart, T. Bjarnsholt. 2022. The biofilm life cycle: Expanding the conceptual model of biofilm formation. *Nat. Rev. Microbiol.* 20(10). 608-620. DOI: 10.1038/s41579-022-00767-0.

[2] Matarredona, L., M. Camacho, B. Zafrilla, M.J. Bonete, J. Esclapez. 2020. The role of stress proteins in Haloarchaea and their adaptive response to environmental

ISSN. 2087-2852
E-ISSN. 2338-1655

shifts. *Biomolecules.* 10(10). 1390. DOI: 10.3390/biom10101390.

[3] Sayed, A.M., M.H. Hassan, H.A. Alhadrami, H.M. Hassan, M. Goodfellow, M.E. Rateb. 2020. Extreme environments: microbiology leading to specialized metabolites. *J. Appl. Microbiol.* 128(3). 630-657. DOI: 10.1111/jam.14386.

[4] Kajale, S., N. Deshpande, Y. Shouche, A. Sharma. 2020. Cultivation of diverse microorganisms from hipersalin lake and impact of delay in sample processing on cell viability. *Curr. Microbiol.* 77(5). 716-721. DOI: 10.1007/s00284-019-01857-8.

[5] Musa, H., F.H. Kasim, A.A.N. Gunny, S.C. Gopinath. 2018. Salt-adapted moulds and yeasts: Potentials in industrial and environmental biotechnology. *Process Biochem.* 69. 33-44. DOI: 10.1016/ j.procbio.2018.03.026.

[6] Filliazati, M. 2013. Pengolahan limbah cair domestik dengan biofilter aerob menggunakan media bioball dan tanaman kiambang. *Jurnal Teknologi Lingkungan Lahan Basah*. 1(1). DOI: 10.26418/jtllb. v1i1.4028.

[7] Kurniawan, A., T. Yamamoto. 2019. Accumulation of and inside biofilms of natural microbial consortia: implication on nutrients seasonal dynamic in aquatic ecosystems. *Int. J. Microbiol.* 6473690. DOI: 10.1155/2019/6473690.

[8] Marlina, D., M. Kurniati, F. Hamid, F. Larasathi, F. Irnawita. 2018. Visualisasi matriks biofilm *Eschericia coli* dengan media bacteriological peptone, sucrose dan ethanol. *Jurnal Kesehatan*. 9(1). 26-32.

[9] Seviour, T., N. Derlon, M.S. Dueholm, H.C. Flemming, E. Girbal-Neuhauser, H. Hornet *al.* 2019. Extracellular polymeric substances of biofilms: Suffering from an identity crisis. *Water Res.* 151, 1-7. DOI: 10.1016/j.watres.2018.11.020.

[10] Wang, L., W. Chen, X. Song, Y. Li, W. Zhang, H. Zhang, L. Niu. 2020. Cultivation substrata differentiate the properties of river biofilm EPS and their binding of heavy metals: A spectroscopic insight. Environ. Res. 182. 109052. DOI: 10.1016/ j.envres.2019.109052.

[11] Robika, R., R. Lingga, B. Afriyansyah. 2022. Identification of biofilm-producing bacteria from Nangka Island marine water in District of Bangka Tengah. *Jurnal Pembelajaran dan Biologi Nukleus.* 8(1). 179-191. DOI: 10.36987/jpbn.v8i1.2492.

[12] Kurniawan, A., M. Musa, L.N. Salamah, T. Yamamoto, A.A. Prihanto, A.A. Amin 2019. Analysis of physicochemical properties of natural biofilm matrices formed in a sub-tropical region (Lake Biwa, Japan) and a tropical region (Karangkates Reservoir, Indonesia). *Aquacult. Aquarium Conserv. Legis.* 12(5). 1951-1960.

[13] Pramudia, Z., A.T. Yanuar, I.M. Al Zamzami, R. Kurniaty, R.A. Lestariadi, S.M. Ulfa, *et al.* 2023. Induksi metode *Continuously Dynamic Mixing* (CDM) untuk optimasi produksi garam dengan teknologi *Greenhouse Salt Tunnel* (GST) di pesisir selatan Kabupaten Malang. *J. Innov. Appl. Technol.* 9(1). 49-56.

[14] Atlas, R.M. 2010. Handbook of microbiological media. CRC press. Boca Raton. DOI: 10.1201/EBK1439804063.

[15] Oren, A. 2015. Pyruvate: a key nutrient in hipersalin environments?. *Microorganisms.* 3(3). 407-416.

[16] Hiraki, A., Y. Tsuchiya, Y. Fukuda, T. Yamamoto, A. Kurniawan, H. Morisaki. 2009. Analysis of how a biofilm forms on the surface of the aquatic macrophyte Phragmites australis. *Microbes Environ.* 24(3). 265-272.

[17] Chagas, P.A., R, Schneider, D. dos Santos, M., A.J. Otuka, C.R. Mendonça, D.S. Correa. 2021. Bilayered electrospun membranes composed of poly (lactic-acid)/natural rubber: A strategy against curcumin photodegradation for wound dressing application. *React. Funct. Polym.* 163. 104889.

[18] Virgianti, D.P., R. Suhartati. 2020. *Clitoria ternatea* Linn Extract as natural pH indicator in mannitol salt agar medium. In: 2nd Bakti Tunas Husada-Health Science International Conference (BTH-HSIC 2019). Atlantis Press. 326-328.

[19] Virginia, L.J., C. Peterbauer. 2023. Localization of Pyranose 2-Oxidase from *Kitasatospora aureofaciens*: A step closer to elucidate a biological role. *Int. J. Mol. Sci.* 24(3). 1975.

[20] Bhagat, C., S. Bhavsar, R. Patel, A. Ghelani, P. Dudhagara, R. Chaudhari. 2022. Effect of different calcium salts on calcium carbonates formation induced by halophilic *Bacillus oceanisediminis* CB1. *Acta Chimica Asiana.* 5(2). 212-217.

ISSN. 2087-2852
E-ISSN. 2338-1655

[21] Halimah, N., I. Apriani, R.N. Sunarti. 2022. Tepung umbi gadung (*Dioscorea hispida* Dennst) sebagai alternatif media pengganti media PDA (Potato Dextrose Agar). *Organisms.* 2(2). 85-94.

[22] Wingfield, L.K., N. Jitprasitporn, N. Che-Alee. 2023. Isolation and characterization of halophilic and halotolerant fungi from man-made solar salterns in Pattani Province, Thailand. *Plos One*. 18(2). e0281623.

[23] Jia, H., S. Qiu, F. Hu, L. Wang, J. Shi, X. Xie. 2020. Adsorption-doping for preparing N-doped porous carbon for promising electrochemical capacitors-using peptone and polymer porous resin as precursors. *J. Energy Storage*. 28. 101297. DOI: 10.1016/j.est.2020.101297.

[24] Kim, M., S.C. Jee, S.K. Shinde, B.M. Mistry, R.G. Saratale, G.D. Saratale, *et al.* 2019. Green-synthesis of anisotropic peptone-silver nanoparticles and its potential application as anti-bacterial agent. *Polymers*. 11(2). 271. DOI: 10.3390/polym 11020271.

[25] Xie, G., S. Du, Q. Huang, M. Mo, Y. Gao, M. Li, *et al*. 2022. Photonic hydrogels for synergistic visual bacterial detection and on-site photothermal disinfection. *ACS Appl. Mater. Interfaces*. 14(4), 5856-5866. DOI: 10.1021/acsami.1c22586.

[26] Nazhifan, S.F., K. Dewi, E.N.N. Asih. 2023. Bakteri halofilik dan halotoleran dari air baku tambak garam Universitas Trunojoyo Madura. *Jurnal Pengolahan Hasil Perikanan Indonesia*. 26(1). 67-76. DOI: 10.17844/jphpi.v26i1.44536

[27] Ali, A., L. Chen, M.S. Nasir, C. Wu, B. Guo, Y. Yang. 2023. Piezocatalytic removal of water bacteria and organic compounds: a review. *Environ. Chem. Lett.* 21(2). 1075-1092. DOI: 10.1007/s10311-022-01537-3.

[28] Liu, K., Y. Liu, N. Jiao, L. Zhu, J. Wang, A. Hu, X. Liu. 2016. Vertical variation of bacterial community in Nam Co, a large stratified lake in central Tibetan Plateau. *Antonie Van Leeuwenhoek*. 109. 1323-1335.

[29] Wu, K., W. Zhao, Q. Wang, X. Yang, L. Zhu, J. Shen, *et al.* 2019. The relative abundance of benthic bacterial phyla along a water-depth gradient in a plateau lake: physical, chemical, and biotic drivers. *Front. Microbiol.* 10, 1521.

[30] Comini, S., N. Mandras, M.R. Iannantuoni, F. Menotti, A.G. Musumeci, G. Piersigilli, *et al.* 2021. Positive and negative ions potently inhibit the viability of airborne gram-positive and gram-negative bacteria. *Microbiol. Spectr.* 9(3). e00651-21.

[31] Liu, Y., J. Wang, B. Jung, U. Rao, E. Sedighi, E.M. Hoek, *et al.* 2022. Desalinating a real hyper-saline pre-treated produced water via direct-heat vacuum membrane distillation. *Water Res.* 218. 118503. DOI: 10.1016/j.watres.2022.118503.

ISSN. 2087-2852
E-ISSN. 2338-1655

Numerical Simulation and Sensitivity Analysis of COVID-19 Transmission Involves Virus in the Environment

Maratus Sholihatul Azizah[1*], Trisilowati[2], Nur Shofianah[2]

[1]Master Program of Mathematics, Faculty of Mathematics and Natural Sciences, University of Brawijaya, Malang, Indonesia
[2]Departement of Mathematics, Faculty of Mathematics and Natural Sciences, University of Brawijaya, Malang, Indonesia

Abstract

This paper is aimed to develop a new COVID-19 mathematical model involving viruses in the environment. In this mathematical model, the human population is divided into five subpopulations: susceptible, exposed, infected, hospitalized, and cured individuals. In addition, the model also contains the virus population in the environment. Infection in the model occurs due to interactions between susceptible individual subpopulations and infected individuals and hospitalizations, as well as the spread of the virus in the environment. Based on the results of dynamic analysis, this model has two equilibrium points, the disease-free and endemic equilibrium points. The disease-free equilibrium point always exists, and both equilibrium points are locally asymptotically stable if they meet the Routh-Hurwitz criteria. Model sensitivity analysis was carried out on model parameters that affect the basic reproduction number with the most sensitive parameters are the natural death rate, the recruitment rate, the transmission rate of the virus in the environment, the virus clearance rate, and the rate of wearing PPE (Personal Protective Equipment), as well as the parameter that does not affect the basic reproduction number that is the rate of leaving the recovered population. Numerical simulations performed show results in accordance with the analysis, also from the simulations can be concluded that the increase (or decrease) of the transmission rate of the virus in an environment that has a higher sensitivity index has more significant influences on the basic reproduction number and the number of infected population than the transmission rate of hospitalized individuals.

Keywords: Basic Reproduction Number, Dynamics Analysis, Epidemic Models of COVID-19, Local Stability Analysis, Sensitivity Analysis.

INTRODUCTION

Coronavirus is an infectious disease called acute respiratory syndrome by the International Virus Taxonomy community. In general, the coronavirus is known as COVID-19. This disease is transmitted through direct contact such as touch, body fluids, or air when sneezing or coughing [1]. Researchers are still tracking the spread of COVID-19 in all parts of the world. To describe the dynamics of the spread of the virus in a population, a mathematical model is needed so that the solutions can be obtained in handling the spread of the virus.

Mathematical modeling is a field of mathematics that describes real-world problems in mathematical statements. The COVID-19 model is an epidemic model where the model is used to describe the infectious disease COVID-19. The COVID-19 epidemic model has been studied by several researchers.

*Corresponding Address:
Maratus Sholihatul Azizah
E-mail : maratussa@gmail.com
Address : Dept. Mathematics, University of Brawijaya, Veteran Malang, 65145.

Researchers [2-5] developed a model of three SIR subpopulations. Then Victor [6] developed this model by adding a subpopulation of exposed individuals (E) and the assumption that subpopulations of individuals who recovered could be susceptible again (R). Zeb *et al.* [7] also developed the previous model researched [2,4] by adding a subpopulation of exposed individuals (E) and isolated individual subpopulations (Q) to the model.

Naik *et al.* [8] modeled the effect of COVID-19 transmission on contaminated environments in India using seven subpopulations, namely susceptible (S), exposed (E), asymptomatic infected (A), infected with symptoms (I), confirmed (C), hospitalized (H), and recovered (R) with the virus population in the environment (V). The intended population is a combined population that interacts homogeneously where each individual interacts directly, without isolation or quarantine, and without closing access to a particular area.

Masandawa *et al.* [9] presented a COVID-19 model consisting of five subpopulations namely, susceptible (S), exposed (E), infected (I), hospitalized (H), and recovered (R). This model assumes that individuals who have

ISSN. 2087-2852
E-ISSN. 2338-1655

recovered have the possibility to become vulnerable again.

This paper will constructed a mathematical model for COVID-19 by modifying Masandawa et al. [9] model by adding the virus compartment in the environment as in Naik et al. [8]. It is done to determine the virus's behavior in the environment with the constructed model. Then the dynamic analysis of the model is applied by determining the equilibrium point and analyzing its stability. In the final part, a numerical simulation is carried out to describe the results of dynamic analysis using the fourth-order Runge-Kutta method.

MATERIALS AND METHOD

Model Formulation

In this paper, the COVID-19 epidemic model [9] is the main object of the study. The model construction is done by modifying the model of Masandawa *et al.* [9] by adding the virus compartment, such as in the model of Naik *et al.* [8].

Determination of the Equilibrium Points

The first step to be done in dynamics analysis is to determine the equilibrium points. The equilibrium points of the model are obtained when the population rate of the system is unchanged or equal to zero. From this condition, the existence properties of equilibrium points are also obtained.

Stability of the Equilibrium Points

The local stability of equilibrium points is analyzed by linearizing the model using the Taylor series. The linearization is done to change the nonlinear model into its linear form. The approximation used is in the form of a Jacobian matrix. From there, we can determine the eigenvalues or roots of the characteristics equation. The local stability determination is obtained from the absolute of its eigenvalue argument.

Sensitivity Analysis

The sensitivity analysis is done to determine the parameter that mainly affects the spread of the disease. In this stage, the study calculates the sensitivity index of each model parameter that correlates with the basic reproduction number, $\mathcal{R}_0$.

Numerical Simulation

The numerical simulation is used to verify the analytical results and illustrate the model's behavior. The approach used is the fourth-order Runge-Kutta method using MATLAB software. In this stage, it is crucial to determine the parameters that match the condition of existences and stability of equilibrium points. The interpretation results of numerical simulations are done as the last step in this stage.

RESULTS AND DISCUSSION

The COVID-19 Model Construction

This section will give a mathematical model of the COVID-19 epidemic involving viruses in the environment. The epidemic model used as a reference is the Masandawa *et al.* [9] epidemic model involving viruses in the environment, as referred to by Naik *et al.* [8]. The compartment diagram for the COVID-19 epidemic model involving viruses in the environment is shown in Figure 1.

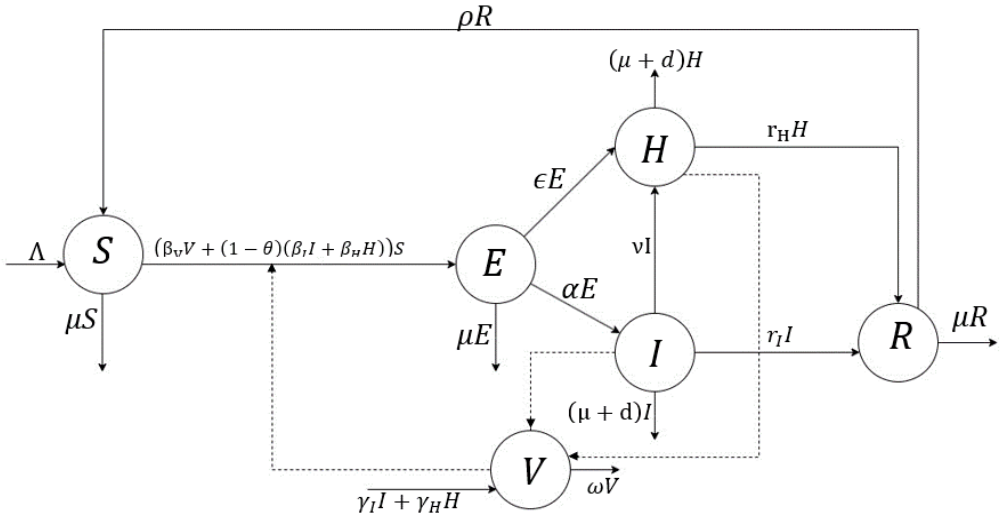

Figure 1. The COVID-19 epidemic model involving viruses in the environment

ISSN. 2087-2852
E-ISSN. 2338-1655

The assumptions used in the mathematical model are as follows: 1) individuals who have recovered will be susceptible again, 2) the virus population in the environment (V) is spread by infected (I) and hospitalized individuals (H), 3) susceptible individuals will be infected with the virus by interacting with infected and hospitalized individuals as well as interactions with viruses in the environment, 4) interactions between susceptible and hospitalized individuals occur when susceptible individuals are in the hospital, and 5) there are significant influences in the use of personal protective equipment (PPE) to prevent the spread of the virus.

The COVID-19 epidemic model involving virus in the environment consists of five groups of human subpopulations; susceptible (S), exposed (E), infected (I), hospitalized (H), and recovered (R) subpopulations, also the virus population in the environment (V). The COVID-19 epidemic model involving virus in the environment is given by the following equation. The parameter description can be seen in Table 1.

$$\begin{aligned}
\frac{dS}{dt} &= \Lambda + \rho R - \big(\mu + \beta_V V + (1-\theta)(\beta_I I + \beta_H H)\big)S \\
\frac{dE}{dt} &= \big(\beta_V V + (1-\theta)(\beta_I I + \beta_H H)\big)S - (\alpha + \epsilon + \mu)E \\
\frac{dI}{dt} &= \alpha E - (r_I + \nu + d + \mu)I \\
\frac{dH}{dt} &= \epsilon E + \nu I - (r_H + d + \mu)H \\
\frac{dR}{dt} &= r_I I + r_H H - (\rho + \mu)R \\
\frac{dV}{dt} &= \gamma_I I + \gamma_H H - \omega V
\end{aligned} \tag{1}$$

and

$N = S + E + I + H + R$

Table 1. Description of all parameters

Para-meter	Description
Λ	Recruitment rate of susceptible
μ	Natural death rate
ρ	Rate of leaving the recovered population
β_V	virus transmission rate in the environment
β_I	Transmission rate of infected individuals
β_H	Transmission rate of hospitalized individuals
θ	The rate of wearing PPE
α	'Exposed individuals become infected' rate
ϵ	'Exposed individuals are hospitalized' rate
ν	'Infected individuals are hospitalized' rate
r_I	Recovery rate of infected individuals
r_H	Recovery rate of hospitalized individuals
d	The disease induced death rate
γ_I	Virus released rate via infected individuals
γ_H	Virus release rate via the hospitalized individuals
ω	The virus clearance rate

Equilibrium points

The system equilibrium points are obtained when $\frac{dS}{dt} = \frac{dE}{dt} = \frac{dI}{dt} = \frac{dH}{dt} = \frac{dR}{dt} = \frac{dV}{dt} = 0$, such that

$$\begin{aligned}
&\Lambda + \rho R - \big(\mu + \beta_V V + (1-\theta)(\beta_I I + \beta_H H)\big)S = 0, \\
&\big(\beta_V V + (1-\theta)(\beta_I I + \beta_H H)\big)S - k_1 E = 0, \\
&\alpha E - k_2 I = 0, \\
&\epsilon E + \nu I - k_3 H = 0, \\
&r_I I + r_H H - k_4 R = 0, \\
&\gamma_I I + \gamma_H H - \omega V = 0,
\end{aligned} \tag{2}$$

where

$k_1 = \alpha + \epsilon + \mu,$
$k_2 = r_I + \nu + d + \mu,$
$k_3 = r_H + d + \mu,$
$k_4 = \rho + \mu.$

Disease-free equilibrium

$$Y_0 = (S_0, E_0, I_0, H_0, R_0, V_0) = \left(\frac{\Lambda}{\mu}, 0,0,0,0,0\right),$$

With assumptions $S \neq 0, E \neq 0, I \neq 0, H \neq 0, R \neq 0$, and $V \neq 0$,we get the endemic equilibrium

$Y^* = (S^*, E^*, I^*, H^*, R^*, V^*)$ where

$$\begin{aligned}
S^* &= \frac{\Lambda + a_3 E^*}{\mu + (a_4 + a_5)E^*} \\
I^* &= \frac{\alpha E^*}{k_2} \\
H^* &= \frac{E^*}{k_3}\left(\epsilon + \frac{\alpha\nu}{k_2}\right) \\
R^* &= \frac{E^*}{k_4}\left(\frac{\alpha r_I}{k_2} + \frac{r_H}{k_3}\left(\epsilon + \frac{\alpha\nu}{k_2}\right)\right) \\
V^* &= \frac{E^*}{\omega}\left(\frac{\alpha\gamma_I}{k_2} + \frac{\gamma_H}{k_3}\left(\epsilon + \frac{\alpha\nu}{k_2}\right)\right)
\end{aligned} \tag{3}$$

and

$$\begin{aligned}
&a_1 = \frac{\alpha}{k_2}, a_2 = \frac{1}{k_3}\left(\epsilon + \frac{\alpha\nu}{k_2}\right), \\
&a_3 = \frac{\rho}{k_4}(a_1 r_I + a_2 r_H), \\
&a_4 = \frac{\beta_V}{\omega}(\gamma_I a_1 + \gamma_H a_2), \\
&a_5 = (1-\theta)(\beta_I a_1 + \beta_H a_2).
\end{aligned}$$

Endemic equilibrium Y^* exists when
$k_1\mu > \Lambda(a_4 + a_5)$ and $a_3 > k_1$
or
$k_1\mu < \Lambda(a_4 + a_5)$ and $a_3 < k_1$.

Basic reproduction number

The next generation matrix method was used to obtain the basic reproduction number $(\mathcal{R}_0)$. The components forming the next generation matrix consist of the infected population group, i.e

$$\begin{aligned}
\frac{dE}{dt} &= \big(\beta_V V + (1-\theta)(\beta_I I + \beta_H H)\big)S - k_1 E, \\
\frac{dI}{dt} &= \alpha E - k_2 I,
\end{aligned} \tag{4}$$

ISSN. 2087-2852
E-ISSN. 2338-1655

$$\frac{dH}{dt} = \epsilon E + \nu I - k_3 H,$$
$$\frac{dV}{dt} = \gamma_I I + \gamma_H H - \omega V.$$

to differ new infection, so (4) is changed to

$$\frac{dx_i}{dt} = \mathcal{F}_i(x) - \mathcal{G}_i(x),$$

Where $\mathcal{F}_i$ is the new infection rate, $\mathcal{G}_i$ is the transfer of infection between subpopulations and x are the infected subpopulations such that $x_1 = E, x_2 = I, x_3 = H, x_4 = V$.

$$\mathcal{F}_i = \begin{pmatrix} (\beta_V V + (1-\theta)(\beta_I I + \beta_H H))S \\ 0 \\ 0 \\ 0 \end{pmatrix},$$
$$\mathcal{G}_i = \begin{pmatrix} k_1 E \\ k_2 I - \alpha E \\ k_3 H - \epsilon E - \nu I \\ \omega V - \gamma_I I - \gamma_H H \end{pmatrix}.$$

The spectral radius of the next generation matrix $\mathcal{K} = \mathcal{F}\mathcal{G}^{-1}$ as the basic reproduction number $\mathcal{R}_0$ and $Y_0 = \left(\frac{\Lambda}{\mu}, 0,0,0,0,0\right)$, where,

$$\mathcal{F} = \left(\frac{\partial f_i(x_i)}{\partial x_i}\right) = \begin{pmatrix} 0 & \frac{\beta_I \Lambda}{\mu}(1-\theta) & \frac{\beta_H \Lambda}{\mu}(1-\theta) & \frac{\beta_V \Lambda}{\mu} \\ 0 & 0 & 0 & 0 \\ 0 & 0 & 0 & 0 \\ 0 & 0 & 0 & 0 \end{pmatrix}$$

and

$$\mathcal{G} = \left(\frac{\partial \mathcal{G}_i(x_i)}{\partial x_i}\right) = \begin{pmatrix} k_1 & 0 & 0 & 0 \\ -\alpha & k_2 & 0 & 0 \\ -\epsilon & -\nu & k_3 & 0 \\ 0 & -\gamma_I & -\gamma_H & \omega \end{pmatrix}.$$

After computing the eigen values of the matrix $\mathcal{K} = \mathcal{F}\mathcal{G}^{-1}$, we have the expression of $\mathcal{R}_0$,

$$\begin{aligned} \mathcal{R}_0 &= \frac{\alpha\beta_I\Lambda(1-\theta)}{\mu k_1 k_2} + \frac{\beta_H\Lambda(1-\theta)(\alpha\nu - \epsilon k_2)}{\mu k_1 k_2 k_3} \\ &\quad + \frac{\beta_V\Lambda(\alpha\gamma_I k_3 + \alpha\gamma_H\nu + \gamma_H\epsilon k_2)}{\mu k_1 k_2 k_3 \omega} \\ &= \frac{\begin{matrix}\omega k_3\alpha\beta_I\Lambda(1-\theta) + \omega\beta_H\Lambda(1-\theta)(\alpha\nu - \epsilon k_2) \\ +\beta_V\Lambda(\alpha\gamma_I k_3 + \alpha\gamma_H\nu + \gamma_H\epsilon k_2)\end{matrix}}{\mu k_1 k_2 k_3 \omega} \\ \mathcal{R}_0 &= \mathcal{R}_0^{isp} + \mathcal{R}_0^{ive}, \end{aligned}$$

where

$$\mathcal{R}_0^{isp} = \frac{\omega k_3\alpha\beta_I\Lambda(1-\theta) + \omega\beta_H\Lambda(1-\theta)(\alpha\nu - \epsilon k_2)}{\mu k_1 k_2 k_3 \omega},$$
$$\mathcal{R}_0^{ive} = \frac{\beta_V\Lambda(\alpha\gamma_I k_3 + \alpha\gamma_H\nu + \gamma_H\epsilon k_2)}{\mu k_1 k_2 k_3 \omega}.$$

Here, $\mathcal{R}_0^{isp}$ indicates the average number of secondary infections generated by a single infected individual introduced to susceptible populations directly during their life cycle. $\mathcal{R}_0^{ive}$ indicates the average number of secondary infections generated by the virus released into the environment during its life cycle.

Local stability analysis

The general Jacobian matrix associated to system (1) is given by

$$J = \begin{pmatrix} -(\mu + \beta_V V + (1-\theta)(\beta_I I + \beta_H H)) & 0 & -(1-\theta)\beta_I S & -(1-\theta)\beta_H S & \rho & -\beta_V \\ \beta_V V + (1-\theta)(\beta_I I + \beta_H H) & -k_1 & (1-\theta)\beta_I S & (1-\theta)\beta_H S & 0 & \beta_V \\ 0 & \alpha & -k_2 & 0 & 0 & 0 \\ 0 & \epsilon & \nu & -k_3 & 0 & 0 \\ 0 & 0 & \gamma_I & \gamma_H & -k_4 & 0 \\ 0 & 0 & \gamma_I & \gamma_H & 0 & -\omega \end{pmatrix}.$$

We will prove the local stability of equilibrium points following theorems with proofs.

Theorem 1. The disease-free equilibrium point Y_0 of the proposed COVID-19 epidemic model (1) is locally asymptotically stable if $\mathcal{R}_0 < 1$ and unstable otherwise.

Proof. Substitute the point Y_0 to the general Jacobian matrix J that yields

$$J(Y_0) = \begin{pmatrix} -\mu & 0 & \frac{-\beta_I\Lambda(1-\theta)}{\mu} & \frac{-\beta_H\Lambda(1-\theta)}{\mu} & \rho & -\beta_V \\ 0 & -k_1 & \frac{\beta_I\Lambda(1-\theta)}{\mu} & \frac{\beta_H\Lambda(1-\theta)}{\text{ì}} & 0 & \beta_V \\ 0 & \alpha & -k_2 & 0 & 0 & 0 \\ 0 & \epsilon & \nu & -k_3 & 0 & 0 \\ 0 & 0 & \gamma_I & \gamma_H & -k_4 & 0 \\ 0 & 0 & \gamma_I & \gamma_H & 0 & -\omega \end{pmatrix}$$

as per the Routh-Hurwitz criterion, for $\mathcal{R}_0 < 1$, the disease-free equilibrium point Y_0 of the proposed model (1) is locally asymptotically stable if all eigenvalues $\lambda_i, i = 1,2,\dots,6$ of the matrix $J(Y_0)$ are negative numbers or have negative real parts. We can evaluate these eigenvalues from the following characteristics polynomial

$$\left|J(Y_0) - \lambda\vec{I}\right| = 0 \quad (5)$$

where $\vec{I}$ is an identity matrix of order six and λ is the eigenvalues. By using cofactor expansion method, we get $\lambda_1 = -\mu < 0$ and $\lambda_2 = -k_4 < 0$ and the fourth-order Routh-Hurwitz matrix such that, we get the characteristic polynomial of the form

$$P^{Y_0}(\lambda) = \lambda^4 + b_1\lambda^3 + b_2\lambda^2 + b_3\lambda + b_4 = 0$$

where b_1, b_2, b_3,and b_4 is given in the Box 1.

Therefore, the stability when $\mathcal{R}_0 < 1$ follows the Routh-Hurwitz criterion for fourth-order polynomials, the disease-free equilibrium point is asymptotically stable if and only if

i) $b_1 > 0$ and $b_4 > 0$,
ii) $h_1 = b_1 b_2 - b_3 > 0$,
iii) $h_2 = b_3(b_1 b_2 - b_3) - b_1^2 b_4 > 0$.

Theorem 2. The endemic equilibrium point Y^* of the proposed COVID-19 epidemic model (1) is locally asymptotically stable if $\mathcal{R}_0 > 1$ and unstable otherwise.

ISSN. 2087-2852
E-ISSN. 2338-1655

Proof. Substitute the point Y^* to the general Jacobian matrix J that yields

$$J(Y^*) = \begin{pmatrix} -(\mu+n_1) & 0 & -n_2 & -n_3 & \rho & -\beta_V \\ n_1 & -k_1 & n_2 & n_3 & 0 & \beta_V \\ 0 & \alpha & -k_2 & 0 & 0 & 0 \\ 0 & \epsilon & \nu & -k_3 & 0 & 0 \\ 0 & 0 & r_I & r_H & -k_4 & 0 \\ 0 & 0 & \gamma_I & \gamma_H & 0 & -\omega \end{pmatrix},$$

where

$n_1 = \beta_V V^* + (1-\theta)(\beta_I I^* + \beta_H H^*)$,
$n_2 = (1-\theta)\beta_I S^*$,
$n_3 = (1-\theta)\beta_H S^*$.

as per the Routh-Hurwitz criterion, for $\mathcal{R}_0 > 1$, the endemic equilibrium Y^* of the proposed model (1) is locally asymptotically stable if all eigenvalues $\lambda_i, i = 1,2,\dots,6$ of the matrix $J(Y^*)$ are negative numbers or have negative real parts. We can evaluate these eigenvalues from the following characteristics polynomial

$$\left|J(Y^*) - \lambda\vec{I}\right| = 0 \quad (6)$$

where $\vec{I}$ is an identity matrix of order six and λ is the eigenvalues. Therefore, we get the characteristic polynomial of the form

$$P^{Y^*}(\lambda) = \lambda^6 + b_1\lambda^5 + b_2\lambda^4 + b_3\lambda^3 + b_4\lambda^2 + b_5\lambda + b_6 = 0$$

where b_1, b_2, b_3, b_4, b_5, and b_6 is given in Box 1.

Therefore, the stability when $\mathcal{R}_0 > 1$ follows the Routh-Hurwitz criterion for sixth-order polynomials, the endemic equilibrium point is asymptotically stable if and only if

i) $b_1 > 0$ and $b_6 > 0$,
ii) $h_3 = b_1b_2 - b_3 > 0$,
iii) $h_4 = b_3(b_1b_2 - b_3) - b_1(b_1b_4 - b_5) > 0$,
iv) $h_5 = b_4\big(b_3(b_1b_2 - b_3) - b_1(b_1b_4 - b_5)\big) - b_5\big(b_2(b_1b_2 - b_3) - (b_1b_4 - b_5)\big) + b_6b_1(b_1b_2 - b_3) > 0$,
v) $h_6 = b_5\Big(b_4\big(b_3(b_1b_2 - b_3) - b_1(b_1b_4 - b_5)\big) - b_5\big(b_2(b_1b_2 - b_3) - (b_1b_4 - b_5)\big) + 2b_6b_1(b_1b_2 - b_3)\Big) - b_6\big(b_3(b_3(b_1b_2 - b_3) - b_1(b_1b_4 - b_5) - b_1^2b_2b_3)\big) > 0$.

Sensitivity analysis

Sensitivity analysis can help analyze the parameters that influence the spread of disease. The normalized forward sensitivity index of a variable $\mathcal{R}_0$, depends on a parameter p, that is defined in Chitnis *et al.* [10].

$$\Omega_p^{\mathcal{R}_0} = \frac{\partial\mathcal{R}_0}{\partial p} \times \frac{p}{\mathcal{R}_0}, \quad (7)$$

where p is one of the parameters whose sensitivity on $\mathcal{R}_0$ is sought. This index implies that the higher the value, the more sensitive $\mathcal{R}_0$ is to the parameter. The positive (or negative) of the index indicates the increases (or decreases) of $\mathcal{R}_0$ as p increase. Based on the parameter values given in Table 2, we get $\mathcal{R}_0 = 6.238762263$. The sensitivity index of the parameters to $\mathcal{R}_0$ given in Table 3.

Table 2. Parameter values and sources

Parameters	Value	Sources
Λ	40	[9]
β_I	0.55	[8]
β_H	0.05	Estimated
β_V	0.3	[8]
θ	0.61	[9]
α	0.08	[9]
ϵ	0.37	[9]
ν	0.08	[9]
r_I	0.2	[9]
r_H	0.65	[9]
γ_I	0.1	[8]
γ_H	0.05	Estimated
d	0.011	Estimated
μ	0.5	Estimated
ω	0.172	[8]
ρ	0.05	Estimated

Table 3. Sensitivity index to $\mathcal{R}_0$

Parameters	Sensitivity index to $\mathcal{R}_0$
μ	-2.07027958
Λ	1
β_V	0.621457651
ω	-0.621457651
θ	-0.592079059
α	0.45676089
γ_H	0.383349503
β_I	0.2928254
r_H	-0.26261257
γ_I	0.238108148
r_I	-0.136781648
β_H	0.085716949
ϵ	0.0695549
ν	-0.044674791
d	-0.011967203

For our proposed COVID-19 epidemic model (1), we follow the analysis done by Chitnis *et al.* [10]. A positive sensitivity index indicates an increase in the parameter leads to an increase of $\mathcal{R}_0$, while a negative sensitivity index indicates an increase in the parameter leads to a decrease of $\mathcal{R}_0$. Among these parameters, $\Lambda, \beta_V, \beta_I, \gamma_H, \gamma_I, \alpha, \epsilon$, and β_H have the positive index and $\mu, \omega, \theta, r_H, r_I, \nu$, and d have the negative index. Thus, the sensitivity analysis results show μ, Λ, β_V, and ω are the most influential parameters for proposed model (1).

In Table 4 and Table 5, we show the influences of the increase (or decrease) of parameters to $\mathcal{R}_0$. The positive sensitivity index given in Table 4 shows that with an increase (or decrease) of one parameter, the $\mathcal{R}_0$ will get an addition (or reduction) and the endemic rate will increase (or decrease). The negative sensitivity index given in Table 5 shows that with an increase (or decrease) of one parameter, the $\mathcal{R}_0$ will get a reduction (or addition) and the endemic rate will decrease (or increase).

ISSN. 2087-2852
E-ISSN. 2338-1655

Disease-free equilibrium

$$b_1 = \omega + k_1 + k_2 + k_3$$
$$b_2 = \omega(k_1 + k_2 + k_3) + k_1(k_2 + k_3) + k_2k_3 - \frac{\Lambda}{\mu}(1-\theta)(\alpha\beta_I + \epsilon\beta_H)$$
$$b_3 = k_1k_2k_3 + \omega(k_1(k_2 + k_3) + k_2k_3) - \frac{\Lambda}{\mu}(1-\theta)\big(\alpha(\nu\beta_H + (\omega + k_3)\beta_I) + \epsilon\beta_H(\omega + k_2)\big) - \beta_V(\alpha\gamma_I + \epsilon\gamma_H)$$
$$b_4 = \omega k_1k_2k_3 - \frac{\Lambda\omega}{\mu}(1-\theta)(\alpha(\nu\beta_H + k_3\beta_I) + \epsilon k_2\beta_H) - \alpha\beta_V(\gamma_H(\nu + k_2) + \gamma_I k_3)$$

Endemic equilibrium

$$b_1 = \mu + \omega + n_1 + k_1 + k_2 + k_3 + k_4,$$
$$b_2 = \mu(\omega + k_1 + k_2 + k_3 + k_4) + \omega(n_1 + k_1 + k_2 + k_3 + k_4) + k_1(k_2 + k_3 + k_4) + k_2(k_3 + k_4) + k_3k_4 + n_1(k_1 + k2 + k_3 + k_4) - \alpha n_2 - \epsilon n_3,$$
$$b_3 = \mu(\omega(k_1 + k_2 + k_3 + k_4) + k_1(k_2 + k_3 + k_4) + k_2(k_3 + k_4) + k_3k_4) + \omega(n_1(k_1 + k_2 + k_3 + k_4) + k_1(k_2 + k_3 + k_4) + k_2(k_3 + k_4) + k_3k_4) + k_1\big(k_2(k_3 + k_4)\big) + k_3k_4(k_1 + k_2) + n_1(k_1(k_2 + k_3 + k_4) + k_2(k_3 + k_4) + k_3k_4) - \alpha(n_2(\mu + \omega + k_3 + k_4) + \nu n_3 + \beta_V\gamma_I) - \epsilon(n_3(\mu + \omega + k_2 + k_4) + \beta_V\gamma_H),$$
$$b_4 = \mu\big(\omega(k_1(k_2 + k_3 + k_4) + k_2(k_3 + k_4) + k_3k_4) + k_1k_2(k_3 + k_4) + k_3k_4(k_1 + k_2)\big) + \omega\big(k_1(k_2(k_3 + k_4) + k_3k_4) + n_1(k_1(k_2 + k_3 + k_4) + k_2(k_3 + k_4) + k_3k_4)\big) + n_1\big(k_1k_2(k_3 + k_4) + k_3k_4(k_1 + k_2)\big) + k_1k_2k_3k_4 - \alpha\big(\mu(n_2(\omega + k_3 + k_4) + n_3\nu + \beta_V\gamma_I) + \nu(n_3(\omega + k_4) + \beta_V\gamma_H) + \omega n_2(k_3 + k_4)\big) - \epsilon(\mu(n_3(\omega + k_2 + k_4) + \beta_V\gamma_H) + \omega n_3(k_2 + k_4) + \beta_V\gamma_H(k_2 + k_4) + n_3k_2k_4 + \tilde{n}n_1r_H),$$
$$b_5 = \mu\omega\big(k_1k_2(k_3 + k_4) + k_3k_4(k_1 + k_2)\big) + (\mu + \omega + n_1)k_1k_2k_3k_4 + \omega n_1\big(k_1k_2(k_3 + k_4) + k_3k_4(k_1 + k_2)\big) - \alpha\big(\mu(\nu(n_3(\omega + k_4) + \beta_V\gamma_H) + (\omega n_2 + \beta_V\gamma_I)(k_3 + k_4) + n_2k_3k_4) + \nu(k_4(n_3\omega + \beta_V\gamma_H) + \rho n_1r_H) + \omega(\rho n_1r_I + n_2k_3k_4) + k_3(\rho n_1r_I + \beta_V\gamma_Ik_4)\big) - \epsilon\Big(\mu\big((\omega n_3 + \beta_V\gamma_H)(k_2 + k_4) + n_3k_2k_4\big) + \omega(\rho n_1r_H + n_3k_3k_4) + k_2(\rho n_1r_H + \beta_V\gamma_Hk_4)\Big),$$
$$b_6 = \omega\big(k_1k_2k_3k_4(\mu + n_1)\big) - \alpha\Big(\mu\Big(k_4\big(\nu(\omega n_3 + \beta_V\gamma_H) + k_3(\omega n_2 + \beta_V\gamma_I)\big)\Big) + \omega\rho n_1(\nu r_H + k_3r_I)\Big) - \epsilon\big(k_2(\mu k_4(\omega n_3 + \beta_V\gamma_H) + \omega\rho n_1r_H)\big).$$

Box 1

Numerical simulations

This section aids in predicting the stability of the model (1) numerically using the fourth-order Runge-Kutta method with the help of MATLAB software. The numerical simulations are used to verify the analytical results.

Table 4. Influences of the positive sensitivity index parameters to $\mathcal{R}_0$

No.	Parameter ($\boldsymbol{p}$)	$\mathcal{R}_0$ value	
		$\boldsymbol{p} + 10\%$	$\boldsymbol{p} - 10\%$
1.	Λ	6.862638485	5.614886035
2	β_V	6.626474917	5.851049609
3.	α	6.521344877	5.951379936
4.	γ_H	6.477924903	5.999599620
5.	β_I	6.421449069	6.056075458
6.	γ_I	6.387312276	6.090212250
7.	β_H	6.292239030	6.185285497
8.	ϵ	6.280529198	6.193610053

Table 5. Influences of the negative sensitivity index parameters to $\mathcal{R}_0$

No.	Parameter ($\boldsymbol{p}$)	$\mathcal{R}_0$ value	
		$\boldsymbol{p} + 10\%$	$\boldsymbol{p} - 10\%$
1.	μ	5.110513732	7.738847295
2.	ω	5.886296211	6.6695541
3.	θ	5.869378215	6.608146312
4.	r_H	6.083610862	6.412316656
5.	r_I	6.155531881	6.326310693
6.	ν	6.211169788	6.266918568
7.	d	6.231305433	6.246237566

Simulation on disease-free equilibrium points

The parameters used for this simulation is from Table 2 except $d = 0.5, \mu = 0.8, \omega = 1.72$, and $\beta_V = 0.03$ with $\mathcal{R}_0 = 0.5942745861 < 1$. The disease-free equilibrium point $Y_0 = \left(\frac{\Lambda}{\mu}, 0,0,0,0,0\right) = (50,0,0,0,0,0)$.

ISSN. 2087-2852
E-ISSN. 2338-1655

Local stability analysis based on Routh-Hurwitz criterion where

i) $b_1 = 6.5 > 0$ and $b_4 = 2.7539565 > 0$,
ii) $h_1 = 81.832575 > 0$,
iii) $h_2 = 897.8537228 > 0$.

where $b_2 = 14.49635$, and $b_3 = 12.3937$.

These show that Routh-Hurwitz criterion is fulfilled and the characteristics polynomial have negative real parts.

Figure 2 shows that using initial condition $NA = (100,60,20,20,10,50)$, the susceptible subpopulation ends at equilibrium point 50, and the other subpopulations end at equilibrium points. It means that the numerical simulation approve of the analytical results.

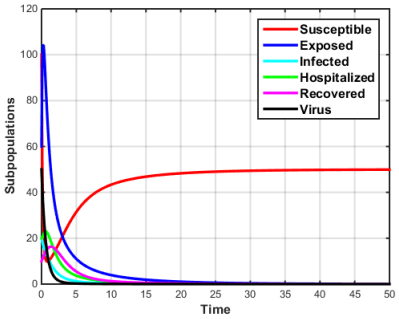

Figure 2. Numerical simulation when $\mathcal{R}_0 < 1$

Simulation on endemic equilibrium points

The parameters used for this simulation is from Table 2 with $\mathcal{R}_0 = 6.238762263 > 1$. Y^* exists where $k_1\mu < \Lambda(a_4 + a_5) = 0.475 < 2.963412073$ and $a_3 < k_1 = 0.02108240255 < 0.95$. Based on those parameters we get the endemic equilibrium

$Y^* = (S^*, E^*, I^*, H^*, R^*, V^*)$
$= (12.82305634, 36.15872058, 3.657013458,$
$11.77544159, 15.24625405, 5.549264101).$

Local stability analysis based Routh-Hurwitz criterion where

i) $b_1 = 6.802829728 > 0$ and
$b_6 = 0.24046706 > 0$,
ii) $h_3 = 91.79853862 > 0$,
iii) $h_4 = 1209.367776 > 0$,
iv) $h_5 = 8872.761805 > 0$,
v) $h_6 = 93025.31869 > 0$.

where $b_2 = 16.17011194, b_3 = 18.20397962,$ $b_4 = 18.20397962$, and $b_5 = 2.705938479$.

These show that Routh-Hurwitz criterion is fulfilled and the characteristics polynomial have negative real parts. Figure 3 shows that using initial condition $NA = (100,60,20,20,10,50)$, all of the subpopulations end at the equilibrium point Y^*. It means that the numerical simulation approves the analytical results.

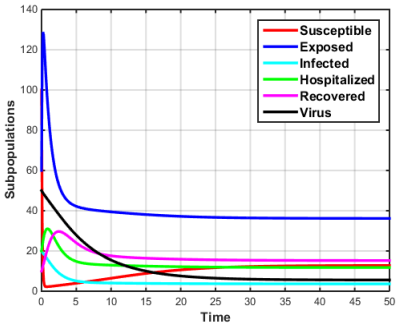

Figure 3. Numerical simulation when $\mathcal{R}_0 > 1$

Numerical simulations of the influences of the changed parameters to E and I

From the sensitivity analysis, we got parameters that have influences on $\mathcal{R}_0$. Here, we give numerical simulations for the high sensitivity index and the low sensitivity index to see which one has the gretest influence on the population.

It can be seen that in Figure 4 and Figure 5, when β_V value is increased, $\mathcal{R}_0$ will increase from 6.238762263 to 6.626474917 and the subpopulations of E and I also increase. When β_V value is decreased then $\mathcal{R}_0$ will decrease to 5.851049609 and the subpopulations of E and I also decrease.

In Figure 6 and Figure 7, when β_H value is increased, $\mathcal{R}_0$ will increase from 6.238762263 to 6.292239030 and the subpopulations of E and I also increase. When β_V value is decreased then $\mathcal{R}_0$ will decrease to 6.185285497 and the subpopulations of E and I also decrease.

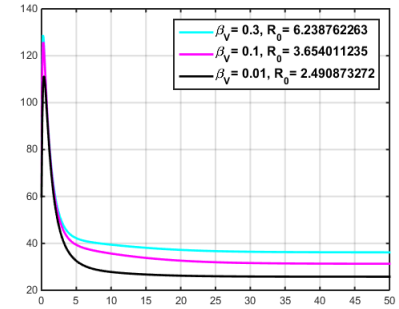

Figure 4. Influence of β_V to E

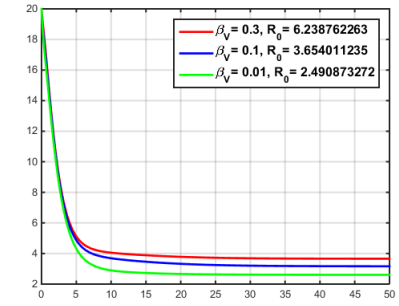

Figure 5. Influence of β_V to I

ISSN. 2087-2852
E-ISSN. 2338-1655

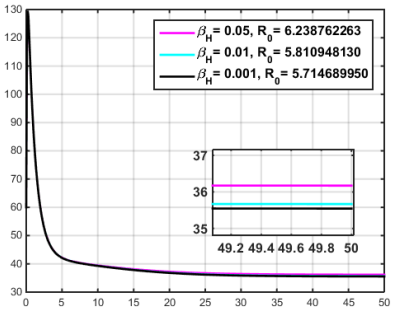

Figure 6. Influence of β_H to E

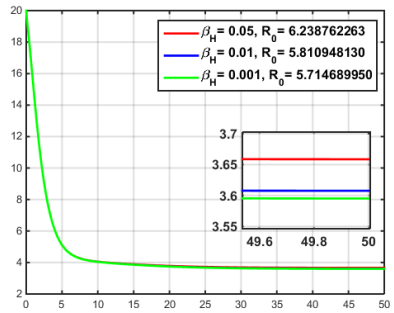

Figure 7. Influence of β_H to I

From the description above, we can conclude as follows. β_V, as a parameter with higher sensitivity index, have a more significant influences to the increase (or decrease) of $\mathcal{R}_0$ for each change of parameter value than β_H that has lower sensitivity index.

CONCLUSION

In this paper, we have proposed and investigated a mathematical model of the COVID-19 epidemic involving viruses in the environment. This model has been used to describe the transmission in the dynamics of the infection and affirms the role of the virus in the environment to the spread of COVID-19 disease. The model is numerically simulated to aid the analytical results that have been done. We have proposed a detailed analysis of the model, including the derivation of equilibrium points, disease-free and endemic, and the basic reproduction number $\mathcal{R}_0$. The local stability analysis of the model fulfilled the Routh-Hurwitz criterion and the sensitivity analysis was also done to know the parameters that have more influence on $\mathcal{R}_0$. The numerical simulations are used to aid and approve the analytical results and prove the sensitivity analysis of the model's parameters. The simulations show that β_V has more influences on $\mathcal{R}_0$ for it has a more sensitivity index than β_H.

ACKNOWLEDGEMENTS

Part of this research is supported by Faculty of Mathematics and Natural Sciences (FMIPA), University of Brawijaya, through Public Funds PDA, with the Research Contract No. 3110.18/ UN10.F09/PN/2022.

REFERENCES

[1] World Health Organization (WHO). 2022. Global situation COVID-19. WHO. Available at: https://covid19.who.int/.

[2] Batista, M. 2020. Estimation of the final size of the COVID-19 epidemic. *Proceedings in MedRxiv* (Preprint). 1-10. DOI: 10.1101/2020.02.16.20023606.

[3] Sun, H., Y. Qiu, H. Yan, Y. Huang, Y. Zhu, S.X. Chen. 2020. Tracking and predicting COVID-19 epidemic in China Mainland. *J. Data Sci.* 18(3). 455-472.

[4] Ming, W.K., C.J. Zhang, J.V. Huang. 2020. Breaking down the healthcare system: Mathematical modelling for controlling the novel coronavirus (2019-nCoV) outbreak in Wuhan, China. *Reseach Gate*. 1-24.

[5] Nesteruk, I. 2020. Statistics-based predictions of coronavirus epidemic spreading in mainland China. *Innov. Biosyst. Bioeng.* 4(1). 13-18.

[6] Victor, A.O. 2020. Mathematical predictions for COVID-19 as a global pandemic. *SSRN Electronic Journal.* 1-16.

[7] Zeb, A., E. Alzahrani, V.S. Erturk, G. Zaman. 2020. Mathematical model for Coronavirus Disease 2019 (COVID-19) containing isolation class. *Biomed Res. Int.* 1-7.

[8] Naik, P.A., J. Zu, M.B. Ghori, M. Naik. 2021. Modeling the effects of the contaminated environments on COVID-19 transmission in India. *Results Phys.* 29. 104774. DOI: 10.1016/j.rinp.2021.104774.

[9] Masandawa, L., S.S. Mirau, I.S. Mbalawata, J.N. Paul, K. Kreppel, O.M. Msamba. 2022. Modeling nosocomial infection of COVID-19 transmission dynamics. *Results Phys.* 37(10). 105503. DOI: 10.1016/j.rinp.2022.105503.

[10] Chitnis, N., J.M. Hyman, J.M. Cushing. 2008. Determining important parameters in the spread of malaria through the sensitivity analysis of a mathematical model. *Bull. Math. Biol.* 70. 1272-1296. DOI: 10.1007/s11538-008-9299-0.

The Impact of Releasing Domestic Dogs on the Spread of Rabies Disease and Its Prevention

Ahmad Fitri*, Marsudi, Trisilowati

Department of Mathematics, Faculty of Mathematics and Natural Sciences, University of Brawijaya, Malang, Indonesia

Abstract

The government's program to achieve rabies-free status by 2030 is an initiative to accelerate the eradication of rabies cases in Indonesia. Rabies is a highly contagious disease with a 100% fatality rate, and dogs are the main carriers of the virus. The government's efforts to minimize rabies cases include vaccination of susceptible animals, eliminating rabid dogs, and implementing dog population management (MPA). Field observations indicate that the practice of releasing domestic dogs allowing them to roam freely, has led to an increase in rabies cases. Using mathematical modeling, this husbandry system's impact can be simulated. Based on the model analysis, it is determined that a maximum of 15% of domestic dogs should be allowed to roam freely. If this threshold is exceeded, it becomes necessary to ensure a minimum of 20% vaccination coverage and eliminate at least 1% of rabid dogs.

Keywords: Dogs, Rabies Disease, Releasing Domestic Dogs.

INTRODUCTION

The national government's program is to make Indonesia rabies-free by 2030. However, in 2019, the number of provinces declared rabies-free decreased from the previous year, with only 8 out of 9 provinces declared rabies-free in 2018 [1]. This information highlights the government's seriousness in eradicating rabies to achieve the national program's goal. Government efforts to prevent rabies transmission include vaccination of susceptible animals, elimination of animals suspected of being exposed to rabies, and the implementation of dog population management (MPA).

Dogs are known as the main rabies transmitters, and the virus is fatal to all mammal species [2]. Out of 150 countries worldwide, in Asia and Africa, more than 95% of rabies deaths occur, with 40% being children under 15 years old. The total number of rabies-related deaths is approximately 59,000 people per year, with 99% of them caused by dog bites [3]. In Indonesia, the number of deaths due to rabies is still relatively high, ranging from 100 to 156 deaths per year, with an almost 100% fatality rate [4]. From 2015 to 2019, there were 404,306 recorded cases of rabies bites, resulting in 544 deaths.

*Corresponding Address:
Ahmad Fitri
E-mail : fitri.ahmad.afit@gmail.com
Address : Dept. Mathematics, University of Brawijaya, Veteran Malang, 65145.

Regarding rabies incidence rates from 2018 to 2020, Bali has been identified as one of the regions with the highest incidence rates, with 26,130 cases in 2018, 37,372 cases in 2019, and almost 27,000 in 2020 [5]. A large number of stray dogs in Bali contributes to the increased spread of rabies, likely due to a lack of public education on responsible dog ownership [6]. As reported in 2021 [5], out of 96 people bitten by dogs in Kuta Utara Sub-district, 70% of them were bitten by stray dogs. Given these circumstances, further research is needed to analyze a mathematical model of the spread of rabies in the context of releasing domestic dogs.

The phenomena occurring in the development of rabies in dogs can be described through mathematical modeling. Analysis can be conducted analytically and through numerical simulation approaches. The analytical approach allows for obtaining exact solutions that closely approximate the actual solutions. It is crucial to understand the model's properties and the effects of the involved parameters, especially in the case of releasing dogs. By analyzing the differential equations analytically, we can identify the relationships between the involved subpopulations, determine equilibrium points, study the system's stability properties, and analyze the model's behavior. Once the analytical solutions are obtained, it is essential to complement them with numerical simulation approaches. We can obtain good approximations of the system's solutions

numerically with numerical methods, even when no analytical solutions are known. This approach allows us to model a more comprehensive system by considering a more significant number of parameters and conditions that occur in real-life situations.

This research utilizes a combination of quantitative data analysis and mathematical modeling. Epidemiological data on dog rabies cases, vaccination coverage, and dog demographics were collected from the affected area and used as comparative data. The data used in this study is the rabies cases data in dogs obtained from the Bali Provincial Department of Agriculture, 2008-2018 [7]. A mathematical model was developed to simulate the dynamics of rabies transmission in the context of releasing domestic dogs.

Self-modeling of rabies has been widely conducted, including [8], who introduced a simple model of rabies in dogs in Bali. The model consists of two compartments, namely S for healthy dogs and I for rabid dogs. The analysis results not only suggest the administration of vaccines to reduce the spread of rabies but also the need to limit the birth rate in the population of healthy dogs.

Based on the recommendations of a previous study [8], a model can be developed by dividing the dog population into two groups, stray dogs and domestic dogs, based on the level of interaction of each group. In 2018, a research [9] further developed the model proposed [8] by adding a vaccinated compartment (V), resulting in a model with three compartments. The analysis results indicated the need to reduce the birth rate and increase vaccination to reduce rabies transmission. Hailemichael *et al.* [10] discuss the population dynamics of rabies in dogs by dividing them into two categories: stray and domestic dogs. The basic model used is $SEIV$, resulting in a model consisting of eight compartments: four for stray dogs and four for domestic dogs. The model assumes that only stray dogs can transmit the disease and rabies is incurable. The designed model goes beyond a typical model by incorporating vaccination control and elimination measures. An effective method is to combine two measures: vaccination and elimination of rabies-infected dogs to reduce the spread of the rabies virus. The birth rate of the susceptible dog population, both domestic and stray dogs, is also an essential factor in the spread of rabies.

The mathematical model in this study is a development of the model proposed by Fitri *et al.* [8], dividing the dog population into two groups: domestic dogs and stray dogs, like the developed model by Nugraha *et al.* [6]. Then, the model is developed by adding a subpopulation of vaccinated/immune dogs, both domestic and stray, so that the model becomes similar to Roberta *et al.* [9]. The development of the model can help understand the impact of vaccination on the dog population. The designed model consists of four nonlinear differential equations. The impact of releasing domestic dogs and the influence of prevention measures such as vaccination and elimination are analyzed in the model. The study concludes with numerical simulations using the fourth-order Runge-Kutta method to strengthen the analytical results.

MATERIALS AND METHODS

This research utilizes a nonlinear differential equation approach to model a system involving the interaction (physical contact) between susceptible and infected subpopulations of dogs. This is because physical contact between susceptible and infected dogs can pose a risk for disease transmission. The interactions between subpopulations in the model are often nonlinear, meaning that changes in one subpopulation can affect the changes in other subpopulations. Therefore, this study employs a nonlinear differential equation approach to understand the development of the rabies subpopulations. Figure 1 shows cases of rabies in dogs in Bali from 2008 to 2018. The data is used as comparative data.

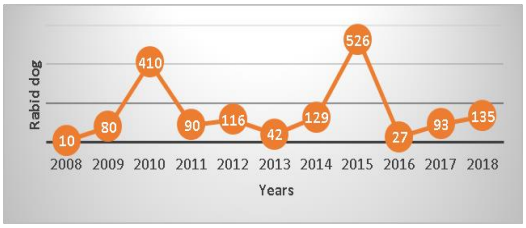

Figure 1. Rabid dogs in Bali, 2008-2018

Construction Model

In this study, the rabies transmission model in dogs consists of two population groups: stray dogs and domestic dogs. Each population group consists of susceptible and infected subpopulations. Both population groups assume there is interaction and only stray dogs can transmit the rabies disease. The model is expressed in the form of a nonlinear autonomous system.

The presence of released domestic dogs

contributes to the increasing population of stray dogs, especially those susceptible to rabies. A mathematical model was developed to simulate the dynamics of rabies transmission in the population of released domestic dogs. By analyzing this model, we can determine the threshold level of released domestic dogs to prevent increased rabies cases. If the level of released domestic dogs exceeds this threshold, it indicates an endemic tendency. Therefore, preventive measures such as vaccination and elimination of rabid dogs are implemented in this model.

Determination of the Equilibrium Points

The equilibrium points of a differential equation remain unchanged. Therefore, when the solution of a system is constant, equilibrium points are obtained. Generally, the equilibrium points of the model consist of two types: disease-free equilibrium point, which represents the extinction of rabies in dogs, and endemic equilibrium point, where rabies in dogs continues to persist.

Stability of the Equilibrium Points

The equilibrium point of a nonlinear model is asymptotically stable if the eigenvalues of the linearized Jacobian matrix have negative real parts. It is unstable if any of the eigenvalues of the linearized Jacobian matrix have positive real parts.

Numerical Simulation

Numerical simulations are performed to strengthen the analytical results and illustrate the model's behavior. The simulations are conducted using the fourth-order Runge-Kutta method. The parameter values and constraint level of released domestic dogs are determined to verify the results obtained analytically.

RESULT AND DISCUSSION

Model Formulation

Domestic dogs' susceptibility decreases when released, resulting in an increase in susceptible stray dogs. Both populations also increase due to births and decrease due to deaths and rabies transmission. Rabies transmission occurs through physical contact with infected stray dogs. This transmission process can be prevented through vaccination and elimination. If both susceptible domestic and stray dogs are late in prevention during transmission, the population of infected stray and pet dogs will increase. Rabid dogs, whether stray or domestic, decrease due to natural deaths.

Furthermore, we assume the existence of four subpopulations: susceptible dogs and dogs infected with rabies, each divided into stray and domestic dogs. Therefore, the model to be designed is similar to the interaction model between the two groups.

The susceptible (S_d) and infected (I_d) subpopulations of domestic dogs: Λ_d represents the recruitment rate of susceptible dogs, along with μ_d as the natural death rate. β_{ds} denotes the disease transmission rate within this group. The susceptible (S_s) and infected (I_s) subpopulations of stray dogs: Λ_s represents the recruitment rate of susceptible dogs (births) and μ_s as the natural death rate. The disease transmission rate within this group is denoted by β_{ss}. The rate of domestic dog release is donated by ϕ, resulting in a decrease in the susceptible subpopulation of domestic dogs and an increase in the susceptible subpopulation of stray dogs. The illustration of rabies transmission in stray and domestic dogs in the context of release is depicted in the diagram:

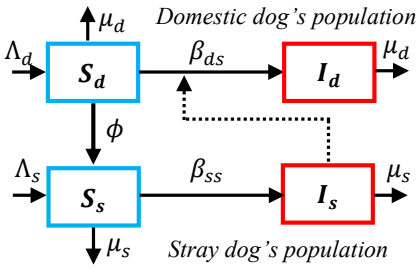

Figure 2. The compartmental model for rabies transmission

Model Equation

Based on Figure 2 above, the rabies transmission model with the presence of a system for releasing domestic dogs is formulated as the following system of nonlinear differential equations. The following Table 1 provides the model parameters along with their descriptions:

$$\left.\begin{aligned}
\frac{dS_d}{dt} &= \Lambda_d - \phi S_d - \beta_{ds} S_d I_s - \mu_d S_d \\
\frac{dI_d}{dt} &= \beta_{ds} S_d I_s - \mu_d I_d \\
\frac{dS_s}{dt} &= \Lambda_s + \phi S_d - \beta_{ss} S_s I_s - \mu_s S_s \\
\frac{dI_s}{dt} &= \beta_{ss} S_s I_s - \mu_s I_s
\end{aligned}\right\} \quad (1)$$

ISSN. 2087-2852
E-ISSN. 2338-1655

Table 1. Model Parameter

Symbol	Information	Value	Source
Λ_d	Number of domestic dog recruitment	120	[10]
Λ_s	Number of stray dog recruitment	32	[10]
β_{ds}	Rate of stray dog transmission to domestic dogs	0.00027	Assumed
β_{ss}	Rate of transmission from stray dog to stray dog	0.00054	[8]
μ_d	The natural death rate of domestic dogs	0.11	[10]
μ_s	The natural death rate of stray dogs	0.24	[10]
ϕ	The rate of releasing domestic dogs	[0,1]	Assumed

Disease-Free Equilibrium Points (DFE)

Equilibrium points when the left-hand of system (1) side equals zero are as follows:

$$\begin{aligned}\Lambda_d - \phi S_d - \beta_{ds} S_d I_s - \mu_d S_d &= 0,\\ \beta_{ds} S_d I_s - \mu_d I_d &= 0,\\ \Lambda_s + \phi S_d - \beta_{ss} S_s I_s - \mu_s S_s &= 0,\\ \beta_{ss} S_s I_s - \mu_s I_s &= 0.\end{aligned}$$

Based on the equation, two equilibrium points are obtained: disease-free equilibrium point and endemic equilibrium point. The disease-free equilibrium point

$$E_0 = \left(\frac{\Lambda_d}{\phi + \mu_d}, 0, \frac{\Lambda_s(\phi + \mu_d) + \phi\Lambda_d}{(\mu_s)(\phi + \mu_d)}, 0\right)$$

and the endemic equilibrium point are as follows.

$$S_s^* = \frac{\mu_s}{\beta_{ss}}, I_s^* = \frac{-B + \sqrt{B^2 - 4AC}}{2A},$$
$$S_d^* = \frac{\Lambda_d}{\beta_{ds} I_s^* + (\phi + \mu_d)}, I_d^* = \frac{\beta_{ds}}{\mu_d} S_d^* I_s^*.$$

$$A = 1,\ B = \frac{\beta_{ds}(\mu_s)^2 + (\phi+\mu_d)\mu_s - \beta_{ds}\beta_{ss}\Lambda_s}{\beta_{ds}\mu_s},$$
$$C = \frac{(\phi+\mu_d)((\mu_s)^2 - \beta_{ss}\Lambda_s) - \beta_{ss}\phi\Lambda_d}{\beta_{ds}\mu_s}$$

Stability Analysis

The stability of the equilibrium point of system (1), namely the equilibrium point E_0, will be analyzed. The linear approximation obtained in the section around the equilibrium points of system (1) can help determine the system's stability. The linear approximation of system (1) at the equilibrium point E_0 results in the Jacobian matrix.

$$J(E_0) = \begin{pmatrix} -(\phi + \mu_d) & 0 & 0 & -\beta_{ds} S_d^0 \\ 0 & -\mu_d & 0 & \beta_{ds} S_d^0 \\ \phi & 0 & -\mu_s & -\beta_{ss} S_s^0 \\ 0 & 0 & 0 & \beta_{ss} S_s^0 - \mu_s \end{pmatrix}$$

The characteristic values at this equilibrium point are given by:

$$\begin{vmatrix} \lambda + (\phi + \mu_d) & 0 & 0 & \beta_{ds} S_d^0 \\ 0 & \lambda + \mu_d & 0 & -\beta_{ds} S_d^0 \\ -\phi & 0 & \lambda + \mu_s & \beta_{ss} S_s^0 \\ 0 & 0 & 0 & \lambda - (\beta_{ss} S_s^0 - \mu_s) \end{vmatrix} = 0.$$

The resulting eigenvalues are:

$$\lambda_1 = -(\phi + \mu_d),$$
$$\lambda_2 = -\mu_d,$$
$$\lambda_3 = -\mu_s,$$
$$\lambda_4 = \beta_{ss} S_s^0 - \mu_s.$$

All four eigenvalues are real numbers, so for the equilibrium point E_0 to be stable, fourth characteristic values must be negative. Since $S_s^0 > 0$, we have $\lambda_4 = \beta_{ss} S_s^0 - \mu_s < 0$, which implies that $\frac{\beta_{ss}(\Lambda_s(\phi+\mu_d)+\phi\Lambda_d)}{(\phi+\mu_d)(\mu_s)^2} < 1$. Thus, based on stability theory, the equilibrium point E_0 is locally asymptotically stable if

$$\phi < \frac{\mu_d((\mu_s)^2 - \beta_{ss}\Lambda_s)}{\beta_{ss}(\Lambda_d + \Lambda_s) - (\mu_s)^2}.$$

If this is fulfilled, it can be said that rabies in dogs will experience extinction.

Model with Intervention

If interventions such as vaccination of susceptible dogs against rabies ($\nu_d = \nu_d = \nu$) and elimination ($\xi_d = \xi_s = \xi$) of rabid dogs are implemented, the two interventions are described as follows. ν_d represents vaccination in domestic dogs, and ν_s represents vaccination in stray dogs (assuming it remains constant). These interventions are periodically given according to the vaccination schedule, ensuring that the level of immunity against rabies in dogs is maintained. The elimination ξ_d is implemented in the infected subpopulation of domestic dogs, while in stray dogs, infected subpopulations receive the intervention ξ_s. The compartmental model with intervention in the diagram:

ISSN. 2087-2852
E-ISSN. 2338-1655

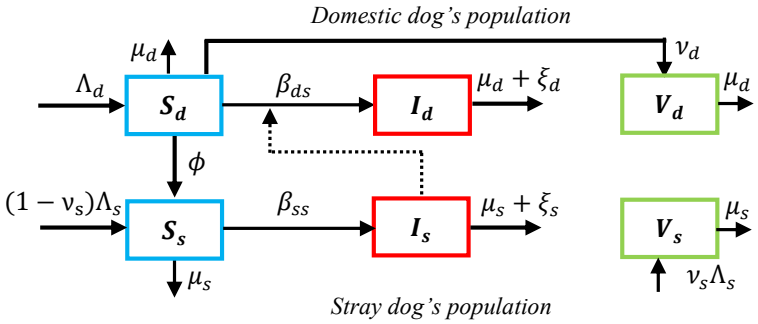

Figure 3. The compartmental model for rabies transmission with intervention

Model (1) becomes the following system.

$$\left.\begin{aligned}
\frac{dS_d}{dt} &= \Lambda_d - \phi S_d - \beta_{ds} S_d I_s - \mu_d S_d - \nu_d S_d \\
\frac{dI_d}{dt} &= \beta_{ds} S_d I_s - \mu_d I_d - \xi_d I_d \\
\frac{dV_d}{dt} &= \nu_d S_d - \mu_d V_d \\
\frac{dS_s}{dt} &= (1-\nu_s)\Lambda_s + \phi S_d - \beta_{ss} S_s I_s - \mu_s S_s \\
\frac{dI_s}{dt} &= \beta_{ss} S_s I_s - \mu_s I_s - \xi_s I_s \\
\frac{dV_s}{dt} &= \nu_s \Lambda_s - \mu_s V_s
\end{aligned}\right\} \quad (2)$$

The first and second equations of system (2) do not depend on the variable V_d, and the fourth and fifth equations of system (2) do not depend on the variable V_s. it is sufficient to analyze the dynamics using only the first, second, fourth, and fifth equations of system (2). Similarly processed, system (2) produces two equilibrium points.

The equilibrium points are disease-free and endemic. The disease-free equilibrium point

$E_0 = (S_d^0, 0, S_s^0, 0)$, with

$$S_d^0 = \frac{\Lambda_d + \alpha}{\phi + \nu_d + \mu_d}$$

$$S_s^0 = \frac{(1-\nu_s)\Lambda_s(\phi + \nu_d + \mu_d) + \phi\Lambda_d}{\mu_s(\phi + \nu_d + \mu_d)}$$

The stability of the disease-free equilibrium point is determined by substituting S_s^0 into the equations $\beta_{ss} S_s^0 - (\mu_s + \xi_s)$. If $S_s^0 < \frac{(\mu_s+\xi_s)}{\beta_{ss}}$, then this equilibrium point is asymptotically stable, meaning rabies in dogs will be eradicated. To ensure this condition is met, the following must be fulfilled:

$$\frac{(1-\nu_s)\Lambda_s(\phi + \nu_d + \mu_d) + \phi(\Lambda_d + \alpha)}{\mu_s(\phi + \nu_d + \mu_d)} < \frac{\mu_s + \xi_s}{\beta_{ss}}$$

Therefore, if interventions are applied to the model, the constraint on the rate of releasing domestic dogs will change according to the magnitude of the interventions performed (vaccination and elimination). It indicates that if the releasing domestic dogs' rate exceeds the limit, actions must be taken on the model to prevent rabies from spreading in dogs, with the following magnitudes.

1. $\xi_s > \frac{\beta_{ss}\phi\Lambda_d}{\mu_s(\phi+\nu_d+\mu_d)} + \frac{\beta_{ss}(1-\nu_s)\Lambda_s - \mu_s^2}{\mu_s}$
2. $\nu_d > \frac{\beta_{ss}\phi\Lambda_d}{\mu_s(\mu_s+\xi_s) - \beta_{ss}(1-\nu_s)\Lambda_s} - (\phi + \mu_d)$
3. $\nu_s > 1 - \left(\frac{\mu_s(\mu_s+\xi_s)}{\beta_{ss}\Lambda_s} + \frac{\phi\Lambda_d}{\Lambda_s(\phi+\nu_d+\mu_d)}\right)$

Numerical Simulation

To strengthen the analysis results, numerical simulations are conducted using fourth-order Runge-Kutta method. The initial values used are presented in Table 2.

ISSN. 2087-2852
E-ISSN. 2338-1655

Table 2. The initial value

Symbol	Value	Source
S_d	3200	[10]
S_s	15	[10]
I_d	2800	[10]
I_s	20	[10]

The parameter values for the numerical simulation are provided in Table 2, resulting in the constraint $\phi = 15\%$. The numerical simulation is conducted based on various values of (ϕ) to observe the model trends without any intervention. If $\phi < 15\%$, the system exhibits local and global asymptotic stability towards the disease-free equilibrium point E_0, while if $\phi > 15\%$, the equilibrium point E_0 is unstable. The simulation results are presented ϕ in Figure 4, with variations in the value of $\{0\%, 10\%, 25\%, 50\%\}$.

The simulation results show differences in the solution curves when the value of $\phi < 15\%$ and $\phi > 15\%$. If $\phi < 15\%$, the curves converge to the disease-free equilibrium point, while if $\phi < 15\%$, the curves converge to the endemic equilibrium point. Thus, rabies in dogs will be eliminated when the percentage of free-roaming domestic dogs is less than 15%. If it exceeds this threshold, preventive measures such as vaccination or elimination of rabies-exposed dogs are necessary. Furthermore, if the percentage of free-roaming domestic dogs is set at $\phi = 50\%$, the role of vaccination $\nu_d = \nu_s = \nu$ or elimination $\xi_d = \xi_s = \xi$ is illustrated in Figure 5.

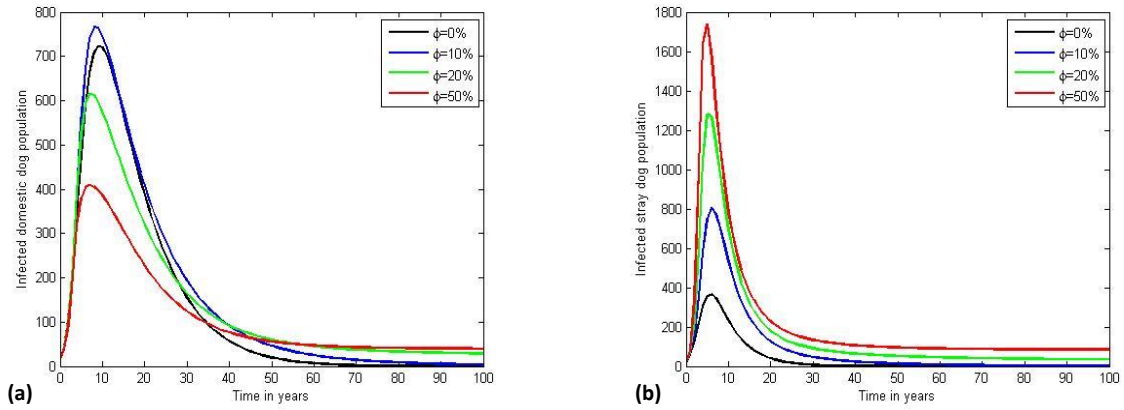

Figure 4. The numerical simulation results of system (1) with variations on the rate of releasing domestic dogs on the (a) Infected domestic dog population and (b) infected stray dog population

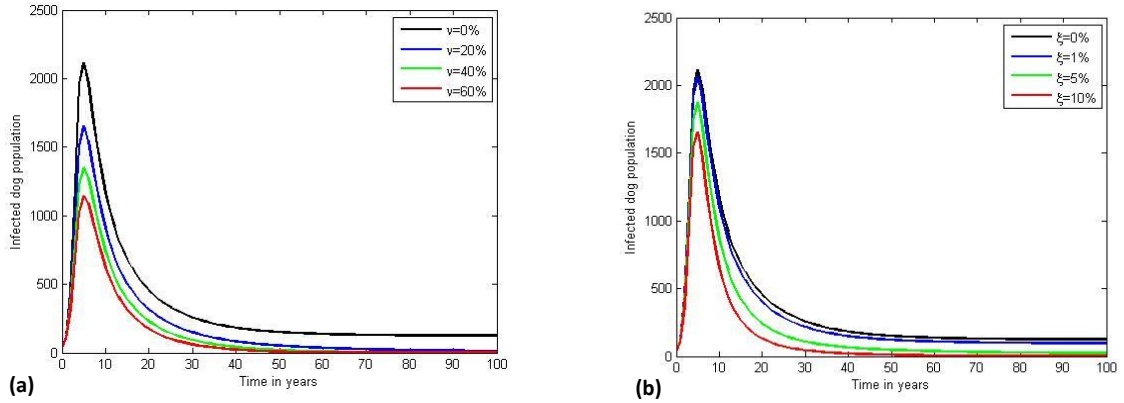

Figure 5. The impact of vaccination (a) and elimination (b) on rabies in dogs can be significant

Figure 5 (a) illustrates the impact of vaccination on the rabies dog subpopulation, while Figure 5 (b) depicts the effect of eliminating rabid dogs. When the value of $\phi > 15\%$, in order to reduce the spread of rabies, it is necessary to carry out a minimum vaccination rate of $\nu > 20\%$ or a minimum elimination of rabid dogs of $\xi > 1\%$.

CONCLUSION

Based on the model's simulation results, the system of releasing domestic dogs plays a crucial role in the spread of rabies. It is evident when the parameters in the designed model are given, as there is a limit to the rate of

ISSN. 2087-2852
E-ISSN. 2338-1655

domestic dog roaming. If the roaming rate exceeds this limit, it indicates the occurrence of rabies transmission. In such conditions, preventive measures such as vaccination or elimination of domestic and stray rabid dogs are necessary.

REFERENCES

[1] Novita, R. 2019. Pemberantasan rabies di Indonesia sebagai upaya mewujudkan *right to life*, *right to health*. *BALABA: Jurnal Litbang Pengendalian Penyakit Bersumber Binatang Banjarnegara.* 15(2).151-162. DOI: 10.22435/blb.v15i2.1581.

[2] Wang, X., J. Lou. 2008. Two dynamic models about rabies between dogs and human. *J. Biol. Syst.* 16(4). 519-529. DOI: 10.1142/S0218339008002666.

[3] Gholami, A., A. Alamdary. 2020. The World Day Rabies 2020: Collaborate and Vaccinate. *Iran. Biomed. J.* 24(5). 264-268. DOI: 10.29252/ibj.24.5.263.

[4] Nugraha, E. Y. 2021. Menuju Indonesia bebas rabies (Studi Kasus di Kabupaten Bangli, Bali). CV Veniks Muda Sejahtera. Bandung, Jawa Barat.

[5] Dewi, D.A.D.N, P.A.S. Astuti, I.G.A.A. Naya. 2022. Perbedaan karakteristik pasien kasus gigitan hewan penular rabies di Puskesmas Kuta Utara Periode Agustus-Oktober tahun 2021. *Intisari Sains Medis*. 13(1). 284-288. DOI: 10.15562/ism.v13i1.1308.

[6] Nugraha, I.M.B., D.G. Purwita, G.L.A.K. Putra. 2021. Perancangan animasi pendek sebagai saran kampanye stop buang anjing di Denpasar. *Jurnal Selaras Rupa.* 2(2). 95-103.

[7] Subrata, M., S.G. Purnama, A. Utami, K.K. Agustina, I.B.N. Swacita. 2020. Peranan pemangku kepentingan dalam pengendalian rabies dengan pendekatan *one health* terintegrasi di Bali. *Jurnal Kebijakan Kesehatan Indonesia.* 9. 20-32.

[8] Fitri, A., T.B. Oka, I.N. Widana. 2015. Model matematika (nonlinier) populasi anjing rabies dengan vaksinasi. *Jurnal Matematika.* 5(1). 14-29.

[9] Roberta, D., M. Kaftiah, W.B. Partiwi. 2018. Analisis kestabilan model dinamika populasi anjing rabies dengan vaksinasi. *Buletin Ilmiah Matematika, Statistika dan Terapannya (Bimaster)*. 7(1). 47-54.

[10] Hailemichael, D.D., G.K. Edessa, P.R. Koya. 2022. Effect of vaccination and culling on the dynamics of rabies transmission from stray dogs to domestic dogs. *J. Appl. Math.* 2022. Article ID 2769494. DOI: 10.1155/2022/2769494.

ISSN. 2087-2852
E-ISSN. 2338-1655

CORRIGENDUM:
Morphological Variation of Asian Small Lizards genus *Tytthoscincus* Linkem, Diesmos & Brown (Squamata : Scincidae) in Indonesia

Richo Firmansyah[1*], Awal Riyanto[2], Nia Kurniawan[1]

[1]Department of Biology, Faculty of Mathematics and Natural Sciences, University of Brawijaya, Malang, Indonesia
[2]Museum Zoologicum Bogoriense, Research Center of Biology, National Research and Innovation Agency (BRIN), Bogor, Indonesia

URL: https://doi.org/10.21776/ub.jels.2023.013.02.10

This is a corrigendum to the article *Morphological Variation of Asian Small Lizards genus Tytthoscincus Linkem, Diesmos & Brown (Squamata : Scincidae) in Indonesia* published online on 2023-08-03 by The Journal of Experimental Life Science (jels.ub.ac.id) with DOI: https://doi.org/10.21776/ub.jels.2023.013.02.05 [1].

The following is the correction for Table 1.

1. Character SVL on the second line should be TD/SVL
2. Added information/notes that all measurements are in millimeters

The corrected Table 1 is below.

Table 1. Mean values and Kruskal-Wallis test statistics on variation in morphometric ratios between OTUs and comparison of meristic characters.

Character	OTU					X^2	*P-value*
	***T. temmincki* type1**	***T. temmincki* type2**	***T. textus* type1**	***T. textus* type2**	***T. parvus***		
N	**type 1 (n=3)**	**type 2 (n=2)**	**type 1(n=12)**	**type 2 (n=4)**	**(n=11)**		
HdL/SVL	0.203 ± 0.007	0.221 ± 0.017	0.200 ± 0.013	0.206 ± 0.014	0.205 ± 0.015	4.0686	0.3968
TD/SVL	0.033 ± 0.004*	0.033 ± 0.003*	0.034 ± 0.003*	0.040 ± 0.003*	0.024 ± 0.003*	24.825*	$5.456e^{-05}$*
AXG/SVL	0.545 ± 0.024	0.479 ± 0.103	0.562 ± 0.020	0.536 ± 0.036	0.546 ± 0.025	6.1551	0.1879
FL/SVL	0.185 ± 0.012	0.175 ± 0.005	0.159 ± 0.016	0.173 ± 0.013	0.158 ± 0.016	8.0561	0.08954
HL/SVL	0.283 ± 0.043	0.229 ± 0.013	0.251 ± 0.024	0.272 ± 0.021	0.257 ± 0.022	7.3068	0.1205
TD/HdL	0.164 ± 0.011*	0.148 ± 0.000*	0.170 ± 0.012*	0.196 ± 0.004*	0.116 ± 0.015*	26.624*	$2.368e^{-05}$*
Supralabials	8(1), 6(2)	6	6	6	7(1), 6(10)		
Infralabials	5	5	5	6(1), 5(3)	5		
Supraoculars	4	4	4	4	4		
Loreals	1	2	2 (10), 1(2)	1	1		
Distribution	West Java, East Java	West Java	Gorontalo, Southeast Sulawesi, Central Sulawesi	South Sulawesi	Sulawesi, Gorontalo, Central Sulawesi		

Notes: * significant; HdL = head length, SVL = snout-vent length, TD = tympanum diameter, AXG = axilla groin length, FL = forelimb length, and HL = hind limb length. All measurements are in millimeters.

REFERENCES

[1] Firmansyah, R., A. Riyanto, N. Kurniawan. 2023. Morphological Variation of Asian Small Lizards genus Tytthoscincus Linkem, Diesmos & Brown (Squamata : Scincidae) in Indonesia. *J. Exp. Life Sci.* 13(2). 101-105.

*Correspondence address:
Richo Firmansyah
Email : richo.firmansyah25@gmail.com
Address : Dept. Biology, University of Brawijaya, Veteran Malang 65145, Indonesia.

MANUSCRIPT SUBMISSION

FOCUS AND SCOPE

Journal of Experimental Life Science (JELS) is scientific journal published by Graduate Program of Brawijaya University as distribution media of Indonesian researcher's results in life science to wider community. JELS is published in every four months. JELS published scientific papers in review, short report, and life sciences especially nanobiology, molecular biology and cellular biology. JELS is scientific journal that published compatible qualified articles to academic standard, scientific and all articles reviewed by expert in their field.

Journal of Experimental Life Science (JELS) have vision to become qualified reference media to publish the best and original research results, and become the foundation of science development through invention and innovation on cellular, molecular, and nanobiology rapidly to community.

Journal of Experimental Life Science (JELS) have objectives to published qualified articles on research's results of Indonesian researchers in life science scope. JELS encompasses articles which discuss basic principles on nature phenomenon with cellular, molecular, and nanobiology approach.

PEER REVIEW PROCESS

Publication of articles by JITODE is dependent primarily on their validity and coherence, as judged by peer reviewers, who are also asked whether the writing is comprehensible and how interesting they consider the article to be. All submitted manuscripts are read by the editorial staff and only those articles that seem most likely to meet our editorial criteria are sent for formal review. All forms of published correction may also be peer-reviewed at the discretion of the editors. Reviewer selection is critical to the publication process, and we base our choice on many factors, including expertise, reputation, and specific recommendations. The editors then make a decision based on the reviewers' advice, from among several possibilities:

Accepted, with or without editorial revisions
Invite the authors to revise their manuscript to address specific concerns before a final decision

Rejected, but indicate to the authors that further work might justify a resubmission

Rejected outright, typically on grounds of specialist interest, lack of novelty, insufficient conceptual advance or major technical and/or interpretational problems

PUBLICATION FREQUENCY

JELS publish 2 Issues per year until 2017. JELS started to publish 3 Issues per year since 2018.

OPEN ACCESS POLICY

This journal provides immediate open access to its content on the principle that making research freely available to the public supports a greater global exchange of knowledge.

COPYRIGHT NOTICE

Authors who publish with this journal agree to the following terms:

Authors retain copyright and grant the journal right of first publication with the work simultaneously licensed under a Creative Commons Attribution License that allows others to share the work with an acknowledgement of the work's authorship and initial publication in this journal.

Authors are able to enter into separate, additional contractual arrangements for the non-exclusive distribution of the journal's published version of the work (e.g., post it to an institutional repository or publish it in a book), with an acknowledgement of its initial publication in this journal.

Authors are permitted and encouraged to post their work online (e.g., in institutional repositories or on their website) prior to and during the submission process, as it can lead to productive exchanges, as well as earlier and greater citation of published work (The Effect of Open Access).

PRIVACY STATEMENT

The names and email addresses entered in this journal site will be used exclusively for the stated purposes of this journal and will not be made available for any other purpose or to any other party.

ETHICS PUBLICATION

Research that using animal, human, and clinical testing is should already have ethical clearance certificate from authorized institution.

Title Typed in Bold, Capitalize each First Letter of Each Word, Except Conjunctive, *Scientific name* should not be Abbreviated (Calibri 14 Bold Center, should not exceed 12 words, except conjuctive)

First Author[1]*, Second Author[2], Third Author[3] (Calibri 12 Center, without title)

[1]First Author Affiliation, Correspondence author should be indicated by * symbol (Calibri 9 Center)
[2]Department of Biology, Faculty of Mathematics and Natural Sciences, University of Brawijaya, Malang, Indonesia
[3]Laboratorium of Physiology, Faculty of Medicine, University of Brawijaya, Malang, Indonesia

Abstract (Calibri 9 Bold Center)

This article illustrates preparation of your paper using MS-WORD (.doc or .rtf). Manuscript was numbered consecutively. Main text typed in two columns (67 characters), except title and abstract in one column. The manuscript should be written in English. The length of manuscript should not exceed 10 pages including table and figure in this format using A4 paper single space. The text should be in the margin of 3 cm up, down and left side, 2.5 cm on right side. Abstract includes the research purposes, research method and research results in one paragraph of *essay,* not *enumerative*. No citation in abstract. Abstract should not exceed 200 words. Keywords typed after abstract. (Calibri 9 Justify).

Keywords: manuscript, English, format, 5 words maximum (Calibri 9 Left)

INTRODUCTION* (Calibri 10 Bold, Left, Capslock)

All submitted manuscripts should contain original research which not previously published and not under consideration for publication elsewhere. Articles must be written in ENGLISH and manuscripts may be submitted for consideration as research report articles, short reports or reviews.

The introduction explains the background of the problem, the study of literature and research purposes. Some initial introduction paragraphs explain the problem and background to these problems [1]. The next few paragraphs explain the study of literature that contains recent knowledge development which is directly related to the issues. The last paragraph of the introductory section contains a description of the purposes of the study. (Calibri 10 Justify)

MATERIAL AND METHOD (Calibri 10 Bold, Left, Capslock)

This section describes the types of methods (qualitative, quantitative or mixed-method) with details of methods of data collection and data analysis [2]. This section also describes the perspective that underlying the selection of a particular method. (Calibri 10 Justify)

Correspondence address: (Calibri 8 Bold, Left)
Full name of correspondence author
Email : sapto@jurnal.ub.ac.id
Address : afiliation address include post code

Data Collection (Calibri 10 Bold, Left)

Explain the data collection methods, i.e. surveys, observations or archive, accompanied by details of the use of such methods. This section also describes the population, sampling and sample selection methods. (Calibri 10 Justify)

The use of English language should followed proper grammar and terms. Name of organism shoul be followed by its full scientific name in the first mention, in *italic* [3]. Author of the scientific name and the word of "var." typed regular. Example: *Stellaria saxatillis* Buch. Ham. First abbreviation typed in colon after the abbreviated phrase.

Author must use International Standard Unit (SI). Negative exponent used to show the denominator unit. Example: g l^{-1}, instead of g/l. The unit spaced after the numbers, except percentage [4]. Example: 25 g l^{-1}, instead of 25gl^{-1}; 35% instead of 35 %. Decimal typed in dot (not coma). All tables and figures should be mentioned in the text.

RESULT AND DISCUSSION (Calibri 10 Bold, Left, Capslock)

This section contains the results of the analysis and interpretation or discussion of the results of the analysis. Describe a structured, detailed, complete and concise explanation, so that the reader can follow the flow of analysis and thinking of researchers [5]. Part of the results study should be integrated with the results of the

analysis and the results and discussion are not separated.

Table

Table should be submitted within the manuscript and in separated file of *Microsoft Excel* (xls.). Table whould not exceed 8 cm (one column) and 17 cm (two columns). Table should be embedded in different page after references.

Table should be numbered in sequence. Table title should be brief and clear above the table, with uppercase in initial sentence. Vertical line should not be used. Footnote use number with colon and superscripted. Symbol of (*) or (**) was used to show difference in confidence interval of 95 and 99%.

Table 1. Example of the Table (Calibri 8.5 Left)

No	Point (Calibri 8.5 Justify)	Description
1		
2		
3		
4		
5		

Sources: Journal of PPSUB (Calibri 8.5 Left)

Figures

Figures should be in high resolution and well contrast in JPEG or PDF with the following conditions:

- Monochrome image (line art), figures of black and white diagram (solid/no shades of gray), resolution 1000-1200 dpi (dot per inch).
- Combination Halftone, combine figure and text (image containing text) and coloured graphic or in grayscale format. Resolution 600-900 dpi.
- Halftone, coloured figure or grayscale format without text. Resolution 300 dpi.
- Black and white figure should be in the grayscale mode, while coloured figures should be in RGB mode.
- Figure should not exceed the width of 8 cm (one column), 12.5 cm (1.5 columns) or 17 cm (two columns).
- Figures title typed clearly below the figure.
- Figure with pointing arrow should be grouped (grouping).
- Figures were recommended in black and white.
- Legend or figure description should be clear and complete. If compressed, the figure should be readable.
- Statistic graphic should be supplemented with data sources.
- If the figures come from the third party, it should have the copyright transfer from the sources.

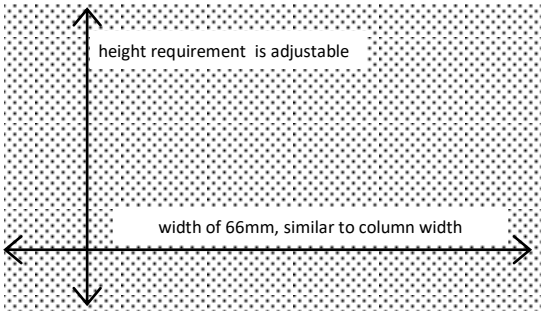

Figure 1. Illustration of Dimensional Figure of one column width. Figure dimension adjusted to the width of one column. Name the figure (diagram) written below the image. (Calibri 8.5 Justify)

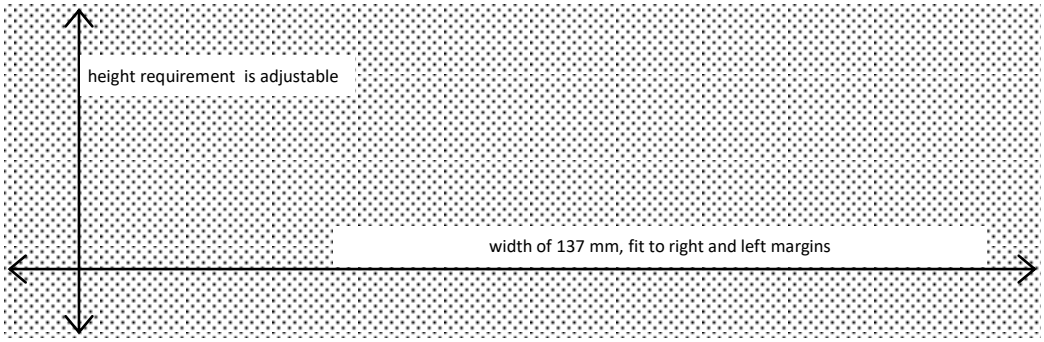

Figure 2. . Illustration of Dimensional Figure of two column width. Figure dimension adjusted to the width of two columns (137 mm). Figure were align top or bottom of the page. (Calibri 8.5 Justify)

References

1. Primary references include journal, patent, dissertation, thesis, paper in proceeding and text book.
2. Avoid self citation.
3. Author should avoid reference in reference, popular book, and internet reference except journal and private ana state institution.
4. Author was not allowed to use abstract as references.
5. References should been published (book, research journal or proceeding). Unpublished references or not displayed data can not be used as references.
6. References typed in numbering list (format number 1,2,3,…), ordered sequentially as they appear in the text (system of Vancouver or author-number style).
7. Citation in the manuscript typed only the references number (not the author and year), example: Obesity is an accumulation of fat in large quantities which would cause excessive body weight (overweight) [1]. Obesity is a risk factor of diabetic, hypertension dan atherosclerosis [2].

CONCLUSION (Calibri 10 Bold, Left, Capslock)

Conclusion of the study's findings are written in brief, concise and solid, without more additional new interpretation. This section can also be written on research novelty, advantages and disadvantages of the research, as well as recommendations for future research.(Calibri 10 Justify)

ACKNOWLEDGEMENT (Calibri 10 Bold, Left, Capslock)

This section describes gratitude to those who have helped in substance as well as financially. (Calibri 10 Justify)

REFERENCES (Calibri 10 Bold, Left, Capslock)

[1]. (Calibri 10 Justify, citation labelling by references numbering)
[2]. Vander, A., J. Sherman., D. Luciano. 2001. Human Physiology: The Mecanisms of Body Function. McGraw-Hill Higher Education. New York. (Book)
[3]. Shi, Z., M. Rifa'i, Y. Lee, K. Isobe, H. Suzuki. 2007. Importance of CD80/CD86-CD28 interaction in the recognation of target cells by $CD8^{+}CD122^{+}$ regulatory T cells. *Journal Immunology.* 124. 1:121-128. (Article in Journal)
[4]. Syafi'i, M., Hakim, L., dan Yanuwiyadi, B. 2010. Potential Analysis of Indigenous Knowledge (IK) in Ngadas Village as Tourism Attraction. pp. 217-234. In: Widodo, Y. Noviantari (eds.) Proceed-ing *Basic Science National Seminar 7* Vol.4. Universitas Brawijaya, Malang. (Article within conference proceeding)
[5]. Dean, R.G. 1990. Freak waves: A possible explanation. p. 1-65. *In* Torum, A., O.T. Gudmestad (eds). Water wave kinetics. CRC Press. New York. (Chapter in a Book)
[6]. Astuti, A.M. 2008. The Effect of Water Fraction of *Stellaria* sp. on the Content of TNF-α in Mice (*Mus musculus* BALB-C). Thesis. Department of Biology. University of Brawijaya. Malang. (Thesis)

Cover Image
3D Structure of EGCG (Epigallocatechin-3-Gallate)
Green Tea Component
Created by ::
Prof. Widodo, S.Si.,M.Si.,Ph.D MED Sc.

Address :
Building B, 1st Floor, Graduate Program Universitas Brawijaya
Jl. Mayor Jenderal Haryono 169, Malang, 65145,
East Java, Indonesia
Tel.: (+62341) 571260; Fax: (+62341) 580801
Email: jels@ub.ac.id
Web: jels.ub.ac.id

9 772087 285007